



# Search for heavy neutrinos and $W$ bosons with right-handed couplings in proton-proton collisions at $\sqrt{s} = 8 \text{ TeV}$

The CMS Collaboration\*

## Abstract

A search for heavy, right-handed neutrinos,  $N_\ell$  ( $\ell = e, \mu$ ), and right-handed  $W_R$  bosons, which arise in the left-right symmetric extensions of the standard model, has been performed by the CMS experiment. The search was based on a sample of two lepton plus two jet events collected in proton-proton collisions at a center-of-mass energy of 8 TeV corresponding to an integrated luminosity of  $19.7 \text{ fb}^{-1}$ . For models with strict left-right symmetry, and assuming only one  $N_\ell$  flavor contributes significantly to the  $W_R$  decay width, the region in the two-dimensional  $(M_{W_R}, M_{N_\ell})$  mass plane excluded at a 95% confidence level extends to approximately  $M_{W_R} = 3.0 \text{ TeV}$  and covers a large range of neutrino masses below the  $W_R$  boson mass, depending on the value of  $M_{W_R}$ . This search significantly extends the  $(M_{W_R}, M_{N_\ell})$  exclusion region beyond previous results.

*Published in the European Physical Journal C as doi:10.1140/epjc/s10052-014-3149-z.*



## 1 Introduction

The standard model (SM) [1–3] explicitly incorporates the parity violation observed in weak interactions through the use of a left-handed chiral  $SU_L(2)$  gauge group which includes the left-handed gauge bosons  $W_L^\pm$  and  $Z_L$ . One of the attractive features of left-right (LR) symmetric extensions [4–7] to the standard model is that these models explain parity violation in the SM as the consequence of spontaneous symmetry breaking of a larger gauge group to  $SU_L(2) \times SU_R(2)$  at a multi-TeV mass scale. The LR extensions introduce an additional right-handed  $SU_R(2)$  symmetry group to the SM, which includes heavy charged ( $W_R^\pm$ ) and neutral ( $Z_R$ ) gauge bosons that could be produced at LHC energies.

In addition to addressing parity non-conservation in weak interactions, LR theories also provide an explanation for the mass of SM neutrinos. The observation of neutrino oscillations [8, 9] requires that neutrinos have mass, and the fact that the neutrino mass scale [10] is far below that of quarks and charged leptons suggests that the origin of neutrino mass may be distinct from the origin of mass for the other SM fermions. Heavy right-handed Majorana neutrinos ( $N_e, N_\mu,$  and  $N_\tau$ ), which are naturally present in LR models, provide a possible explanation for the mass of SM neutrinos through the see-saw mechanism [11, 12].

We search for  $W_R$  bosons produced in a sample of proton-proton collisions at a center-of-mass energy  $\sqrt{s} = 8$  TeV and collected by the CMS detector at the CERN LHC. This search, which expands upon a previous search using  $\sqrt{s} = 7$  TeV data [13], assumes the production of a  $W_R$  boson that decays to a charged lepton (we consider  $\ell = e, \mu$ ) and to a right-handed neutrino  $N_\ell$ . The decay of the right-handed neutrino produces a second charged lepton of the same flavor together with a virtual right-handed charged boson  $W_R^*$ . When the  $W_R^*$  decays to a pair of quarks, we arrive at the decay chain:

$$W_R \rightarrow \ell_1 N_\ell \rightarrow \ell_1 \ell_2 W_R^* \rightarrow \ell_1 \ell_2 q \bar{q}.$$

The quarks hadronize into jets ( $j$ ), resulting in an observable final state containing two same-flavor charged leptons and two jets. Although the potential Majorana nature of the right-handed neutrinos implies the final-state charged leptons can have the same sign, we do not impose any charge requirements on the final-state electrons or muons in this analysis.

This search is characterized by the masses of the  $W_R$  boson ( $M_{W_R}$ ) and the right-handed neutrino  $N_\ell$  ( $M_{N_\ell}$ ), which are allowed to vary independently. Although  $M_{N_\ell} > M_{W_R}$  is allowed in the LR symmetric model, it is not considered in this analysis in favor of the dominant  $q\bar{q}' \rightarrow W_R$  production mechanism. As the branching fraction for  $W_R \rightarrow \ell N_\ell$  depends on the number of heavy-neutrino flavors accessible at LHC energies, results are first interpreted assuming that only one neutrino flavor, namely  $N_e$  or  $N_\mu$ , is light enough to contribute significantly to the  $W_R$  boson decay width. Results are then interpreted assuming degenerate  $N_e, N_\mu,$  and  $N_\tau$  masses.

For given  $W_R$  boson and  $N_\ell$  mass assumptions, the signal cross section can be predicted from the value of the coupling constant  $g_R$ , which denotes the strength of the gauge interactions of  $W_R$  bosons. We assume strict LR symmetry, such that  $g_R$  is equal to the (left-handed) weak interaction coupling strength  $g_L$  at  $M_{W_R}$ , and we also assume identical quark and neutrino mixing matrices for the left- and right-handed interactions. The  $W_R$  boson production cross section can then be calculated by the FEWZ program [14] using the left-handed  $W'$  model [15]. Finally, the left-right boson and lepton mixing angles are assumed to be small [16].

The theoretical lower limit on  $W_R$  mass of  $M_{W_R} \gtrsim 2.5$  TeV [17, 18] is estimated from the measured size of the  $K_L$ – $K_S$  mass difference. Searches for  $W_R \rightarrow t\bar{b}$  decays at the LHC using  $\sqrt{s} = 7$

and 8 TeV data [19–21] have excluded  $W_R$  boson masses below 2.05 TeV at 95% confidence level (CL), and previous searches for  $W_R \rightarrow \ell N_\ell$  at the LHC excluded at 95% CL a region in the two-dimensional parameter space  $(M_{W_R}, M_{N_\ell})$  extending to nearly  $M_{W_R} = 2.5$  TeV [13, 22]. This paper describes the first direct search that is sensitive to  $M_{W_R}$  values beyond the theoretical lower mass limit.

## 2 The CMS detector

The central feature of the CMS apparatus is a superconducting solenoid, of 6 m internal diameter, providing a field of 3.8 T. Within the field volume are the silicon pixel and strip tracker, the  $\text{PbWO}_4$  crystal electromagnetic calorimeter (ECAL) and the brass and scintillator hadron calorimeter (HCAL). Muons are measured in gas-ionization detectors embedded in the steel flux-return yoke. The ECAL has an energy resolution of better than 0.5% for unconverted photons with transverse energies  $E_T \equiv E/\cosh\eta > 100$  GeV. The muons are measured in the pseudorapidity window  $|\eta| < 2.4$ , where  $\eta = -\ln[\tan(\theta/2)]$  and  $\theta$  is the polar angle with respect to the counterclockwise-beam direction. The muon system detection planes are made of three technologies: drift tubes, cathode strip chambers, and resistive-plate chambers. Matching the muons to the tracks measured in the silicon tracker results in a transverse momentum ( $p_T \equiv |p|/\cosh\eta$ ) resolution between 1 and 10% for  $p_T < 1$  TeV. The inner tracker measures charged particles within the range  $|\eta| < 2.5$  and provides an impact parameter resolution of  $\sim 15$   $\mu\text{m}$  and a  $p_T$  resolution of about 1.5% for 100 GeV particles. The first level of the CMS trigger system, composed of custom hardware processors, uses information from the calorimeters and muon detectors to select up to 100 kHz of events of interest. The high-level trigger (HLT) processor farm uses information from all CMS subdetectors to further decrease the event rate to about 400 Hz before data storage. A more detailed description of the CMS detector, together with a definition of the coordinate system used and the relevant kinematic variables, can be found elsewhere [23].

The particle-flow event reconstruction technique [24, 25] used to reconstruct jets in this analysis consists in reconstructing and identifying each single particle with an optimized combination of all subdetector information. The energy of photons is directly obtained from the ECAL measurement, corrected for zero-suppression effects. The energy of electrons is determined from a combination of the track momentum at the main interaction vertex, the corresponding ECAL cluster energy, and the energy sum of all bremsstrahlung photons attached to the track. The energy of muons is obtained from the corresponding track momentum. The energy of charged hadrons is determined from a combination of the track momentum and the corresponding ECAL and HCAL energy, corrected for zero-suppression effects and for the response function of the calorimeters to hadronic showers. Finally, the energy of neutral hadrons is obtained from the corresponding corrected ECAL and HCAL energy.

## 3 Data and Monte Carlo samples

The search for  $W_R$  boson production described in this paper is performed using pp collision data collected with the CMS detector at  $\sqrt{s} = 8$  TeV in 2012. The data sample corresponds to an integrated luminosity of 19.7  $\text{fb}^{-1}$ . Candidate  $W_R \rightarrow eN_e$  events are collected using a double-electron trigger that requires two clusters in ECAL with  $E_T > 33$  GeV each. These ECAL clusters are loosely matched at the HLT stage to tracks formed from hits in the pixel detector. To reject hadronic backgrounds, only a small amount of energy in the HCAL may be associated with the HLT electron candidates. Muon channel events are selected with a single-

muon trigger that requires at least one candidate muon with  $p_T > 40 \text{ GeV}$  and  $|\eta| < 2.1$ , as reconstructed by the HLT.

Simulated  $W_R \rightarrow \ell N_\ell$  signal samples are generated assuming  $M_{N_\ell} = \frac{1}{2} M_{W_R}$  using PYTHIA 6.4.26 [26], a tree-level Monte Carlo (MC) generator, with CTEQ6L1 parton distribution functions (PDF) [27] and underlying event tune Z2\* [28]. The MC generator includes the LR symmetric model with the assumptions previously mentioned. The final state leptons and jets in these signal events are sufficiently energetic to allow reconstruction effects to be addressed apart from the kinematic requirements discussed below. With this separation, the extension from  $M_{N_\ell} = \frac{1}{2} M_{W_R}$  to the full two-dimensional  $(M_{W_R}, M_{N_\ell})$  mass plane for signal events is straight-forward, as is discussed in Section 7. The dominant backgrounds to  $W_R$  boson production include SM processes with at least two charged leptons with large transverse momentum, namely  $t\bar{t} \rightarrow bW^+ \bar{b}W^-$  and Drell–Yan (DY)+jets processes. All remaining SM background events, which collectively contribute less than 10% to the total background level, are dominated by diboson and single top quark processes. The  $t\bar{t}$  background is estimated using control samples in data and a simulated sample of fully leptonic  $t\bar{t}$  decays, which are generated using the tree-level matrix element MC generator MADGRAPH 5.1.4.8 [29]. The DY+jets background is estimated using exclusive DY+n jets ( $n = 0, 1, 2, 3, 4$ ) simulated samples generated with MADGRAPH 5.1.3.30. For the above MADGRAPH samples, parton showering, fragmentation, and the underlying event are handled by PYTHIA. A statistically comparable sample of DY+jets events generated with the tree-level MC event generator SHERPA 1.4.2 [30], which incorporates parton showering and other effects in addition to the hard process, is used to help quantify the systematic uncertainty in the DY+jets background estimation. Simulated diboson (WW, WZ, and ZZ) events are generated using PYTHIA 6.4.26, with the additional small contributions from diboson scattering processes generated with MADGRAPH 5.1.3.30. The simulated single top quark (namely,  $tW$ ) background sample is generated via the next-to-leading-order MC generator POWHEG 1.0 [31–34]. Parton showering and other effects are handled by PYTHIA for the diboson and single top quark background samples.

The generated signal and SM background events pass through a full CMS detector simulation based on GEANT4 [35], and are reconstructed with the same software used to reconstruct collision data, unless otherwise noted. The simulation is compared to data using various control samples, and when necessary the simulation is adjusted to account for slight deviations seen with respect to data. Additional pp collisions in the same beam crossing (pileup) are also included for each simulated event to realistically describe the  $\sqrt{s} = 8 \text{ TeV}$  collision environment.

## 4 Event selection and object reconstruction

We assemble  $W_R$  boson candidates from the two highest- $p_T$  (leading) jets and two highest- $p_T$  same-flavor leptons (electrons or muons) reconstructed in collision data or simulation events. Candidate events are first selected by the CMS trigger system using the lepton triggers described previously. The electron and muon trigger efficiencies are determined using the “tag and probe” techniques applied to  $Z \rightarrow \ell\ell$  candidates [36–38]. Simple triggers, requiring a single ECAL cluster with  $E_T > 300 \text{ GeV}$ , collected events with high- $p_T$  electrons to help evaluate the trigger efficiency for electron channel events with high dielectron mass [39]. Following the application of object and event selection requirements mentioned below, the trigger efficiency for  $W_R \rightarrow \ell N_\ell$  candidate events is greater than 99% (98%) in the electron (muon) channel.

Because of the large expected mass of the  $W_R$  boson, electron and muon reconstruction and identification are performed using algorithms optimized for objects with large transverse momentum [36, 39]. Non-isolated muon backgrounds are suppressed by computing the transverse

momentum sum of all additional tracks within a cone of  $\Delta R < 0.3$  about the muon direction, where  $\Delta R = \sqrt{(\Delta\eta)^2 + (\Delta\phi)^2}$  (azimuthal angle  $\phi$  in radians), and requiring the  $p_T$  sum to be less than 10% of the muon transverse momentum. This isolation requirement is only weakly dependent on the number of pileup collisions in the event, as tracks with a large  $\Delta z$  separation from the muon, i.e., tracks from other pp collisions, are not included in the isolation sum. Electrons are expected to have minimal associated HCAL energy and also to appear isolated in both calorimeters and in the tracker. To minimize the effects of pileup, electrons must be associated with the primary vertex, which is the collision vertex with the highest  $\sum p_T^2$  of all associated tracks. As pileup collisions also produce extra energy in the calorimeters and can make the electron appear non-isolated, calorimeter isolation for electron candidates is corrected for the average energy density in the event [40].

Jets are reconstructed using the anti- $k_T$  clustering algorithm [41] with a distance parameter of 0.5. Charged and neutral hadrons, photons, and leptons reconstructed with the CMS particle-flow technique are used as input to the jet clustering algorithm. To reduce the contribution to jet energy from pileup collisions, charged hadrons that do not originate from the primary vertex in the event are not used in jet clustering. After jet clustering, the pileup calorimeter energy contribution from neutral particles is removed by applying a residual average area-based correction [40, 42]. Jet identification requirements [43] suppress jets from calorimeter noise and beam halo, and the event is rejected if either of the two highest- $p_T$  jet candidates fails the identification criteria. The jet four-momenta are corrected for zero-suppression effects and for the response function of the calorimeters to hadronic showers based on studies with simulation and data [44]. As the electrons and muons from  $W_R$  boson decay are likely to be spatially separated from jets in the detector, we reject any lepton found within a cone of radius  $\Delta R < 0.5$  from the jet axis for either of the two leading jets.

After selecting jets and isolated electrons or muons in the event,  $W_R \rightarrow \ell N_\ell$  candidates are formed using the two leading same-flavor leptons and the two leading jets that satisfy the selection criteria. The leading (subleading) lepton is required to have  $p_T > 60$  (40) GeV, while the  $p_T$  of each jet candidate must exceed 40 GeV. Electrons and jets are reconstructed within the tracker acceptance ( $|\eta| < 2.5$ ). Muon acceptance extends to  $|\eta| < 2.4$ , although at least one muon is restricted to  $|\eta| < 2.1$  in order to be selected by the trigger.

We perform a shape-based analysis, searching for evidence of  $W_R$  boson production using the four-object mass distribution ( $M_{\ell\ell jj}$ ), where we consider events with  $M_{\ell\ell jj} > 600$  GeV. To reduce the contribution from DY+jets and other SM backgrounds, we also impose a requirement of  $M_{\ell\ell} > 200$  GeV on the mass of the lepton pair associated with the  $W_R$  boson candidate.

The decay of a  $W_R$  boson tends to produce final-state objects that have high  $p_T$  and are separated in the detector. We define the signal acceptance to include the kinematic and detector acceptance requirements for the leptons and jets, lepton-jet separation, and the minimum  $M_{\ell\ell}$  and  $M_{\ell\ell jj}$  requirements. This signal acceptance, typically near 80% at  $M_{N_\ell} \sim M_{W_R}/2$ , varies by less than 1% between the electron and muon channels because of differences in detector acceptance for leptons. Provided that the  $W_R$  boson decay satisfies acceptance requirements, the ability to reconstruct all four final-state particles is near 75% 2.8 (85%) for the electron (muon) channel, with some dependence on  $W_R$  boson and  $N_\ell$  masses. However, if the mass of the  $W_R$  boson is sufficiently heavy compared to that of the right-handed neutrino, the  $N_\ell \rightarrow \ell jj$  decay products tend to overlap and it becomes difficult to reconstruct two distinct jets or find leptons outside of the jet cone. As a result, the signal acceptance as a function of  $M_{N_\ell}$  decreases rapidly as  $M_{N_\ell}$  drops below about 10% of the  $W_R$  boson mass.

## 5 Standard model backgrounds

The  $t\bar{t}$  background contribution to the  $eejj$  and  $\mu\mu jj$  final states is estimated using a control sample of  $e\mu jj$  events reconstructed in data. Studies of simulated  $t\bar{t} \rightarrow eejj$ ,  $\mu\mu jj$ , and  $e\mu jj$  decays confirm that the  $M_{eejj}$  and  $M_{\mu\mu jj}$  distributions can be modeled by the  $M_{e\mu jj}$  distribution, so we apply selection requirements to  $e\mu jj$  events that parallel those applied to electron and muon channel events. The  $e\mu jj$  events are collected using the same HLT selection as  $\mu\mu jj$  events, although in this case only one muon is available for selection by the trigger. This sample is dominated by  $t\bar{t}$  events, and small contributions from other SM processes are subtracted using simulation. The relative fractions of  $t\bar{t} \rightarrow eejj$ ,  $\mu\mu jj$ , and  $e\mu jj$  events that pass the selection criteria are determined from simulation. Using this information, the  $M_{e\mu jj}$  distribution for the  $e\mu jj$  control sample from data is scaled to match the expected  $t\bar{t}$  background contribution to the  $M_{eejj}$  and  $M_{\mu\mu jj}$  distributions. The scale factor derived from simulation is determined after requiring  $M_{e\mu} > 200 \text{ GeV}$  and  $M_{e\mu jj} > 600 \text{ GeV}$ , which is equivalent to the third and final selection stage in Table 1. The scale factors for the  $t\bar{t}$  background sample are  $0.524 \pm 0.007$  and  $0.632 \pm 0.008$  in the electron and muon channels, respectively, where the uncertainty in the values reflects the number of simulated  $t\bar{t}$  events that satisfy all object and event requirements. The trigger efficiency for  $e\mu jj$  events is over 90% for events with central muons ( $|\eta| < 0.9$ ) and decreases for events with more forward muons. Consequently, both the electron and muon scale factors are larger than the expected value of 0.5, given the relative branching fractions for  $t\bar{t} \rightarrow eejj$ ,  $\mu\mu jj$ , and  $e\mu jj$  decays.

The  $t\bar{t}$  scale factors, determined from simulation, are checked using control regions in data. We first consider events in both simulation and data where one or both jets are identified as originating from a bottom quark. After all selection requirements are applied, reconstructed  $t\bar{t}$  decays dominate the event samples. Accounting for contributions from other SM processes using simulation, we compute scale factors for  $e\mu jj$  events in data with  $60 < M_{e\mu} < 200 \text{ GeV}$  to estimate the  $t\bar{t}$  contribution to the SM background when one or both jets are tagged as b jets using the medium working point of the combined secondary vertex tagging algorithm [45]. The  $M_{ee}$  and  $M_{\mu\mu}$  distributions in b-tagged data agree with expectations based on simulation and the  $e\mu jj$  control sample, and the derived scale factors agree with those obtained from simulation within statistical precision. For another cross-check, we compute the scale factor based on the expectation that  $t\bar{t} \rightarrow e\mu jj$  should be twice the rate of  $t\bar{t} \rightarrow eejj$  or  $t\bar{t} \rightarrow \mu\mu jj$ . Deviation from this expected ratio depends primarily on the differences in electron and muon reconstruction and identification efficiencies. The number of electron and muon channel events in data in the  $120 < M_{\ell\ell} < 200 \text{ GeV}$  control region are thus used to derive the relative efficiency difference between electrons and muons and then extract the  $t\bar{t}$  scale factors. The scale factors determined from this control region in data are consistent with those derived from simulation, and the larger statistical uncertainty (2%) of this cross-check is taken as the systematic uncertainty in the  $t\bar{t}$  normalization.

The DY+jets background contribution is estimated from  $Z/\gamma^* \rightarrow \ell\ell$  decays reconstructed in simulation and data. The simulated DY+jets background contribution is normalized to data using events in the dilepton mass region  $60 < M_{\ell\ell} < 120 \text{ GeV}$  after kinematic requirements are applied on the leptons and jets, which is the first selection stage indicated in Table 1. After removing the small contribution from other SM background processes, the simulated DY+jets distributions are normalized to data using scale factors of  $1.000 \pm 0.007$  and  $1.027 \pm 0.006$  for the electron and muon channels, respectively, relative to inclusive next-to-next-to-leading-order cross section calculations. The uncertainty in this value reflects the number of events from data with  $60 < M_{\ell\ell} < 120 \text{ GeV}$ . The shape of the  $M_{\ell\ell}$  distribution in data is in agreement with SM expectations for  $M_{\ell\ell} > 60 \text{ GeV}$ , as shown in Fig. 1.

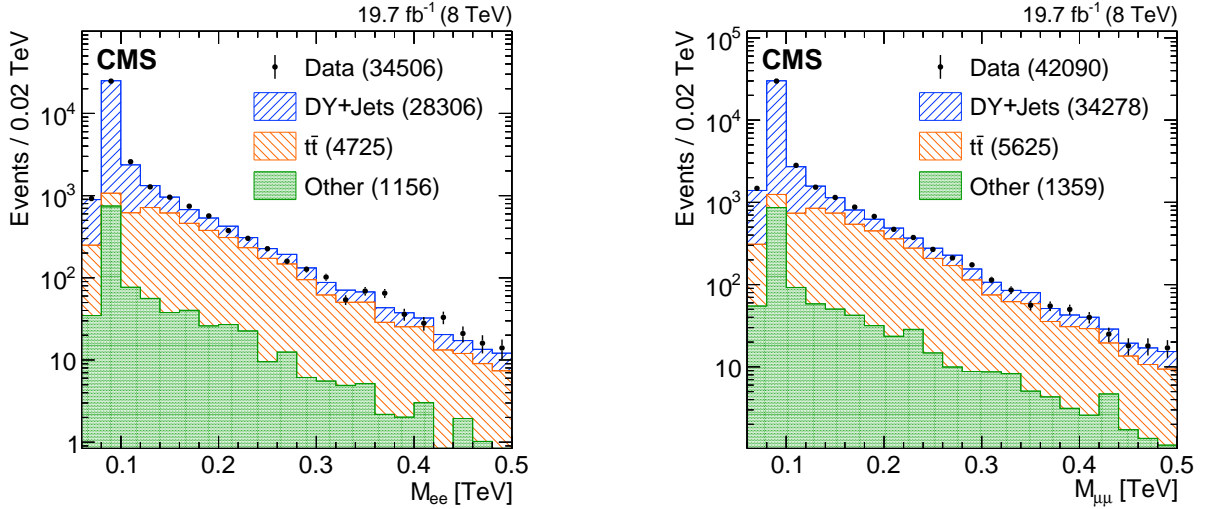


Figure 1: Distribution of the invariant mass  $M_{ee}$  (left) and  $M_{\mu\mu}$  (right) for events in data (points with error bars) with  $p_T > 60$  (40) GeV for the leading (subleading) lepton and at least two jets with  $p_T > 40$  GeV, and for background contributions (hatched stacked histograms) from data control samples ( $t\bar{t}$ ) and simulation. The numbers of events from each SM process are included in parentheses in the legend, where the contributions from diboson and single top quark processes have been collected in the “Other” background category.

The diboson and single top quark contributions to the total background are estimated from simulation, based on next-to-leading-order [46] and approximate next-to-next-to-leading-order [47] production cross sections, respectively. The background from  $W$ +jets processes, also estimated from simulation, is negligible starting from the earliest selection stage. Finally, the background contribution from multijet processes is estimated using control samples in data and is also found to be negligible at every selection stage.

The observed and expected numbers of events surviving the selections are summarized in Table 1, which explicitly lists the contributions from  $t\bar{t}$  and  $DY$ +jets processes while including all other SM background contributions in a single column. The yields reflect the numbers of background events surviving each selection stage, with normalization factors obtained from simulation and control sample studies or taken directly from simulation. The numbers of events observed at each selection stage agree with SM expectations in both channels.

## 6 The $M_{W_R}$ distribution and systematic uncertainties

Once all object and event selection criteria are applied, the  $M_{\ell\ell jj}$  distributions in data and simulation are used to search for evidence of  $W_R$  boson production, where the expected SM  $M_{\ell\ell jj}$  distribution is computed as the sum of the individual background  $M_{\ell\ell jj}$  distributions. The  $M_{\ell\ell jj}$  distribution is measured in 200 GeV wide bins up to 1.8 TeV, as this bin width is comparable to the mass resolution of the  $W_R$  boson for  $M_{W_R} < 2.5$  TeV. Beyond 1.8 TeV, events are summed in two bins,  $1.8 < M_{\ell\ell jj} < 2.2$  TeV and  $M_{\ell\ell jj} > 2.2$  TeV, to account for the small number of background events in the simulated and data control samples at high mass. The  $M_{\ell\ell jj}$  distributions for  $DY$ +jets, diboson, and single top quark processes are taken from simulation, with the normalization of each distribution as discussed previously. The  $M_{e\mu jj}$  distribution from data is used to model the  $t\bar{t}$  background contribution in the electron and muon channels.

In our previous search for  $W_R \rightarrow \mu N_\mu$  production using 7 TeV collision data [13], we mod-



Table 1: The total numbers of events reconstructed in data, and the expected contributions from signal and background samples, after successive stages of the selection requirements are applied. For the first selection stage, all kinematic and identification requirements are imposed on the leptons and jets as described in the text. The ‘‘Signal’’ column indicates the expected contribution for  $M_{W_R} = 2.5$  TeV, with  $M_{N_\ell} = 1.25$  TeV. The ‘‘Other’’ column represents the combined background contribution from diboson and single top quark processes. The uncertainties in the background expectation are derived for the final stage of selection and more details are given in Section 6. The total experimental uncertainty is summarized in the first signal uncertainty, and the second signal uncertainty represents the PDF cross section uncertainty. The yields from earlier stages of the selection have greater relative uncertainty than that for the final  $M_{\ell\ell jj} > 600$  GeV selection stage.

	Data	Signal	SM Backgrounds			
			Total	t $\bar{t}$	DY+jets	Other
Two electrons, two jets	34506	30	34154	4725	28273	1156
$M_{ee} > 200$ GeV	1717	29	1747	1164	475	108
$M_{eejj} > 600$ GeV	817	$29 \pm 1 \pm 3$	$783 \pm 51$	$476 \pm 42$	$252 \pm 24$	$55 \pm 12$
Two muons, two jets	42090	35	41204	5625	34220	1359
$M_{\mu\mu} > 200$ GeV	2042	35	2064	1382	549	133
$M_{\mu\mu jj} > 600$ GeV	951	$35 \pm 1 \pm 4$	$913 \pm 58$	$562 \pm 50$	$287 \pm 26$	$64 \pm 12$

eled the shape of each background  $M_{\mu\mu jj}$  distribution using an exponential lineshape. For this search, we again find that an exponential function can be used to describe each background  $M_{\ell\ell jj}$  distribution below 2 TeV, but these  $M_{\ell\ell jj}$  distributions begin to deviate from the assumed exponential shape at high mass. As a result, in this updated search we use the  $M_{\ell\ell jj}$  distributions from each background process directly instead of relying on exponential fits to model the shape of the SM backgrounds.

As the  $t\bar{t}$  background shape is taken from a control sample of  $e\mu jj$  events in data, we examine the shape of the  $t\bar{t}$  background  $M_{e\mu jj}$  distributions in both simulation and data. Based on the method to extract the background shape in our earlier search, we fit each  $M_{e\mu jj}$  distribution to an exponential lineshape for events surviving all selection criteria for  $e\mu jj$  events. The  $t\bar{t}$  background distribution is again expected to decrease exponentially as  $M_{\ell\ell jj}$  increases, although we allow for deviations at high mass (beyond 2 TeV) where the DY+jets background is more significant. The simulated  $M_{e\mu jj}$  distribution agrees with the exponential lineshape for  $M_{e\mu jj} < 2$  TeV, as expected, while we find that the  $M_{e\mu jj}$  distribution in the data control sample noticeably deviates from fit expectations for  $1.0 < M_{e\mu jj} < 1.2$  TeV. While the fit expects 94 events, only 78 events are found in data in this region. As a result, we correct the  $M_{e\mu jj}$  distribution from the data control sample to the expected number of events from the exponential fit for  $1.0 < M_{e\mu jj} < 1.2$  TeV, and this correction is reflected in Table 1. The size of the correction is taken as a systematic uncertainty in the shape of the  $t\bar{t}$   $M_{\ell\ell jj}$  distribution.

The  $M_{\ell\ell jj}$  distributions for events satisfying all selection criteria appear in Fig. 2. A comparison of the observed data to SM expectations yields a normalized  $\chi^2$  of 1.4 (0.9) for electron (muon) channel events. We observe an excess in the electron channel in the region  $1.8 < M_{eejj} < 2.2$  TeV, where 14 events are observed compared to 4 events expected from SM backgrounds. This excess has a local significance of  $2.8\sigma$  estimated using the method discussed in Section 7. This excess does not appear to be consistent with  $W_R \rightarrow eN_e$  decay. We examined additional distributions for events with  $1.8 < M_{eejj} < 2.2$  TeV, including the mass distributions  $M_{eij}$  (for both the leading and subleading electrons),  $M_{ee}$ , and  $M_{jj}$ , as well as the  $p_T$  distributions for each of the final state particles. In this examination, we find no compelling evidence in favor of

the signal hypothesis over the assumption of an excess of SM background events in this region. Examining the charge of the electrons used to build  $W_R$  boson candidates in data events with  $1.8 < M_{eejj} < 2.2$  TeV, we find same-sign electrons in one of the 14 reconstructed events. In this region, the same-sign SM background is expected to be on the order of half an event due to SM diboson processes and charge misidentification in DY+jets events. No same-sign events are observed in the same mass region of the distribution for the muon channel. For comparison, making plausible assumptions for the properties of a signal contributing in this region, one would expect half of the additional events to have electrons with the same sign.

The uncertainties in modeling the shape of the background  $M_{\ell\ell jj}$  distributions dominate the background systematic uncertainty, as shown in Fig. 2. The background  $M_{\ell\ell jj}$  uncertainty is determined in each mass bin based on the number of events surviving all selection criteria for each background sample. For the two dominant backgrounds, an additional shape uncertainty is included as part of the background shape uncertainty.

The additional  $t\bar{t}$  shape uncertainty is included for the  $1.0 < M_{\ell\ell jj} < 1.2$  TeV mass region based on the previously discussed correction to the  $M_{e\mu jj}$  distribution for  $1.0 < M_{e\mu jj} < 1.2$  TeV. No additional  $t\bar{t}$  shape uncertainty is applied at other  $M_{\ell\ell jj}$  values as the  $M_{e\mu jj}$  distributions in both data and simulation agree with the assumed exponential lineshape below 1.8 TeV, and the statistical uncertainty of the  $e\mu jj$  control sample dominates at high mass. For the DY+jets background, the  $M_{\ell\ell jj}$  shape uncertainty is determined using simulated samples from two different MC generators, MADGRAPH and SHERPA. The difference between these two  $M_{\ell\ell jj}$  distributions, computed as a function of mass, is taken as an additional systematic uncertainty in the DY+jets shape.

The uncertainty associated with the background normalization is taken as the quadratic sum of the uncertainty in the scale factors determined from the cross-check for  $t\bar{t}$  background performed on a control region in data, the uncertainty estimated from the difference in the values obtained for DY+jets scale factors in the electron and muon channels, and the combined cross section and luminosity uncertainties for the remaining backgrounds. This overall background normalization uncertainty is small compared to the uncertainties determined for the background shape.

Lepton reconstruction and identification uncertainties, which also contribute to the total signal and background systematic uncertainty, are determined using  $Z \rightarrow ee, \mu\mu$  events reconstructed in both data and simulation. Uncertainties in the jet and lepton energy scales and resolutions also contribute to the systematic uncertainty. These uncertainties dominate the signal efficiency uncertainty, resulting in a total systematic uncertainty of up to 10% for the signal efficiency, depending on the  $W_R$  boson mass assumption. The combination of lepton and jet energy scale, resolution, and efficiency uncertainties is less than 5% for the background estimates taken from simulation.

The systematic uncertainties related to pileup, uncertainties in the proton PDFs, and initial- or final-state radiation are computed for the simulated background samples and are found to be small when compared to the background shape uncertainty. Additional theoretical uncertainties for the SM background processes are covered by the shape uncertainty. The total uncertainty for signal and background is determined for the final selection stage and presented in Table 1. Figure 2 summarizes the background uncertainty as a function of  $M_{\ell\ell jj}$  and displays the dominant background shape uncertainty relative to the total background uncertainty.

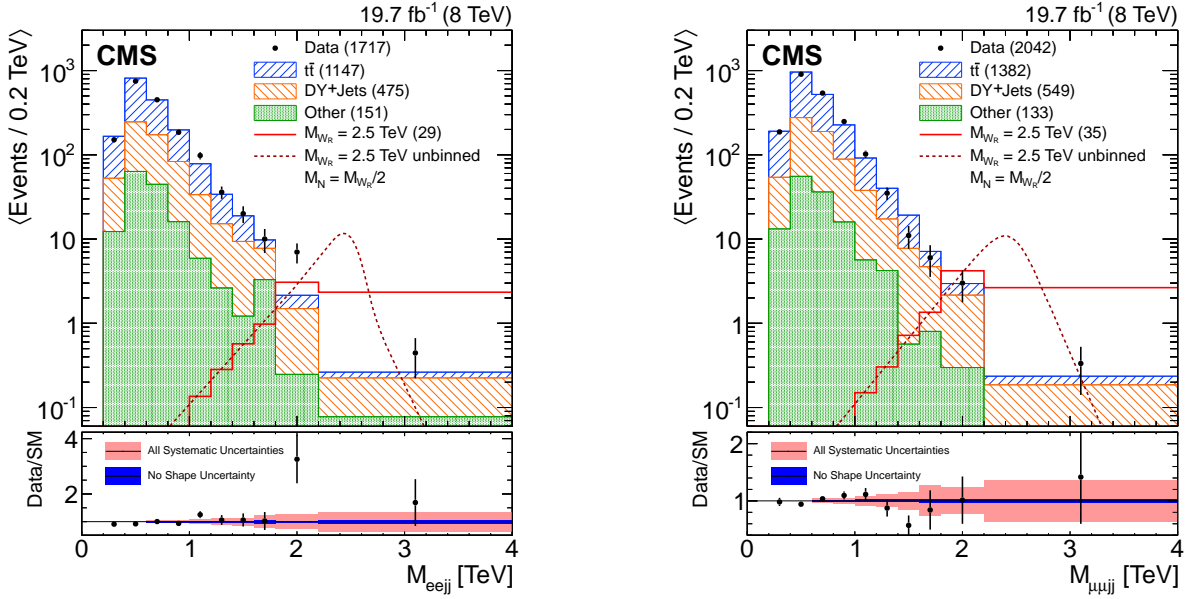


Figure 2: Distribution of the invariant mass  $M_{eejj}$  (left) and  $M_{\mu\mu jj}$  (right) for events in data (points with error bars) with  $M_{\ell\ell} > 200 \text{ GeV}$  and for background contributions (hatched stacked histograms) from data control samples ( $t\bar{t}$ ) and simulation. The signal mass point  $M_{W_R} = 2.5 \text{ TeV}$ ,  $M_{N_\ell} = 1.25 \text{ TeV}$ , is included for comparison (open red histogram, and also as a dotted line for the unbinned signal shape). The numbers of events from each background process (and the expected number of signal events) are included in parentheses in the legend, where the contributions from diboson and single top quark processes have been collected in the “Other” background category. The data are compared with SM expectations in the lower portion of the figure. The total background uncertainty (light red band) and the background uncertainty after neglecting the uncertainty due to background modeling (dark blue band) are included as a function of  $M_{\ell\ell jj}$  for  $M_{\ell\ell jj} > 600 \text{ GeV}$  (dashed line).

## 7 Limits on $W_R$ boson production

We estimate limits on  $W_R$  boson production using a multibin  $CL_S$  limit setting technique [48–50]. The  $M_{\ell\ell jj}$  distributions obtained from signal MC, each of the SM backgrounds, and the observed data all serve as limit inputs. The systematic uncertainties mentioned previously are included as nuisance parameters in the limit calculations. We estimate the 95% CL upper limit on the  $W_R$  boson cross section multiplied by the  $W_R \rightarrow \ell\ell jj$  branching fraction as a function of  $M_{W_R}$  and  $M_{N_\ell}$ . These results (available in tabular form in Appendix A) can be used for the evaluation of models other than those considered in this paper.

The limits are computed for a set of  $W_R$  boson and  $N_\ell$  mass assumptions, where  $M_{W_R}$  starts at 1 TeV and increases in 100 GeV steps and the  $N_\ell$  mass is taken to be half the  $W_R$  boson mass. For these determinations, the  $W_R$  boson signal samples include the full CMS detector simulation.

The procedure to determine the limits on  $W_R$  boson production for a range of  $N_\ell$  mass assumptions ( $M_{N_\ell} < M_{W_R}$ ) proceeds as follows. For a fixed value of  $M_{W_R}$ , the limits on  $W_R \rightarrow \ell N_\ell \rightarrow \ell\ell jj$  are determined as a function of  $M_{N_\ell}$  (up to  $M_{W_R}$ ) based on differences in kinematic acceptance, lepton-jet overlap, and  $M_{\ell\ell jj}$  shape relative to  $M_{N_\ell} = \frac{1}{2}M_{W_R}$ . As mentioned previously, the combined reconstruction and identification efficiency for the  $W_R$  boson and  $N_\ell$  decay products varies by  $\mathcal{O}(1\%)$  as a function of  $M_{W_R}$  once acceptance requirements are satisfied. Consequently, for  $M_{N_\ell}$  values other than  $M_{N_\ell} = \frac{1}{2}M_{W_R}$ , the  $W_R$  boson production cross section limits are computed using information from signal samples that do not include the simulated detector response.

The cross section limit calculation based on the kinematic acceptance is compared with the results for fully simulated samples using a spectrum of  $N_\ell$  mass assumptions for  $M_{W_R} = 1, 1.5, 2,$  and  $3$  TeV. The difference between the two methods is at the percent level or smaller for  $M_{N_\ell}$  masses greater than 10–20% of the generated  $W_R$  boson mass. Differences grow to  $\mathcal{O}(10)\%$  for lighter right-handed neutrinos. The ratio of the products of efficiency and acceptance for the two approaches is computed as a function of  $M_{N_\ell}/M_{W_R}$ , and a global fit to this distribution is used to correct the cross section limits determined as a function of  $M_{N_\ell}$  for all  $M_{W_R}$  values.

The uncertainty in this correction is computed using the maximum difference in the efficiency times acceptance ratio for the set of simulated samples as a function of  $M_{N_\ell}/M_{W_R}$ , unless the statistical uncertainty in the ratio calculation dominates. The impact of this uncertainty on signal acceptance is propagated to the cross section limit calculations. The overall effect on the limits from this uncertainty is negligible for most  $M_{N_\ell}$  values, but can degrade the cross section limit by 5–10% for  $N_\ell$  masses below 10% of  $M_{W_R}$ .

Finally, we account for variations in the shape of the  $M_{\ell\ell jj}$  distribution. As  $M_{N_\ell} \rightarrow 0$ , neutrino production via a virtual  $W_R$  boson becomes more significant. As a result, the shape of the signal  $M_{\ell\ell jj}$  distribution is expected to vary as a function of both  $M_{W_R}$  and  $M_{N_\ell}$ . This effect is included in the limit calculations.

The largest uncertainty related to the  $W_R \rightarrow \ell N_\ell$  production estimation arises from the variation in the predicted signal production cross section as a result of the uncertainties in the proton PDFs, where we use the CTEQ6L1 PDF set for signal events. The cross section uncertainty, which is not considered in the limit calculations, ranges from 5% for  $M_{W_R} = 1$  TeV to 26% for  $M_{W_R} = 3$  TeV and is computed following the PDF4LHC prescriptions [51, 52] for the CT10 [53], MSTW2008 [54], and NNPDF2.1 [55] PDF sets. The PDF uncertainties in the signal acceptance, which are small compared to the systematic uncertainties for signal events mentioned previously, are included in the limit calculations.

For the results presented in Fig. 3, we indicate a range of  $N_\ell$  masses that are excluded as a function of  $M_{W_R}$  assuming that only one heavy neutrino flavor (electron or muon) is accessible from 8 TeV pp collisions, with the other  $N_{\ell'}$  ( $\ell' = e, \mu, \tau$ , with  $\ell' \neq \ell$ ) too heavy to be produced. These  $(M_{W_R}, M_{N_\ell})$  limits are obtained by comparing the observed and expected cross section upper limits with the expected cross section for each mass point. The limits extend to roughly  $M_{W_R} = 3.0$  TeV in each channel and exclude a wide range of heavy neutrino masses for  $W_R$  boson mass assumptions below this maximal value. The inclusion of the results from the previous iteration of this analysis [13], which searched for  $W_R$  boson production in the  $\mu\mu jj$  final state using 7 TeV data, does not significantly affect the limit results. The excess in the electron channel at approximately 2 TeV has a local significance of  $2.8\sigma$  for a  $W_R$  boson candidate with a mass of 2.1 TeV. Assuming contributions from SM backgrounds only, the p-value for the local excess in the  $M_{eejj}$  distribution is 0.0050. We also present limits as a function of  $W_R$  boson mass for a right-handed neutrino with  $M_{N_\ell} = \frac{1}{2}M_{W_R}$  in Fig. 4. For the electron (muon) channel, we exclude  $W_R$  bosons with  $M_{W_R} < 2.87$  (3.00) TeV, with an expected exclusion of 2.99 (3.04) TeV.

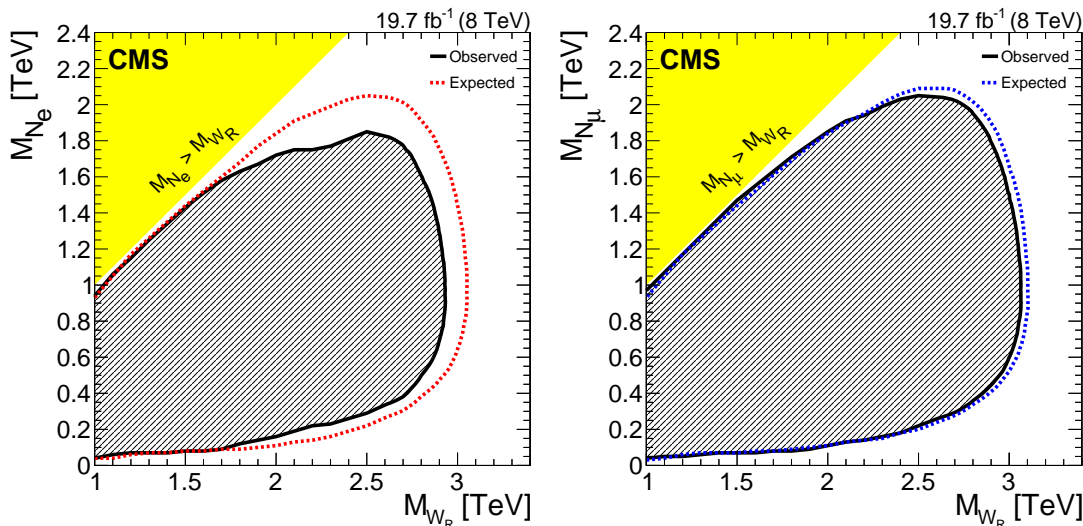


Figure 3: The 95% CL exclusion region (hatched) in the  $(M_{W_R}, M_{N_\ell})$  plane, assuming the model described in the text (see Section 1), for the electron (left) and muon (right) channels. Neutrino masses greater than  $M_{W_R}$  (yellow shaded region) are not considered in this search.

We additionally consider the case where all  $N_\ell$  masses are degenerate and can be produced via  $W_R$  boson production and decay in 8 TeV pp collisions. In this case, the electron and muon results can be combined as shown in Fig. 5. The  $(M_{W_R}, M_{N_\ell})$  exclusion for the combination extends slightly further than the single-channel exclusion limits, with an observed (expected) exclusion for the combined channel of  $M_{W_R} < 3.01$  (3.10) TeV for  $M_{N_\ell} = \frac{1}{2}M_{W_R}$ .

## 8 Summary

A search for right-handed bosons ( $W_R$ ) and heavy right-handed neutrinos ( $N_\ell$ ) in the left-right symmetric extension of the standard model has been presented. The data sample is in agreement with expectations from standard model processes in the  $\mu\mu jj$  final state. An excess is observed in the electron channel with a local significance of  $2.8\sigma$  at  $M_{eejj} \approx 2.1$  TeV. The excess does not appear to be consistent with expectations from left-right symmetric theory. Considering  $W_R \rightarrow eN_e$  and  $W_R \rightarrow \mu N_\mu$  searches separately, regions in the  $(M_{W_R}, M_{N_\ell})$  mass space are excluded at 95% confidence level that extend up to  $M_{W_R} < 3.0$  TeV for both channels. Assuming  $W_R \rightarrow \ell N_\ell$  with degenerate  $N_\ell$  mass for  $\ell = e, \mu$ ,  $W_R$  boson production is excluded at 95%

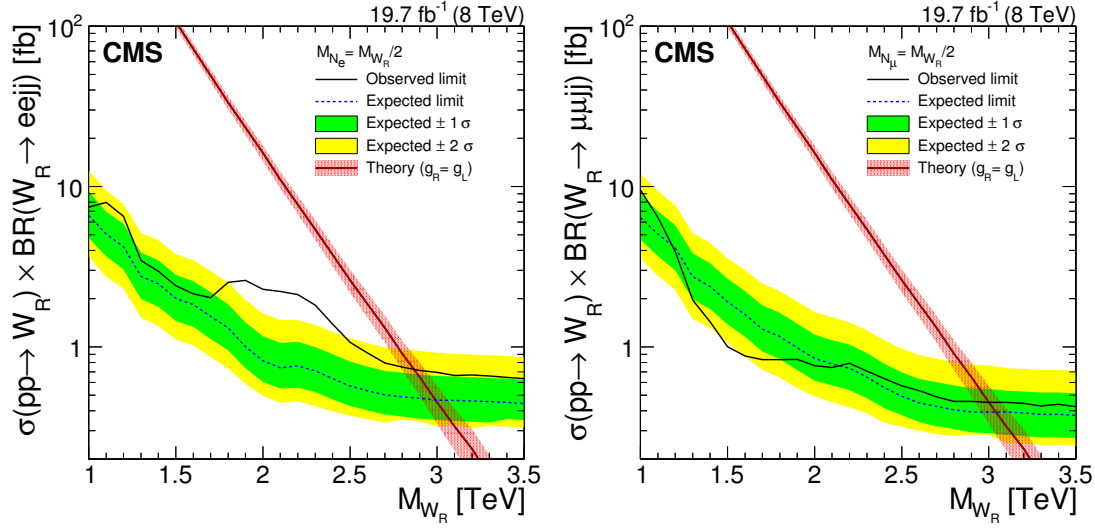


Figure 4: The 95% CL exclusion for  $W_R$  boson production cross section times branching fraction, computed as a function of  $M_{W_R}$  assuming the right-handed neutrino has half the mass of the  $W_R$  boson, for the electron (left) and muon (right) channels. The signal cross section PDF uncertainties (red band surrounding the theoretical  $W_R$ -boson production cross section curve) are included for illustration purposes only.

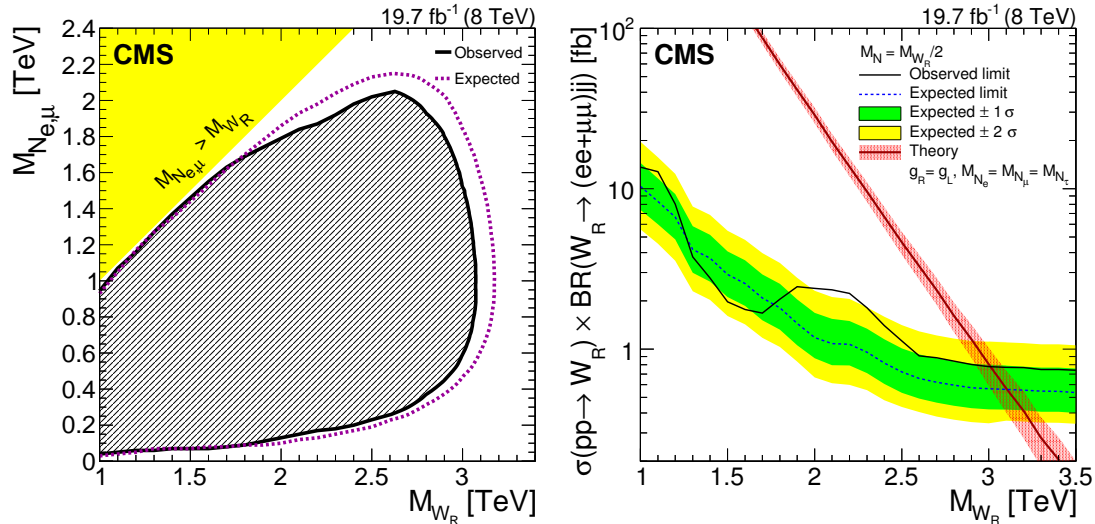


Figure 5: The 95% CL exclusion region in the  $(M_{W_R}, M_{N_\ell})$  plane (left), and as a function of  $W_R$  boson mass with  $M_N = \frac{1}{2}M_{W_R}$  (right) obtained combining the electron and muon channels. The signal cross section PDF uncertainties (red band surrounding the theoretical  $W_R$ -boson production cross section curve) are included for illustration purposes only. Neutrino masses greater than  $M_{W_R}$  (yellow shaded region in the left figure) are not considered in this search.

confidence level up to  $M_{W_R} < 3.0$  TeV. This search has significantly extended the exclusion region in the two-dimensional  $(M_{W_R}, M_{N_\ell})$  mass plane compared to previous searches, and for the first time this search has excluded  $M_{W_R}$  values beyond the theoretical lower mass limit of  $M_{W_R} \gtrsim 2.5$  TeV.

## Acknowledgments

We congratulate our colleagues in the CERN accelerator departments for the excellent performance of the LHC and thank the technical and administrative staffs at CERN and at other CMS institutes for their contributions to the success of the CMS effort. In addition, we gratefully acknowledge the computing centres and personnel of the Worldwide LHC Computing Grid for delivering so effectively the computing infrastructure essential to our analyses. Finally, we acknowledge the enduring support for the construction and operation of the LHC and the CMS detector provided by the following funding agencies: BMWFW and FWF (Austria); FNRS and FWO (Belgium); CNPq, CAPES, FAPERJ, and FAPESP (Brazil); MES (Bulgaria); CERN; CAS, MoST, and NSFC (China); COLCIENCIAS (Colombia); MSES and CSF (Croatia); RPF (Cyprus); MoER, ERC IUT and ERDF (Estonia); Academy of Finland, MEC, and HIP (Finland); CEA and CNRS/IN2P3 (France); BMBF, DFG, and HGF (Germany); GSRT (Greece); OTKA and NIH (Hungary); DAE and DST (India); IPM (Iran); SFI (Ireland); INFN (Italy); NRF and WCU (Republic of Korea); LAS (Lithuania); MOE and UM (Malaysia); CINVESTAV, CONACYT, SEP, and UASLP-FAI (Mexico); MBIE (New Zealand); PAEC (Pakistan); MSHE and NSC (Poland); FCT (Portugal); JINR (Dubna); MON, RosAtom, RAS and RFBR (Russia); MESTD (Serbia); SEIDI and CPAN (Spain); Swiss Funding Agencies (Switzerland); MST (Taipei); ThEPCenter, IPST, STAR and NSTDA (Thailand); TUBITAK and TAEK (Turkey); NASU and SFFR (Ukraine); STFC (United Kingdom); DOE and NSF (USA).

Individuals have received support from the Marie-Curie programme and the European Research Council and EPLANET (European Union); the Leventis Foundation; the A. P. Sloan Foundation; the Alexander von Humboldt Foundation; the Belgian Federal Science Policy Office; the Fonds pour la Formation à la Recherche dans l'Industrie et dans l'Agriculture (FRIA-Belgium); the Agentschap voor Innovatie door Wetenschap en Technologie (IWT-Belgium); the Ministry of Education, Youth and Sports (MEYS) of the Czech Republic; the Council of Science and Industrial Research, India; the HOMING PLUS programme of Foundation for Polish Science, cofinanced from European Union, Regional Development Fund; the Compagnia di San Paolo (Torino); the Consorzio per la Fisica (Trieste); MIUR project 20108T4XTM (Italy); the Thalys and Aristeia programmes cofinanced by EU-ESF and the Greek NSRF; and the National Priorities Research Program by Qatar National Research Fund.

## References

- [1] S. L. Glashow, "Partial-symmetries of weak interactions", *Nucl. Phys.* **22** (1961) 579, doi:10.1016/0029-5582(61)90469-2.
- [2] S. Weinberg, "A Model of Leptons", *Phys. Rev. Lett.* **19** (1967) 1264, doi:10.1103/PhysRevLett.19.1264.
- [3] A. Salam, "Weak and electromagnetic interactions", in *Elementary particle physics: relativistic groups and analyticity*, N. Svartholm, ed., p. 367. Almqvist & Wiskell, 1968. Proceedings of the eighth Nobel symposium.

- [4] J. C. Pati and A. Salam, "Lepton number as the fourth 'color'", *Phys. Rev. D* **10** (1974) 275, doi:10.1103/PhysRevD.10.275.
- [5] R. N. Mohapatra and J. C. Pati, "A Natural Left-Right Symmetry", *Phys. Rev. D* **11** (1975) 2558, doi:10.1103/PhysRevD.11.2558.
- [6] G. Senjanović and R. N. Mohapatra, "Exact left-right symmetry and spontaneous violation of parity", *Phys. Rev. D* **12** (1975) 1502, doi:10.1103/PhysRevD.12.1502.
- [7] W.-Y. Keung and G. Senjanović, "Majorana Neutrinos and the Production of the Right-Handed Charged Gauge Boson", *Phys. Rev. Lett.* **50** (1983) 1427, doi:10.1103/PhysRevLett.50.1427.
- [8] W. M. Alberico and S. M. Bilenky, "Neutrino Oscillations, Masses and Mixing", *Phys. Part. Nucl.* **35** (2003) 297, arXiv:hep-ph/0306239.
- [9] C. Giunti and M. Laveder, "Neutrino mixing", in *Developments in Quantum Physics – 2004*, F. Columbus and V. Krasnoholovets, eds. Nova Science Publishers, Inc., 2003. arXiv:hep-ph/0310238.
- [10] Particle Data Group, J. Beringer et al., "Review of Particle Physics", *Phys. Rev. D* **86** (2012) 010001, doi:10.1103/PhysRevD.86.010001.
- [11] R. N. Mohapatra and G. Senjanović, "Neutrino Mass and Spontaneous Parity Nonconservation", *Phys. Rev. Lett.* **44** (1980) 912, doi:10.1103/PhysRevLett.44.912.
- [12] M. Gell-Mann, P. Ramond, and R. Slansky, "Complex Spinors and Unified Theories", in *Supergravity*, P. van Nieuwenhuizen and D. Z. Freedman, eds. North Holland Publishing Co., 1979. arXiv:1306.4669.
- [13] CMS Collaboration, "Search for heavy neutrinos and  $W_R$  bosons with right-handed couplings in a left-right symmetric model in pp collisions at  $\sqrt{s} = 7\text{ TeV}$ ", *Phys. Rev. Lett.* **109** (2012) 261802, doi:10.1103/PhysRevLett.109.261802, arXiv:1210.2402.
- [14] R. Gavin, Y. Li, F. Petriello, and S. Quackenbush, "FEWZ 2.0: A code for hadronic Z production at next-to-next-to-leading order", *Comput. Phys. Commun.* **182** (2011) 2388, doi:10.1016/j.cpc.2011.06.008, arXiv:1011.3540.
- [15] R. Hamberg, W. van Neerven, and T. Matsuura, "A complete calculation of the order  $\alpha_s^2$  correction to the Drell-Yan K-factor", *Nucl. Phys. B* **359** (1991) 343, doi:10.1016/0550-3213(91)90064-5. See also the erratum at doi:10.1016/S0550-3213(02)00814-3.
- [16] E. Nardi, E. Roulet, and D. Tommasini, "New Neutral Gauge Bosons and New Heavy Fermions in the Light of the New LEP Data", *Phys. Lett. B* **344** (1995) 225, doi:10.1016/0370-2693(95)91542-M, arXiv:hep-ph/9409310.
- [17] G. Beall, M. Bander, and A. Soni, "Constraint on the Mass Scale of a Left-Right-Symmetric Electroweak Theory from the  $K_L - K_S$  Mass Difference", *Phys. Rev. Lett.* **48** (1982) 848, doi:10.1103/PhysRevLett.48.848.
- [18] A. Maiezza, M. Nemevšek, F. Nesti, and G. Senjanović, "Left-right symmetry at LHC", *Phys. Rev. D* **82** (2010) 055022, doi:10.1103/PhysRevD.82.055022, arXiv:1005.5160.



- [19] ATLAS Collaboration, "Search for  $t\bar{b}$  resonances in proton-proton collisions at  $\sqrt{s} = 7$  TeV with the ATLAS detector", *Phys. Rev. Lett.* **109** (2012) 081801, doi:10.1103/PhysRevLett.109.081801, arXiv:1205.1016.
- [20] CMS Collaboration, "Search for a  $W'$  boson decaying to a bottom quark and a top quark in pp collisions at  $\sqrt{s} = 7$  TeV", *Phys. Lett. B* **718** (2013) 1229, doi:10.1016/j.physletb.2012.12.008, arXiv:1208.0956.
- [21] CMS Collaboration, "Search for  $W' \rightarrow t\bar{b}$  decays in the lepton+jets final state at  $\sqrt{s} = 8$  TeV", *JHEP* **1405** (2014) 108, doi:10.1007/JHEP05(2014)108, arXiv:1402.2176.
- [22] ATLAS Collaboration, "Search for heavy neutrinos and right-handed  $W$  bosons in events with two leptons and jets in pp collisions at  $\sqrt{s} = 7$  TeV with the ATLAS detector", *Eur. Phys. J. C* **72** (2012) 2056, doi:10.1140/epjc/s10052-012-2056-4, arXiv:1203.5420.
- [23] CMS Collaboration, "The CMS experiment at the CERN LHC", *JINST* **03** (2008) S08004, doi:10.1088/1748-0221/3/08/S08004.
- [24] CMS Collaboration, "Commissioning of the Particle-Flow Event Reconstruction with the first LHC collisions recorded in the CMS detector", CMS Physics Analysis Summary CMS-PAS-PFT-10-001, 2010.
- [25] CMS Collaboration, "Particle-Flow Event Reconstruction in CMS and Performance for Jets, Taus, and MET", CMS Physics Analysis Summary CMS-PAS-PFT-09-001, 2009.
- [26] T. Sjöstrand, S. Mrenna, and P. Skands, "PYTHIA 6.4 physics and manual", *JHEP* **05** (2006) 026, doi:10.1088/1126-6708/2006/05/026, arXiv:hep-ph/0603175.
- [27] J. Botts et al., "CTEQ parton distributions and flavor dependence of sea quarks", *Phys. Lett. B* **304** (1993) 159, doi:10.1016/0370-2693(93)91416-K, arXiv:hep-ph/9303255.
- [28] R. Field, "Early LHC Underlying Event Data - Findings and Surprises", (2010). arXiv:1010.3558.
- [29] J. Alwall et al., "The automated computation of tree-level and next-to-leading order differential cross sections, and their matching to parton shower simulations", (2014). arXiv:1405.0301.
- [30] T. Gleisberg et al., "Event generation with SHERPA 1.1", *JHEP* **02** (2009) 007, doi:10.1088/1126-6708/2009/02/007, arXiv:0811.4622.
- [31] P. Nason, "A New method for combining NLO QCD with shower Monte Carlo algorithms", *JHEP* **11** (2004) 040, doi:10.1088/1126-6708/2004/11/040, arXiv:hep-ph/0409146.
- [32] S. Frixione, P. Nason, and C. Oleari, "Matching NLO QCD computations with Parton Shower simulations: the POWHEG method", *JHEP* **11** (2007) 070, doi:10.1088/1126-6708/2007/11/070, arXiv:0709.2092.
- [33] S. Alioli, P. Nason, C. Oleari, and E. Re, "A general framework for implementing NLO calculations in shower Monte Carlo programs: the POWHEG BOX", *JHEP* **06** (2010) 043, doi:10.1007/JHEP06(2010)043, arXiv:1002.2581.

- [34] E. Re, “Single-top Wt-channel production matched with parton showers using the POWHEG method”, *Eur. Phys. J. C* **71** (2011) 1547, doi:10.1140/epjc/s10052-011-1547-z, arXiv:1009.2450.
- [35] GEANT4 Collaboration, “GEANT4—a simulation toolkit”, *Nucl. Instrum. Meth. A* **506** (2003) 250, doi:10.1016/S0168-9002(03)01368-8.
- [36] CMS Collaboration, “Search for narrow resonances in dilepton mass spectra in pp collisions at  $\sqrt{s} = 7$  TeV”, *Phys. Lett. B* **714** (2012) 158, doi:10.1016/j.physletb.2012.06.051.
- [37] CMS Collaboration, “Performance of CMS muon reconstruction in pp collision events at  $\sqrt{s} = 7$  TeV”, *J. Instrum.* **7** (2012) P10002, doi:10.1088/1748-0221/7/10/P10002.
- [38] CMS Collaboration, “Electron Reconstruction and Identification at  $\sqrt{s} = 7$  TeV”, CMS Physics Analysis Summary CMS-PAS-EGM-10-004, 2010.
- [39] CMS Collaboration, “Search for heavy narrow dilepton resonances in pp collisions at  $\sqrt{s} = 7$  TeV and  $\sqrt{s} = 8$  TeV”, *Phys. Lett. B* **720** (2012) 63, doi:10.1016/j.physletb.2013.02.003.
- [40] M. Cacciari and G. P. Salam, “Pileup subtraction using jet areas”, *Phys. Lett. B* **659** (2008) 119, doi:10.1016/j.physletb.2007.09.077, arXiv:0707.1378.
- [41] M. Cacciari, G. P. Salam, and G. Soyez, “The anti- $k_t$  jet clustering algorithm”, *JHEP* **04** (2008) 063, doi:10.1088/1126-6708/2008/04/063, arXiv:0802.1189.
- [42] M. Cacciari, G. P. Salam, and G. Soyez, “The Catchment Area of Jets”, *JHEP* **04** (2008) 005, doi:10.1088/1126-6708/2008/04/005, arXiv:0802.1188.
- [43] CMS Collaboration, “Jet Performance in pp Collisions at  $\sqrt{s} = 7$  TeV”, CMS Physics Analysis Summary CMS-PAS-JME-10-003, 2010.
- [44] CMS Collaboration, “Determination of jet energy calibration and transverse momentum resolution in CMS”, *J. Instrum.* **6** (2011) P11002, doi:10.1088/1748-0221/6/11/P11002.
- [45] CMS Collaboration, “Performance of b tagging at  $\sqrt{s} = 8$  TeV in multijet,  $t\bar{t}$  and boosted topology events”, CMS Physics Analysis Summary CMS-PAS-BTV-13-001, 2013.
- [46] J. M. Campbell, R. K. Ellis, and C. Williams, “Vector boson pair production at the LHC”, *JHEP* **07** (2011) 018, doi:10.1007/JHEP07(2011)018, arXiv:1105.0020.
- [47] N. Kidonakis, “Differential and total cross sections for top pair and single top production”, (2012). arXiv:1205.3453.
- [48] A. L. Read, “Presentation of search results: the  $CL_s$  technique”, *J. Phys. G* **28** (2002) 2693, doi:10.1088/0954-3899/28/10/313.
- [49] T. Junk, “Confidence level computation for combining searches with small statistics”, *Nucl. Instrum. Meth. A* **434** (1999) 435, doi:10.1016/S0168-9002(99)00498-2, arXiv:hep-ex/9902006.
- [50] L. Moneta et al., “The RooStats Project”, in *13<sup>th</sup> International Workshop on Advanced Computing and Analysis Techniques in Physics Research*. SISSA, 2010. arXiv:1009.1003.

- 
- [51] PDF4LHC Working Group, “PDF4LHC Recommendations”, (2011).  
arXiv:1101.0536.
- [52] PDF4LHC Working Group, “The PDF4LHC Working Group Interim Recommendations”, (2011). arXiv:1101.0538.
- [53] H.-L. Lai et al., “New parton distributions for collider physics”, *Phys. Rev. D* **82** (2010) 074024, doi:10.1103/PhysRevD.82.074024, arXiv:1007.2241.
- [54] A. D. Martin, W. J. Stirling, R. S. Thorne, and G. Watt, “Uncertainties on  $\alpha_s$  in global PDF analyses and implications for predicted hadronic cross sections”, *Eur. Phys. J. C* **64** (2009) 653, doi:10.1140/epjc/s10052-009-1164-2, arXiv:0905.3531.
- [55] NNPDF Collaboration, “Unbiased global determination of parton distributions and their uncertainties at NNLO and at LO”, *Nucl. Phys. B* **855** (2012) 153, doi:10.1016/j.nuclphysb.2011.09.024, arXiv:1107.2652.

**A 95% CL exclusion limits as a function of  $W_R$  and  $N_\ell$  mass (tabular format)**

Table A1: The 95% CL observed (Obs.) and expected (Exp.) exclusion limits (in fb) on the  $W_R$  production cross section times branching fraction for  $W_R \rightarrow eejj$  as a function of  $W_R$  and  $N_e$  mass (in GeV) for  $1000 \leq M_{W_R} \leq 1600$  GeV. The signal acceptance (Acc.) is also included for each  $(M_{W_R}, M_{N_e})$  entry.

$M_{W_R}$	$M_{N_e}$	Obs.	Exp.	Acc.	$M_{W_R}$	$M_{N_e}$	Obs.	Exp.	Acc.
1000	100	65.7	58.5	$0.073 \pm 0.110$	1400	100	60.1	50.2	$0.043 \pm 0.164$
1000	200	14.6	13.0	$0.298 \pm 0.031$	1400	200	9.07	7.57	$0.241 \pm 0.061$
1000	300	9.77	8.69	$0.447 \pm 0.014$	1400	300	4.91	4.09	$0.428 \pm 0.027$
1000	400	8.17	7.27	$0.549 \pm 0.011$	1400	400	3.76	3.13	$0.549 \pm 0.015$
1000	500	7.44	6.63	$0.596 \pm 0.009$	1400	500	3.29	2.75	$0.630 \pm 0.011$
1000	600	7.14	6.35	$0.620 \pm 0.009$	1400	600	3.09	2.58	$0.688 \pm 0.010$
1000	700	7.16	6.38	$0.617 \pm 0.009$	1400	700	2.97	2.48	$0.711 \pm 0.011$
1000	800	7.71	6.86	$0.573 \pm 0.009$	1400	800	2.89	2.41	$0.729 \pm 0.009$
1000	900	10.2	9.05	$0.435 \pm 0.010$	1400	900	2.89	2.41	$0.729 \pm 0.009$
1100	100	97.0	61.6	$0.062 \pm 0.124$	1400	1000	2.90	2.42	$0.725 \pm 0.009$
1100	200	17.6	11.2	$0.290 \pm 0.038$	1400	1100	2.96	2.47	$0.712 \pm 0.009$
1100	300	10.3	6.56	$0.441 \pm 0.016$	1400	1200	3.17	2.64	$0.664 \pm 0.009$
1100	400	8.61	5.47	$0.548 \pm 0.011$	1400	1300	3.77	3.15	$0.558 \pm 0.010$
1100	500	8.05	5.11	$0.609 \pm 0.010$	1500	100	59.4	49.4	$0.038 \pm 0.176$
1100	600	7.69	4.89	$0.655 \pm 0.010$	1500	200	8.23	6.86	$0.221 \pm 0.070$
1100	700	7.59	4.82	$0.663 \pm 0.009$	1500	300	3.97	3.31	$0.411 \pm 0.031$
1100	800	7.82	4.96	$0.644 \pm 0.010$	1500	400	3.00	2.50	$0.545 \pm 0.017$
1100	900	8.30	5.27	$0.606 \pm 0.009$	1500	500	2.64	2.20	$0.625 \pm 0.012$
1100	1000	10.6	6.75	$0.473 \pm 0.010$	1500	600	2.49	2.07	$0.686 \pm 0.010$
1200	100	91.5	59.2	$0.052 \pm 0.139$	1500	700	2.41	2.01	$0.716 \pm 0.010$
1200	200	16.2	10.5	$0.275 \pm 0.045$	1500	800	2.37	1.98	$0.739 \pm 0.011$
1200	300	9.76	6.32	$0.442 \pm 0.019$	1500	900	2.35	1.95	$0.746 \pm 0.009$
1200	400	7.81	5.05	$0.556 \pm 0.012$	1500	1000	2.32	1.93	$0.755 \pm 0.009$
1200	500	6.98	4.52	$0.627 \pm 0.010$	1500	1100	2.37	1.97	$0.739 \pm 0.009$
1200	600	6.53	4.23	$0.671 \pm 0.009$	1500	1200	2.46	2.05	$0.711 \pm 0.009$
1200	700	6.39	4.14	$0.684 \pm 0.009$	1500	1300	2.59	2.16	$0.675 \pm 0.009$
1200	800	6.36	4.12	$0.687 \pm 0.009$	1500	1400	3.06	2.55	$0.573 \pm 0.009$
1200	900	6.48	4.20	$0.674 \pm 0.009$	1600	100	58.8	50.4	$0.033 \pm 0.187$
1200	1000	6.98	4.52	$0.626 \pm 0.009$	1600	200	8.08	6.93	$0.212 \pm 0.078$
1200	1100	8.71	5.64	$0.502 \pm 0.009$	1600	300	3.91	3.35	$0.402 \pm 0.036$
1300	100	61.7	49.2	$0.047 \pm 0.152$	1600	400	2.89	2.48	$0.536 \pm 0.019$
1300	200	9.48	7.55	$0.254 \pm 0.054$	1600	500	2.49	2.13	$0.627 \pm 0.017$
1300	300	4.99	3.97	$0.446 \pm 0.023$	1600	600	2.27	1.95	$0.680 \pm 0.010$
1300	400	3.95	3.14	$0.558 \pm 0.013$	1600	700	2.21	1.89	$0.723 \pm 0.009$
1300	500	3.60	2.86	$0.635 \pm 0.010$	1600	800	2.14	1.84	$0.747 \pm 0.010$
1300	600	3.46	2.76	$0.684 \pm 0.010$	1600	900	2.10	1.80	$0.760 \pm 0.009$
1300	700	3.41	2.72	$0.699 \pm 0.009$	1600	1000	2.09	1.79	$0.763 \pm 0.009$
1300	800	3.32	2.65	$0.716 \pm 0.009$	1600	1100	2.10	1.80	$0.761 \pm 0.009$
1300	900	3.35	2.67	$0.710 \pm 0.009$	1600	1200	2.13	1.83	$0.749 \pm 0.009$
1300	1000	3.41	2.72	$0.698 \pm 0.009$	1600	1300	2.18	1.87	$0.732 \pm 0.009$
1300	1100	3.66	2.92	$0.650 \pm 0.009$	1600	1400	2.30	1.97	$0.695 \pm 0.012$
1300	1200	4.43	3.53	$0.536 \pm 0.009$	1600	1500	2.70	2.31	$0.592 \pm 0.009$

Table A2: The 95% CL observed (Obs.) and expected (Exp.) exclusion limits (in fb) on the  $W_R$  production cross section times branching fraction for  $W_R \rightarrow eejj$  as a function of  $W_R$  and  $N_e$  mass (in GeV) for  $1700 \leq M_{W_R} \leq 2000$  GeV. The signal acceptance (Acc.) is also included for each  $(M_{W_R}, M_{N_e})$  entry.

$M_{W_R}$	$M_{N_e}$	Obs.	Exp.	Acc.	$M_{W_R}$	$M_{N_e}$	Obs.	Exp.	Acc.
1700	100	76.5	58.3	$0.032 \pm 0.197$	1900	100	131	50.7	$0.025 \pm 0.216$
1700	200	9.12	6.95	$0.195 \pm 0.086$	1900	200	14.3	5.51	$0.161 \pm 0.103$
1700	300	3.87	2.95	$0.383 \pm 0.040$	1900	300	5.83	2.25	$0.348 \pm 0.055$
1700	400	2.71	2.07	$0.526 \pm 0.022$	1900	400	3.91	1.51	$0.502 \pm 0.028$
1700	500	2.30	1.75	$0.616 \pm 0.015$	1900	500	3.23	1.25	$0.605 \pm 0.025$
1700	600	2.14	1.63	$0.676 \pm 0.011$	1900	600	2.89	1.12	$0.674 \pm 0.013$
1700	700	2.09	1.59	$0.719 \pm 0.010$	1900	700	2.74	1.06	$0.715 \pm 0.011$
1700	800	2.02	1.54	$0.751 \pm 0.011$	1900	800	2.67	1.03	$0.747 \pm 0.010$
1700	900	2.00	1.52	$0.767 \pm 0.009$	1900	900	2.61	1.01	$0.769 \pm 0.009$
1700	1000	1.98	1.51	$0.774 \pm 0.009$	1900	1000	2.56	0.987	$0.782 \pm 0.011$
1700	1100	1.97	1.50	$0.776 \pm 0.009$	1900	1100	2.55	0.983	$0.784 \pm 0.011$
1700	1200	1.98	1.51	$0.770 \pm 0.009$	1900	1200	2.54	0.980	$0.787 \pm 0.009$
1700	1300	2.01	1.53	$0.762 \pm 0.011$	1900	1300	2.53	0.978	$0.788 \pm 0.009$
1700	1400	2.07	1.58	$0.739 \pm 0.009$	1900	1400	2.54	0.979	$0.787 \pm 0.009$
1700	1500	2.18	1.66	$0.702 \pm 0.009$	1900	1500	2.60	1.00	$0.770 \pm 0.009$
1700	1600	2.51	1.91	$0.609 \pm 0.010$	1900	1600	2.64	1.02	$0.756 \pm 0.009$
1800	100	105	54.5	$0.027 \pm 0.207$	1900	1700	2.79	1.08	$0.715 \pm 0.009$
1800	200	13.0	6.74	$0.178 \pm 0.095$	1900	1800	3.19	1.23	$0.626 \pm 0.010$
1800	300	5.61	2.91	$0.363 \pm 0.045$	2000	100	139	49.5	$0.023 \pm 0.225$
1800	400	3.86	2.00	$0.514 \pm 0.026$	2000	200	15.7	5.62	$0.150 \pm 0.110$
1800	500	3.14	1.63	$0.605 \pm 0.016$	2000	300	6.08	2.17	$0.328 \pm 0.056$
1800	600	2.82	1.46	$0.671 \pm 0.012$	2000	400	3.87	1.38	$0.483 \pm 0.031$
1800	700	2.66	1.38	$0.720 \pm 0.010$	2000	500	3.03	1.08	$0.593 \pm 0.020$
1800	800	2.56	1.33	$0.748 \pm 0.009$	2000	600	2.66	0.952	$0.665 \pm 0.014$
1800	900	2.53	1.31	$0.765 \pm 0.009$	2000	700	2.50	0.892	$0.709 \pm 0.011$
1800	1000	2.49	1.29	$0.776 \pm 0.009$	2000	800	2.38	0.850	$0.743 \pm 0.010$
1800	1100	2.46	1.28	$0.784 \pm 0.015$	2000	900	2.33	0.832	$0.766 \pm 0.009$
1800	1200	2.46	1.28	$0.784 \pm 0.009$	2000	1000	2.29	0.820	$0.784 \pm 0.009$
1800	1300	2.47	1.28	$0.783 \pm 0.009$	2000	1100	2.27	0.811	$0.791 \pm 0.009$
1800	1400	2.51	1.30	$0.769 \pm 0.009$	2000	1200	2.24	0.800	$0.802 \pm 0.009$
1800	1500	2.58	1.34	$0.749 \pm 0.010$	2000	1300	2.23	0.798	$0.803 \pm 0.009$
1800	1600	2.73	1.41	$0.709 \pm 0.015$	2000	1400	2.25	0.805	$0.796 \pm 0.009$
1800	1700	3.15	1.63	$0.613 \pm 0.009$	2000	1500	2.27	0.812	$0.789 \pm 0.009$
					2000	1600	2.30	0.822	$0.779 \pm 0.009$
					2000	1700	2.35	0.838	$0.764 \pm 0.009$
					2000	1800	2.49	0.889	$0.720 \pm 0.011$
					2000	1900	2.84	1.02	$0.631 \pm 0.010$

Table A3: The 95% CL observed (Obs.) and expected (Exp.) exclusion limits (in fb) on the  $W_R$  production cross section times branching fraction for  $W_R \rightarrow eejj$  as a function of  $W_R$  and  $N_e$  mass (in GeV) for  $2100 \leq M_{W_R} \leq 2300$  GeV. The signal acceptance (Acc.) is also included for each  $(M_{W_R}, M_{N_e})$  entry.

$M_{W_R}$	$M_{N_e}$	Obs.	Exp.	Acc.	$M_{W_R}$	$M_{N_e}$	Obs.	Exp.	Acc.
2100	100	173	57.8	$0.024 \pm 0.233$	2300	100	158	61.5	$0.022 \pm 0.251$
2100	200	18.1	6.07	$0.142 \pm 0.117$	2300	200	15.5	6.00	$0.134 \pm 0.133$
2100	300	6.94	2.32	$0.315 \pm 0.061$	2300	300	5.76	2.24	$0.297 \pm 0.072$
2100	400	4.26	1.42	$0.469 \pm 0.034$	2300	400	3.42	1.33	$0.438 \pm 0.042$
2100	500	3.25	1.09	$0.586 \pm 0.021$	2300	500	2.62	1.02	$0.554 \pm 0.026$
2100	600	2.77	0.927	$0.657 \pm 0.015$	2300	600	2.26	0.879	$0.651 \pm 0.018$
2100	700	2.52	0.843	$0.710 \pm 0.012$	2300	700	2.06	0.798	$0.691 \pm 0.014$
2100	800	2.38	0.796	$0.745 \pm 0.010$	2300	800	1.96	0.759	$0.736 \pm 0.011$
2100	900	2.29	0.767	$0.759 \pm 0.010$	2300	900	1.90	0.738	$0.760 \pm 0.010$
2100	1000	2.24	0.750	$0.785 \pm 0.009$	2300	1000	1.85	0.716	$0.779 \pm 0.010$
2100	1100	2.21	0.738	$0.791 \pm 0.009$	2300	1100	1.82	0.704	$0.793 \pm 0.010$
2100	1200	2.19	0.732	$0.797 \pm 0.011$	2300	1200	1.81	0.703	$0.801 \pm 0.012$
2100	1300	2.16	0.724	$0.806 \pm 0.011$	2300	1300	1.79	0.695	$0.809 \pm 0.032$
2100	1400	2.17	0.726	$0.802 \pm 0.011$	2300	1400	1.78	0.691	$0.813 \pm 0.009$
2100	1500	2.18	0.728	$0.800 \pm 0.009$	2300	1500	1.78	0.689	$0.815 \pm 0.009$
2100	1600	2.20	0.734	$0.793 \pm 0.009$	2300	1600	1.78	0.692	$0.812 \pm 0.009$
2100	1700	2.24	0.748	$0.779 \pm 0.011$	2300	1700	1.80	0.697	$0.806 \pm 0.010$
2100	1800	2.29	0.767	$0.759 \pm 0.010$	2300	1800	1.81	0.701	$0.801 \pm 0.030$
2100	1900	2.39	0.801	$0.727 \pm 0.009$	2300	1900	1.83	0.711	$0.790 \pm 0.010$
2100	2000	2.71	0.906	$0.643 \pm 0.010$	2300	2000	1.89	0.734	$0.765 \pm 0.009$
2200	100	161	57.9	$0.024 \pm 0.242$	2300	2100	1.98	0.767	$0.732 \pm 0.013$
2200	200	17.3	6.23	$0.135 \pm 0.125$	2300	2200	2.21	0.856	$0.656 \pm 0.011$
2200	300	6.67	2.40	$0.300 \pm 0.067$					
2200	400	4.17	1.50	$0.459 \pm 0.038$					
2200	500	3.23	1.16	$0.568 \pm 0.023$					
2200	600	2.75	0.990	$0.647 \pm 0.016$					
2200	700	2.48	0.894	$0.704 \pm 0.013$					
2200	800	2.33	0.838	$0.735 \pm 0.012$					
2200	900	2.24	0.804	$0.765 \pm 0.011$					
2200	1000	2.17	0.780	$0.784 \pm 0.009$					
2200	1100	2.12	0.763	$0.793 \pm 0.010$					
2200	1200	2.10	0.757	$0.799 \pm 0.009$					
2200	1300	2.07	0.744	$0.812 \pm 0.009$					
2200	1400	2.10	0.754	$0.801 \pm 0.010$					
2200	1500	2.08	0.747	$0.808 \pm 0.010$					
2200	1600	2.08	0.749	$0.806 \pm 0.009$					
2200	1700	2.10	0.756	$0.798 \pm 0.009$					
2200	1800	2.13	0.768	$0.786 \pm 0.009$					
2200	1900	2.19	0.786	$0.768 \pm 0.009$					
2200	2000	2.30	0.826	$0.730 \pm 0.010$					
2200	2100	2.57	0.925	$0.653 \pm 0.030$					

Table A4: The 95% CL observed (Obs.) and expected (Exp.) exclusion limits (in fb) on the  $W_R$  production cross section times branching fraction for  $W_R \rightarrow eejj$  as a function of  $W_R$  and  $N_e$  mass (in GeV) for  $2400 \leq M_{W_R} \leq 2500$  GeV. The signal acceptance (Acc.) is also included for each  $(M_{W_R}, M_{N_e})$  entry.

$M_{W_R}$	$M_{N_e}$	Obs.	Exp.	Acc.	$M_{W_R}$	$M_{N_e}$	Obs.	Exp.	Acc.
2400	100	160	73.2	$0.025 \pm 0.262$	2500	100	157	83.8	$0.027 \pm 0.270$
2400	200	14.3	6.57	$0.127 \pm 0.139$	2500	200	13.6	7.27	$0.125 \pm 0.149$
2400	300	5.09	2.33	$0.278 \pm 0.078$	2500	300	4.63	2.47	$0.265 \pm 0.085$
2400	400	2.93	1.34	$0.429 \pm 0.060$	2500	400	2.60	1.39	$0.414 \pm 0.059$
2400	500	2.16	0.990	$0.548 \pm 0.028$	2500	500	1.82	0.972	$0.539 \pm 0.032$
2400	600	1.79	0.821	$0.634 \pm 0.019$	2500	600	1.50	0.800	$0.622 \pm 0.021$
2400	700	1.63	0.745	$0.691 \pm 0.015$	2500	700	1.32	0.705	$0.683 \pm 0.015$
2400	800	1.52	0.696	$0.732 \pm 0.012$	2500	800	1.22	0.651	$0.729 \pm 0.013$
2400	900	1.54	0.706	$0.757 \pm 0.011$	2500	900	1.15	0.613	$0.750 \pm 0.011$
2400	1000	1.49	0.683	$0.778 \pm 0.010$	2500	1000	1.12	0.598	$0.776 \pm 0.010$
2400	1100	1.43	0.654	$0.794 \pm 0.009$	2500	1100	1.09	0.581	$0.790 \pm 0.010$
2400	1200	1.39	0.636	$0.807 \pm 0.010$	2500	1200	1.08	0.574	$0.803 \pm 0.010$
2400	1300	1.38	0.630	$0.813 \pm 0.012$	2500	1300	1.07	0.569	$0.809 \pm 0.010$
2400	1400	1.38	0.631	$0.811 \pm 0.009$	2500	1400	1.06	0.565	$0.814 \pm 0.009$
2400	1500	1.37	0.629	$0.814 \pm 0.009$	2500	1500	1.05	0.560	$0.820 \pm 0.011$
2400	1600	1.37	0.626	$0.817 \pm 0.009$	2500	1600	1.04	0.555	$0.827 \pm 0.009$
2400	1700	1.37	0.626	$0.817 \pm 0.011$	2500	1700	1.06	0.563	$0.815 \pm 0.012$
2400	1800	1.38	0.634	$0.807 \pm 0.011$	2500	1800	1.06	0.565	$0.812 \pm 0.009$
2400	1900	1.39	0.638	$0.801 \pm 0.009$	2500	1900	1.06	0.563	$0.814 \pm 0.019$
2400	2000	1.41	0.646	$0.792 \pm 0.009$	2500	2000	1.07	0.569	$0.806 \pm 0.009$
2400	2100	1.44	0.660	$0.775 \pm 0.009$	2500	2100	1.08	0.576	$0.797 \pm 0.009$
2400	2200	1.51	0.693	$0.738 \pm 0.011$	2500	2200	1.12	0.594	$0.772 \pm 0.012$
2400	2300	1.69	0.772	$0.662 \pm 0.014$	2500	2300	1.16	0.620	$0.740 \pm 0.011$
					2500	2400	1.30	0.691	$0.664 \pm 0.011$



Table A5: The 95% CL observed (Obs.) and expected (Exp.) exclusion limits (in fb) on the  $W_R$  production cross section times branching fraction for  $W_R \rightarrow eejj$  as a function of  $W_R$  and  $N_e$  mass (in GeV) for  $2600 \leq M_{W_R} \leq 2700$  GeV. The signal acceptance (Acc.) is also included for each  $(M_{W_R}, M_{N_e})$  entry.

$M_{W_R}$	$M_{N_e}$	Obs.	Exp.	Acc.	$M_{W_R}$	$M_{N_e}$	Obs.	Exp.	Acc.
2600	100	148	86.1	$0.023 \pm 0.276$	2700	100	131	83.0	$0.026 \pm 0.288$
2600	200	13.9	8.07	$0.122 \pm 0.157$	2700	200	13.2	8.35	$0.127 \pm 0.165$
2600	300	4.60	2.67	$0.256 \pm 0.090$	2700	300	4.36	2.76	$0.257 \pm 0.098$
2600	400	2.46	1.43	$0.404 \pm 0.054$	2700	400	2.29	1.45	$0.394 \pm 0.059$
2600	500	1.71	0.993	$0.521 \pm 0.034$	2700	500	1.56	0.986	$0.513 \pm 0.037$
2600	600	1.37	0.794	$0.616 \pm 0.024$	2700	600	1.22	0.770	$0.613 \pm 0.025$
2600	700	1.19	0.689	$0.682 \pm 0.018$	2700	700	1.07	0.678	$0.674 \pm 0.018$
2600	800	1.09	0.632	$0.722 \pm 0.013$	2700	800	0.993	0.628	$0.719 \pm 0.015$
2600	900	1.03	0.596	$0.744 \pm 0.013$	2700	900	0.918	0.580	$0.748 \pm 0.012$
2600	1000	0.977	0.568	$0.771 \pm 0.010$	2700	1000	0.851	0.538	$0.774 \pm 0.012$
2600	1100	0.941	0.547	$0.783 \pm 0.010$	2700	1100	0.824	0.521	$0.785 \pm 0.011$
2600	1200	0.947	0.550	$0.803 \pm 0.010$	2700	1200	0.776	0.491	$0.799 \pm 0.010$
2600	1300	0.918	0.534	$0.807 \pm 0.010$	2700	1300	0.781	0.494	$0.810 \pm 0.009$
2600	1400	0.912	0.530	$0.812 \pm 0.010$	2700	1400	0.794	0.502	$0.814 \pm 0.010$
2600	1500	0.907	0.527	$0.816 \pm 0.012$	2700	1500	0.787	0.498	$0.820 \pm 0.014$
2600	1600	0.897	0.521	$0.825 \pm 0.011$	2700	1600	0.781	0.494	$0.826 \pm 0.014$
2600	1700	0.896	0.521	$0.825 \pm 0.019$	2700	1700	0.784	0.496	$0.823 \pm 0.034$
2600	1800	0.901	0.523	$0.821 \pm 0.010$	2700	1800	0.781	0.494	$0.826 \pm 0.016$
2600	1900	0.903	0.525	$0.819 \pm 0.011$	2700	1900	0.783	0.495	$0.823 \pm 0.010$
2600	2000	0.908	0.528	$0.814 \pm 0.010$	2700	2000	0.783	0.495	$0.823 \pm 0.010$
2600	2100	0.914	0.531	$0.808 \pm 0.011$	2700	2100	0.787	0.498	$0.819 \pm 0.016$
2600	2200	0.927	0.539	$0.797 \pm 0.017$	2700	2200	0.801	0.506	$0.805 \pm 0.011$
2600	2300	0.950	0.552	$0.778 \pm 0.009$	2700	2300	0.811	0.513	$0.795 \pm 0.013$
2600	2400	1.00	0.581	$0.739 \pm 0.010$	2700	2400	0.830	0.525	$0.776 \pm 0.009$
2600	2500	1.11	0.645	$0.666 \pm 0.013$	2700	2500	0.872	0.551	$0.739 \pm 0.010$
					2700	2600	0.954	0.603	$0.676 \pm 0.012$

Table A6: The 95% CL observed (Obs.) and expected (Exp.) exclusion limits (in fb) on the  $W_R$  production cross section times branching fraction for  $W_R \rightarrow eejj$  as a function of  $W_R$  and  $N_e$  mass (in GeV) for  $2800 \leq M_{W_R} \leq 2900$  GeV. The signal acceptance (Acc.) is also included for each  $(M_{W_R}, M_{N_e})$  entry.

$M_{W_R}$	$M_{N_e}$	Obs.	Exp.	Acc.	$M_{W_R}$	$M_{N_e}$	Obs.	Exp.	Acc.
2800	100	138	90.4	$0.028 \pm 0.300$	2900	100	136	91.3	$0.030 \pm 0.307$
2800	200	15.2	9.93	$0.130 \pm 0.175$	2900	200	16.8	11.2	$0.130 \pm 0.187$
2800	300	5.01	3.27	$0.255 \pm 0.108$	2900	300	5.42	3.62	$0.247 \pm 0.115$
2800	400	2.56	1.67	$0.385 \pm 0.064$	2900	400	2.71	1.81	$0.391 \pm 0.071$
2800	500	1.69	1.10	$0.507 \pm 0.041$	2900	500	1.74	1.16	$0.498 \pm 0.045$
2800	600	1.30	0.851	$0.601 \pm 0.027$	2900	600	1.32	0.880	$0.595 \pm 0.029$
2800	700	1.09	0.713	$0.666 \pm 0.020$	2900	700	1.10	0.735	$0.658 \pm 0.022$
2800	800	1.00	0.655	$0.708 \pm 0.015$	2900	800	0.966	0.646	$0.701 \pm 0.016$
2800	900	0.900	0.587	$0.739 \pm 0.012$	2900	900	0.882	0.590	$0.737 \pm 0.014$
2800	1000	0.851	0.556	$0.765 \pm 0.012$	2900	1000	0.830	0.555	$0.758 \pm 0.013$
2800	1100	0.814	0.531	$0.779 \pm 0.018$	2900	1100	0.790	0.528	$0.778 \pm 0.027$
2800	1200	0.785	0.512	$0.799 \pm 0.013$	2900	1200	0.761	0.509	$0.795 \pm 0.013$
2800	1300	0.762	0.497	$0.808 \pm 0.010$	2900	1300	0.737	0.493	$0.810 \pm 0.011$
2800	1400	0.751	0.490	$0.816 \pm 0.010$	2900	1400	0.721	0.482	$0.815 \pm 0.010$
2800	1500	0.743	0.485	$0.823 \pm 0.010$	2900	1500	0.714	0.478	$0.817 \pm 0.011$
2800	1600	0.738	0.482	$0.828 \pm 0.011$	2900	1600	0.706	0.472	$0.826 \pm 0.011$
2800	1700	0.735	0.480	$0.830 \pm 0.011$	2900	1700	0.705	0.472	$0.826 \pm 0.012$
2800	1800	0.736	0.480	$0.829 \pm 0.010$	2900	1800	0.698	0.467	$0.834 \pm 0.019$
2800	1900	0.738	0.481	$0.827 \pm 0.009$	2900	1900	0.699	0.468	$0.833 \pm 0.011$
2800	2000	0.739	0.482	$0.826 \pm 0.009$	2900	2000	0.698	0.467	$0.834 \pm 0.037$
2800	2100	0.740	0.483	$0.824 \pm 0.012$	2900	2100	0.710	0.475	$0.819 \pm 0.010$
2800	2200	0.750	0.489	$0.813 \pm 0.012$	2900	2200	0.706	0.472	$0.824 \pm 0.010$
2800	2300	0.757	0.494	$0.806 \pm 0.010$	2900	2300	0.712	0.476	$0.817 \pm 0.010$
2800	2400	0.764	0.498	$0.799 \pm 0.010$	2900	2400	0.718	0.480	$0.811 \pm 0.018$
2800	2500	0.783	0.511	$0.779 \pm 0.009$	2900	2500	0.727	0.486	$0.801 \pm 0.010$
2800	2600	0.821	0.536	$0.743 \pm 0.017$	2900	2600	0.748	0.500	$0.778 \pm 0.015$
2800	2700	0.898	0.586	$0.680 \pm 0.013$	2900	2700	0.782	0.523	$0.744 \pm 0.010$
					2900	2800	0.846	0.566	$0.688 \pm 0.016$

Table A7: The 95% CL observed (Obs.) and expected (Exp.) exclusion limits (in fb) on the  $W_R$  production cross section times branching fraction for  $W_R \rightarrow eejj$  as a function of  $W_R$  and  $N_e$  mass (in GeV) for  $3000 \leq M_{W_R} \leq 3100$  GeV. The signal acceptance (Acc.) is also included for each  $(M_{W_R}, M_{N_e})$  entry.

$M_{W_R}$	$M_{N_e}$	Obs.	Exp.	Acc.	$M_{W_R}$	$M_{N_e}$	Obs.	Exp.	Acc.
3000	100	134	90.2	$0.030 \pm 0.314$	3100	100	134	94.2	$0.036 \pm 0.318$
3000	200	18.8	12.6	$0.131 \pm 0.196$	3100	200	20.6	14.4	$0.145 \pm 0.204$
3000	300	5.90	3.96	$0.256 \pm 0.124$	3100	300	6.52	4.57	$0.261 \pm 0.136$
3000	400	2.94	1.97	$0.382 \pm 0.082$	3100	400	3.12	2.19	$0.387 \pm 0.089$
3000	500	1.86	1.25	$0.496 \pm 0.052$	3100	500	1.97	1.38	$0.489 \pm 0.057$
3000	600	1.37	0.923	$0.586 \pm 0.033$	3100	600	1.42	0.996	$0.578 \pm 0.037$
3000	700	1.13	0.756	$0.648 \pm 0.022$	3100	700	1.15	0.806	$0.646 \pm 0.028$
3000	800	0.984	0.661	$0.695 \pm 0.019$	3100	800	0.989	0.693	$0.695 \pm 0.018$
3000	900	0.891	0.598	$0.729 \pm 0.017$	3100	900	0.888	0.622	$0.733 \pm 0.019$
3000	1000	0.831	0.558	$0.765 \pm 0.013$	3100	1000	0.823	0.576	$0.752 \pm 0.013$
3000	1100	0.786	0.528	$0.779 \pm 0.017$	3100	1100	0.771	0.540	$0.774 \pm 0.012$
3000	1200	0.755	0.506	$0.790 \pm 0.013$	3100	1200	0.740	0.518	$0.792 \pm 0.028$
3000	1300	0.730	0.490	$0.799 \pm 0.018$	3100	1300	0.713	0.499	$0.803 \pm 0.020$
3000	1400	0.711	0.477	$0.813 \pm 0.012$	3100	1400	0.689	0.482	$0.813 \pm 0.033$
3000	1500	0.695	0.466	$0.825 \pm 0.010$	3100	1500	0.671	0.470	$0.815 \pm 0.010$
3000	1600	0.693	0.465	$0.826 \pm 0.015$	3100	1600	0.664	0.465	$0.827 \pm 0.010$
3000	1700	0.687	0.461	$0.833 \pm 0.009$	3100	1700	0.659	0.461	$0.833 \pm 0.010$
3000	1800	0.688	0.462	$0.831 \pm 0.011$	3100	1800	0.658	0.461	$0.833 \pm 0.010$
3000	1900	0.688	0.462	$0.831 \pm 0.022$	3100	1900	0.659	0.461	$0.832 \pm 0.013$
3000	2000	0.684	0.459	$0.836 \pm 0.011$	3100	2000	0.654	0.458	$0.838 \pm 0.017$
3000	2100	0.686	0.460	$0.833 \pm 0.010$	3100	2100	0.659	0.461	$0.831 \pm 0.024$
3000	2200	0.691	0.464	$0.827 \pm 0.040$	3100	2200	0.657	0.460	$0.834 \pm 0.018$
3000	2300	0.691	0.464	$0.826 \pm 0.011$	3100	2300	0.659	0.462	$0.830 \pm 0.011$
3000	2400	0.696	0.467	$0.821 \pm 0.013$	3100	2400	0.664	0.465	$0.825 \pm 0.011$
3000	2500	0.704	0.473	$0.811 \pm 0.015$	3100	2500	0.670	0.469	$0.817 \pm 0.011$
3000	2600	0.714	0.479	$0.800 \pm 0.009$	3100	2600	0.674	0.472	$0.813 \pm 0.009$
3000	2700	0.729	0.489	$0.784 \pm 0.010$	3100	2700	0.683	0.478	$0.801 \pm 0.010$
3000	2800	0.764	0.513	$0.747 \pm 0.011$	3100	2800	0.701	0.491	$0.781 \pm 0.012$
3000	2900	0.826	0.555	$0.691 \pm 0.013$	3100	2900	0.730	0.511	$0.750 \pm 0.010$
					3100	3000	0.789	0.553	$0.693 \pm 0.019$

Table A8: The 95% CL observed (Obs.) and expected (Exp.) exclusion limits (in fb) on the  $W_R$  production cross section times branching fraction for  $W_R \rightarrow eejj$  as a function of  $W_R$  and  $N_e$  mass (in GeV) for  $M_{W_R} = 3200$  GeV. The signal acceptance (Acc.) is also included for each  $(M_{W_R}, M_{N_e})$  entry.

$M_{W_R}$	$M_{N_e}$	Obs.	Exp.	Acc.
3200	100	139	95.7	$0.039 \pm 0.320$
3200	200	23.5	16.3	$0.147 \pm 0.210$
3200	300	7.35	5.08	$0.277 \pm 0.143$
3200	400	3.56	2.46	$0.391 \pm 0.096$
3200	500	2.19	1.51	$0.485 \pm 0.066$
3200	600	1.57	1.08	$0.574 \pm 0.041$
3200	700	1.25	0.861	$0.639 \pm 0.032$
3200	800	1.06	0.731	$0.690 \pm 0.022$
3200	900	0.936	0.646	$0.721 \pm 0.025$
3200	1000	0.860	0.594	$0.749 \pm 0.019$
3200	1100	0.804	0.555	$0.774 \pm 0.016$
3200	1200	0.760	0.524	$0.787 \pm 0.012$
3200	1300	0.731	0.504	$0.800 \pm 0.017$
3200	1400	0.705	0.487	$0.809 \pm 0.021$
3200	1500	0.684	0.472	$0.818 \pm 0.014$
3200	1600	0.669	0.462	$0.827 \pm 0.014$
3200	1700	0.667	0.461	$0.828 \pm 0.011$
3200	1800	0.662	0.457	$0.834 \pm 0.019$
3200	1900	0.661	0.456	$0.835 \pm 0.011$
3200	2000	0.659	0.455	$0.837 \pm 0.033$
3200	2100	0.664	0.459	$0.831 \pm 0.010$
3200	2200	0.658	0.454	$0.838 \pm 0.018$
3200	2300	0.662	0.457	$0.833 \pm 0.011$
3200	2400	0.666	0.460	$0.828 \pm 0.010$
3200	2500	0.671	0.463	$0.822 \pm 0.011$
3200	2600	0.676	0.467	$0.816 \pm 0.010$
3200	2700	0.678	0.468	$0.813 \pm 0.015$
3200	2800	0.690	0.476	$0.800 \pm 0.010$
3200	2900	0.709	0.489	$0.778 \pm 0.013$
3200	3000	0.730	0.504	$0.755 \pm 0.012$
3200	3100	0.794	0.548	$0.695 \pm 0.028$

Table A9: The 95% CL observed (Obs.) and expected (Exp.) exclusion limits (in fb) on the  $W_R$  production cross section times branching fraction for  $W_R \rightarrow \mu\mu jj$  as a function of  $W_R$  and  $N_\mu$  mass (in GeV) for  $1000 \leq M_{W_R} \leq 1600$  GeV. This signal acceptance (Acc.) is also included for each  $(M_{W_R}, M_{N_\mu})$  entry.

$M_{W_R}$	$M_{N_\mu}$	Obs.	Exp.	Acc.	$M_{W_R}$	$M_{N_\mu}$	Obs.	Exp.	Acc.
1000	100	79.0	53.1	$0.0664 \pm 0.0685$	1400	100	26.9	44.7	$0.037 \pm 0.140$
1000	200	18.1	12.1	$0.283 \pm 0.017$	1400	200	4.17	6.93	$0.224 \pm 0.029$
1000	300	12.4	8.31	$0.435 \pm 0.014$	1400	300	2.31	3.83	$0.410 \pm 0.016$
1000	400	10.4	7.00	$0.539 \pm 0.014$	1400	400	1.79	2.97	$0.533 \pm 0.015$
1000	500	9.53	6.40	$0.586 \pm 0.015$	1400	500	1.58	2.63	$0.618 \pm 0.015$
1000	600	9.12	6.13	$0.612 \pm 0.014$	1400	600	1.49	2.48	$0.676 \pm 0.014$
1000	700	9.16	6.15	$0.609 \pm 0.014$	1400	700	1.43	2.38	$0.702 \pm 0.014$
1000	800	9.83	6.61	$0.567 \pm 0.014$	1400	800	1.40	2.32	$0.720 \pm 0.014$
1000	900	13.0	8.71	$0.430 \pm 0.015$	1400	900	1.40	2.32	$0.721 \pm 0.014$
1100	100	72.9	57.5	$0.0550 \pm 0.0851$	1400	1000	1.40	2.33	$0.717 \pm 0.014$
1100	200	13.7	10.8	$0.275 \pm 0.020$	1400	1100	1.43	2.37	$0.705 \pm 0.014$
1100	300	8.18	6.46	$0.428 \pm 0.015$	1400	1200	1.53	2.54	$0.658 \pm 0.015$
1100	400	6.88	5.43	$0.536 \pm 0.014$	1400	1300	1.82	3.02	$0.553 \pm 0.014$
1100	500	6.47	5.10	$0.599 \pm 0.014$	1500	100	22.8	43.5	$0.033 \pm 0.160$
1100	600	6.17	4.87	$0.647 \pm 0.014$	1500	200	3.26	6.20	$0.205 \pm 0.035$
1100	700	6.10	4.82	$0.654 \pm 0.014$	1500	300	1.60	3.05	$0.391 \pm 0.018$
1100	800	6.29	4.96	$0.635 \pm 0.014$	1500	400	1.23	2.34	$0.528 \pm 0.014$
1100	900	6.67	5.26	$0.599 \pm 0.014$	1500	500	1.09	2.08	$0.611 \pm 0.014$
1100	1000	8.53	6.73	$0.468 \pm 0.015$	1500	600	1.03	1.97	$0.675 \pm 0.014$
1200	100	51.3	54.3	$0.047 \pm 0.103$	1500	700	1.01	1.91	$0.707 \pm 0.014$
1200	200	9.38	9.92	$0.259 \pm 0.022$	1500	800	0.988	1.88	$0.731 \pm 0.014$
1200	300	5.76	6.10	$0.426 \pm 0.015$	1500	900	0.978	1.86	$0.738 \pm 0.014$
1200	400	4.66	4.93	$0.543 \pm 0.014$	1500	1000	0.968	1.84	$0.746 \pm 0.014$
1200	500	4.19	4.43	$0.617 \pm 0.014$	1500	1100	0.986	1.88	$0.732 \pm 0.014$
1200	600	3.93	4.16	$0.661 \pm 0.014$	1500	1200	1.02	1.95	$0.705 \pm 0.015$
1200	700	3.86	4.08	$0.674 \pm 0.014$	1500	1300	1.08	2.05	$0.670 \pm 0.014$
1200	800	3.82	4.04	$0.680 \pm 0.014$	1500	1400	1.27	2.42	$0.568 \pm 0.014$
1200	900	3.90	4.13	$0.666 \pm 0.014$	1600	100	22.1	40.2	$0.029 \pm 0.179$
1200	1000	4.19	4.43	$0.621 \pm 0.014$	1600	200	3.13	5.68	$0.196 \pm 0.041$
1200	1100	5.23	5.53	$0.498 \pm 0.014$	1600	300	1.55	2.81	$0.382 \pm 0.018$
1300	100	32.5	45.4	$0.042 \pm 0.121$	1600	400	1.16	2.11	$0.517 \pm 0.015$
1300	200	5.13	7.18	$0.239 \pm 0.026$	1600	500	1.01	1.83	$0.612 \pm 0.015$
1300	300	2.76	3.86	$0.428 \pm 0.015$	1600	600	0.924	1.68	$0.668 \pm 0.014$
1300	400	2.21	3.09	$0.543 \pm 0.014$	1600	700	0.901	1.64	$0.713 \pm 0.014$
1300	500	2.03	2.84	$0.622 \pm 0.015$	1600	800	0.877	1.59	$0.737 \pm 0.014$
1300	600	1.96	2.74	$0.674 \pm 0.014$	1600	900	0.861	1.57	$0.751 \pm 0.014$
1300	700	1.93	2.71	$0.688 \pm 0.014$	1600	1000	0.855	1.56	$0.755 \pm 0.014$
1300	800	1.88	2.63	$0.707 \pm 0.015$	1600	1100	0.857	1.56	$0.754 \pm 0.014$
1300	900	1.90	2.65	$0.702 \pm 0.014$	1600	1200	0.870	1.58	$0.743 \pm 0.014$
1300	1000	1.93	2.70	$0.690 \pm 0.015$	1600	1300	0.890	1.62	$0.726 \pm 0.014$
1300	1100	2.07	2.89	$0.644 \pm 0.014$	1600	1400	0.936	1.70	$0.690 \pm 0.014$
1300	1200	2.51	3.51	$0.531 \pm 0.017$	1600	1500	1.10	2.00	$0.588 \pm 0.014$

Table A10: The 95% CL observed (Obs.) and expected (Exp.) exclusion limits (in fb) on the  $W_R$  production cross section times branching fraction for  $W_R \rightarrow \mu\mu jj$  as a function of  $W_R$  and  $N_\mu$  mass (in GeV) for  $1700 \leq M_{W_R} \leq 2000$  GeV. This signal acceptance (Acc.) is also included for each  $(M_{W_R}, M_{N_\mu})$  entry.

$M_{W_R}$	$M_{N_\mu}$	Obs.	Exp.	Acc.	$M_{W_R}$	$M_{N_\mu}$	Obs.	Exp.	Acc.
1700	100	28.6	44.3	$0.028 \pm 0.198$	1900	100	38.2	45.2	$0.020 \pm 0.235$
1700	200	3.53	5.46	$0.179 \pm 0.048$	1900	200	4.32	5.11	$0.148 \pm 0.063$
1700	300	1.53	2.36	$0.364 \pm 0.020$	1900	300	1.80	2.12	$0.327 \pm 0.028$
1700	400	1.09	1.68	$0.507 \pm 0.016$	1900	400	1.22	1.45	$0.482 \pm 0.023$
1700	500	0.929	1.44	$0.601 \pm 0.014$	1900	500	1.02	1.21	$0.587 \pm 0.014$
1700	600	0.869	1.35	$0.664 \pm 0.015$	1900	600	0.922	1.09	$0.659 \pm 0.016$
1700	700	0.853	1.32	$0.709 \pm 0.014$	1900	700	0.879	1.04	$0.703 \pm 0.015$
1700	800	0.827	1.28	$0.743 \pm 0.014$	1900	800	0.857	1.01	$0.738 \pm 0.014$
1700	900	0.815	1.26	$0.759 \pm 0.014$	1900	900	0.838	0.991	$0.759 \pm 0.014$
1700	1000	0.809	1.25	$0.765 \pm 0.014$	1900	1000	0.824	0.974	$0.774 \pm 0.016$
1700	1100	0.806	1.25	$0.768 \pm 0.015$	1900	1100	0.820	0.970	$0.777 \pm 0.014$
1700	1200	0.812	1.26	$0.762 \pm 0.014$	1900	1200	0.818	0.967	$0.780 \pm 0.014$
1700	1300	0.819	1.27	$0.755 \pm 0.014$	1900	1300	0.816	0.964	$0.782 \pm 0.016$
1700	1400	0.844	1.31	$0.733 \pm 0.014$	1900	1400	0.817	0.966	$0.781 \pm 0.014$
1700	1500	0.887	1.37	$0.698 \pm 0.015$	1900	1500	0.835	0.987	$0.763 \pm 0.014$
1700	1600	1.02	1.58	$0.605 \pm 0.014$	1900	1600	0.848	1.00	$0.752 \pm 0.014$
1800	100	31.5	43.8	$0.023 \pm 0.216$	1900	1700	0.896	1.06	$0.711 \pm 0.015$
1800	200	4.03	5.61	$0.163 \pm 0.055$	1900	1800	1.02	1.21	$0.622 \pm 0.015$
1800	300	1.77	2.46	$0.343 \pm 0.022$	2000	100	41.5	46.1	$0.019 \pm 0.253$
1800	400	1.24	1.72	$0.494 \pm 0.015$	2000	200	4.92	5.46	$0.137 \pm 0.068$
1800	500	1.02	1.42	$0.589 \pm 0.019$	2000	300	1.93	2.15	$0.308 \pm 0.028$
1800	600	0.922	1.28	$0.657 \pm 0.014$	2000	400	1.25	1.39	$0.461 \pm 0.017$
1800	700	0.872	1.21	$0.709 \pm 0.014$	2000	500	0.992	1.10	$0.573 \pm 0.015$
1800	800	0.841	1.17	$0.738 \pm 0.014$	2000	600	0.878	0.975	$0.648 \pm 0.014$
1800	900	0.833	1.16	$0.756 \pm 0.014$	2000	700	0.826	0.918	$0.696 \pm 0.014$
1800	1000	0.820	1.14	$0.768 \pm 0.015$	2000	800	0.790	0.878	$0.733 \pm 0.014$
1800	1100	0.810	1.13	$0.777 \pm 0.014$	2000	900	0.775	0.861	$0.757 \pm 0.014$
1800	1200	0.811	1.13	$0.777 \pm 0.014$	2000	1000	0.764	0.849	$0.776 \pm 0.014$
1800	1300	0.812	1.13	$0.775 \pm 0.014$	2000	1100	0.755	0.839	$0.785 \pm 0.018$
1800	1400	0.825	1.15	$0.764 \pm 0.014$	2000	1200	0.746	0.829	$0.794 \pm 0.014$
1800	1500	0.848	1.18	$0.743 \pm 0.014$	2000	1300	0.744	0.827	$0.796 \pm 0.015$
1800	1600	0.894	1.24	$0.704 \pm 0.014$	2000	1400	0.752	0.835	$0.788 \pm 0.014$
1800	1700	1.03	1.44	$0.610 \pm 0.015$	2000	1500	0.758	0.842	$0.782 \pm 0.015$
					2000	1600	0.767	0.852	$0.772 \pm 0.014$
					2000	1700	0.781	0.868	$0.758 \pm 0.015$
					2000	1800	0.828	0.920	$0.715 \pm 0.015$
					2000	1900	0.946	1.05	$0.627 \pm 0.014$

Table A11: The 95% CL observed (Obs.) and expected (Exp.) exclusion limits (in fb) on the  $W_R$  production cross section times branching fraction for  $W_R \rightarrow \mu\mu jj$  as a function of  $W_R$  and  $N_\mu$  mass (in GeV) for  $2100 \leq M_{W_R} \leq 2300$  GeV. This signal acceptance (Acc.) is also included for each  $(M_{W_R}, M_{N_\mu})$  entry.

$M_{W_R}$	$M_{N_\mu}$	Obs.	Exp.	Acc.	$M_{W_R}$	$M_{N_\mu}$	Obs.	Exp.	Acc.
2100	100	51.7	54.3	$0.020 \pm 0.271$	2300	100	54.0	49.5	$0.018 \pm 0.306$
2100	200	5.70	5.99	$0.129 \pm 0.076$	2300	200	5.59	5.12	$0.121 \pm 0.095$
2100	300	2.22	2.33	$0.294 \pm 0.029$	2300	300	2.11	1.94	$0.275 \pm 0.037$
2100	400	1.38	1.45	$0.448 \pm 0.018$	2300	400	1.27	1.17	$0.413 \pm 0.020$
2100	500	1.07	1.12	$0.566 \pm 0.025$	2300	500	0.987	0.905	$0.533 \pm 0.016$
2100	600	0.917	0.964	$0.640 \pm 0.014$	2300	600	0.862	0.791	$0.632 \pm 0.015$
2100	700	0.839	0.881	$0.696 \pm 0.014$	2300	700	0.788	0.722	$0.675 \pm 0.014$
2100	800	0.794	0.835	$0.733 \pm 0.015$	2300	800	0.752	0.690	$0.723 \pm 0.014$
2100	900	0.767	0.806	$0.749 \pm 0.014$	2300	900	0.734	0.673	$0.750 \pm 0.014$
2100	1000	0.751	0.789	$0.775 \pm 0.014$	2300	1000	0.714	0.654	$0.769 \pm 0.014$
2100	1100	0.740	0.777	$0.783 \pm 0.014$	2300	1100	0.703	0.644	$0.784 \pm 0.014$
2100	1200	0.734	0.771	$0.789 \pm 0.014$	2300	1200	0.701	0.643	$0.794 \pm 0.014$
2100	1300	0.725	0.762	$0.798 \pm 0.014$	2300	1300	0.693	0.636	$0.802 \pm 0.014$
2100	1400	0.728	0.764	$0.796 \pm 0.014$	2300	1400	0.690	0.633	$0.806 \pm 0.014$
2100	1500	0.729	0.766	$0.794 \pm 0.014$	2300	1500	0.690	0.632	$0.806 \pm 0.015$
2100	1600	0.735	0.773	$0.787 \pm 0.014$	2300	1600	0.690	0.633	$0.806 \pm 0.015$
2100	1700	0.749	0.787	$0.773 \pm 0.014$	2300	1700	0.695	0.637	$0.800 \pm 0.014$
2100	1800	0.768	0.807	$0.754 \pm 0.014$	2300	1800	0.700	0.642	$0.795 \pm 0.014$
2100	1900	0.801	0.841	$0.723 \pm 0.014$	2300	1900	0.709	0.650	$0.785 \pm 0.014$
2100	2000	0.906	0.952	$0.639 \pm 0.014$	2300	2000	0.731	0.671	$0.760 \pm 0.016$
2200	100	53.2	49.5	$0.018 \pm 0.288$	2300	2100	0.764	0.700	$0.728 \pm 0.014$
2200	200	6.05	5.62	$0.123 \pm 0.085$	2300	2200	0.853	0.782	$0.652 \pm 0.014$
2200	300	2.36	2.20	$0.279 \pm 0.033$					
2200	400	1.50	1.40	$0.435 \pm 0.019$					
2200	500	1.17	1.09	$0.547 \pm 0.016$					
2200	600	1.01	0.941	$0.629 \pm 0.015$					
2200	700	0.919	0.854	$0.689 \pm 0.014$					
2200	800	0.865	0.804	$0.721 \pm 0.014$					
2200	900	0.832	0.774	$0.754 \pm 0.014$					
2200	1000	0.808	0.751	$0.775 \pm 0.014$					
2200	1100	0.791	0.736	$0.783 \pm 0.015$					
2200	1200	0.782	0.727	$0.792 \pm 0.040$					
2200	1300	0.770	0.716	$0.804 \pm 0.015$					
2200	1400	0.780	0.725	$0.794 \pm 0.015$					
2200	1500	0.774	0.719	$0.801 \pm 0.015$					
2200	1600	0.775	0.720	$0.800 \pm 0.015$					
2200	1700	0.782	0.727	$0.792 \pm 0.014$					
2200	1800	0.795	0.739	$0.780 \pm 0.017$					
2200	1900	0.814	0.756	$0.762 \pm 0.016$					
2200	2000	0.854	0.794	$0.725 \pm 0.015$					
2200	2100	0.955	0.888	$0.649 \pm 0.016$					

Table A12: The 95% CL observed (Obs.) and expected (Exp.) exclusion limits (in fb) on the  $W_R$  production cross section times branching fraction for  $W_R \rightarrow \mu\mu jj$  as a function of  $W_R$  and  $N_\mu$  mass (in GeV) for  $2400 \leq M_{W_R} \leq 2500$  GeV. This signal acceptance (Acc.) is also included for each  $(M_{W_R}, M_{N_\mu})$  entry.

$M_{W_R}$	$M_{N_\mu}$	Obs.	Exp.	Acc.	$M_{W_R}$	$M_{N_\mu}$	Obs.	Exp.	Acc.
2400	100	63.9	56.1	$0.020 \pm 0.325$	2500	100	72.8	62.7	$0.021 \pm 0.345$
2400	200	6.12	5.36	$0.116 \pm 0.105$	2500	200	6.78	5.83	$0.112 \pm 0.116$
2400	300	2.20	1.93	$0.258 \pm 0.041$	2500	300	2.33	2.01	$0.245 \pm 0.047$
2400	400	1.29	1.13	$0.407 \pm 0.022$	2500	400	1.33	1.14	$0.389 \pm 0.024$
2400	500	0.961	0.843	$0.526 \pm 0.016$	2500	500	0.944	0.813	$0.515 \pm 0.017$
2400	600	0.804	0.705	$0.614 \pm 0.015$	2500	600	0.784	0.675	$0.602 \pm 0.016$
2400	700	0.735	0.645	$0.675 \pm 0.014$	2500	700	0.697	0.600	$0.665 \pm 0.014$
2400	800	0.690	0.605	$0.718 \pm 0.014$	2500	800	0.647	0.557	$0.714 \pm 0.014$
2400	900	0.702	0.616	$0.745 \pm 0.016$	2500	900	0.611	0.526	$0.738 \pm 0.014$
2400	1000	0.681	0.597	$0.768 \pm 0.014$	2500	1000	0.597	0.514	$0.766 \pm 0.014$
2400	1100	0.653	0.572	$0.784 \pm 0.014$	2500	1100	0.581	0.500	$0.781 \pm 0.014$
2400	1200	0.635	0.557	$0.800 \pm 0.014$	2500	1200	0.574	0.494	$0.794 \pm 0.014$
2400	1300	0.631	0.553	$0.805 \pm 0.015$	2500	1300	0.569	0.490	$0.802 \pm 0.014$
2400	1400	0.632	0.554	$0.804 \pm 0.014$	2500	1400	0.565	0.486	$0.807 \pm 0.014$
2400	1500	0.630	0.552	$0.806 \pm 0.014$	2500	1500	0.561	0.483	$0.813 \pm 0.015$
2400	1600	0.626	0.549	$0.811 \pm 0.015$	2500	1600	0.556	0.479	$0.820 \pm 0.016$
2400	1700	0.627	0.550	$0.810 \pm 0.022$	2500	1700	0.564	0.485	$0.809 \pm 0.019$
2400	1800	0.634	0.556	$0.802 \pm 0.021$	2500	1800	0.566	0.487	$0.806 \pm 0.018$
2400	1900	0.639	0.561	$0.795 \pm 0.014$	2500	1900	0.564	0.485	$0.810 \pm 0.016$
2400	2000	0.646	0.566	$0.786 \pm 0.014$	2500	2000	0.570	0.491	$0.800 \pm 0.014$
2400	2100	0.660	0.579	$0.769 \pm 0.014$	2500	2100	0.576	0.496	$0.791 \pm 0.014$
2400	2200	0.692	0.607	$0.734 \pm 0.014$	2500	2200	0.595	0.512	$0.766 \pm 0.016$
2400	2300	0.771	0.676	$0.659 \pm 0.017$	2500	2300	0.621	0.534	$0.735 \pm 0.015$
					2500	2400	0.691	0.594	$0.661 \pm 0.015$



Table A13: The 95% CL observed (Obs.) and expected (Exp.) exclusion limits (in fb) on the  $W_R$  production cross section times branching fraction for  $W_R \rightarrow \mu\mu jj$  as a function of  $W_R$  and  $N_\mu$  mass (in GeV) for  $2600 \leq M_{W_R} \leq 2700$  GeV. This signal acceptance (Acc.) is also included for each  $(M_{W_R}, M_{N_\mu})$  entry.

$M_{W_R}$	$M_{N_\mu}$	Obs.	Exp.	Acc.	$M_{W_R}$	$M_{N_\mu}$	Obs.	Exp.	Acc.
2600	100	74.3	62.3	$0.019 \pm 0.359$	2700	100	68.8	59.9	$0.021 \pm 0.378$
2600	200	7.52	6.30	$0.110 \pm 0.127$	2700	200	7.51	6.55	$0.114 \pm 0.142$
2600	300	2.53	2.12	$0.236 \pm 0.053$	2700	300	2.52	2.20	$0.237 \pm 0.060$
2600	400	1.37	1.15	$0.379 \pm 0.029$	2700	400	1.34	1.17	$0.369 \pm 0.032$
2600	500	0.963	0.807	$0.498 \pm 0.018$	2700	500	0.923	0.805	$0.487 \pm 0.019$
2600	600	0.777	0.651	$0.594 \pm 0.015$	2700	600	0.728	0.635	$0.589 \pm 0.015$
2600	700	0.680	0.570	$0.663 \pm 0.014$	2700	700	0.646	0.564	$0.652 \pm 0.015$
2600	800	0.627	0.526	$0.707 \pm 0.014$	2700	800	0.602	0.525	$0.701 \pm 0.014$
2600	900	0.593	0.497	$0.732 \pm 0.014$	2700	900	0.558	0.487	$0.733 \pm 0.014$
2600	1000	0.567	0.475	$0.760 \pm 0.014$	2700	1000	0.519	0.453	$0.761 \pm 0.014$
2600	1100	0.547	0.458	$0.773 \pm 0.015$	2700	1100	0.504	0.439	$0.775 \pm 0.019$
2600	1200	0.551	0.462	$0.794 \pm 0.014$	2700	1200	0.475	0.414	$0.789 \pm 0.016$
2600	1300	0.535	0.448	$0.799 \pm 0.014$	2700	1300	0.479	0.417	$0.802 \pm 0.016$
2600	1400	0.531	0.445	$0.805 \pm 0.015$	2700	1400	0.487	0.424	$0.806 \pm 0.025$
2600	1500	0.529	0.443	$0.808 \pm 0.014$	2700	1500	0.482	0.421	$0.813 \pm 0.014$
2600	1600	0.522	0.438	$0.818 \pm 0.017$	2700	1600	0.479	0.418	$0.818 \pm 0.014$
2600	1700	0.522	0.438	$0.819 \pm 0.014$	2700	1700	0.481	0.419	$0.816 \pm 0.014$
2600	1800	0.525	0.440	$0.814 \pm 0.035$	2700	1800	0.479	0.417	$0.820 \pm 0.015$
2600	1900	0.526	0.441	$0.812 \pm 0.014$	2700	1900	0.480	0.419	$0.817 \pm 0.014$
2600	2000	0.529	0.444	$0.807 \pm 0.014$	2700	2000	0.480	0.419	$0.816 \pm 0.014$
2600	2100	0.533	0.446	$0.802 \pm 0.014$	2700	2100	0.482	0.420	$0.813 \pm 0.016$
2600	2200	0.540	0.452	$0.792 \pm 0.016$	2700	2200	0.491	0.428	$0.799 \pm 0.014$
2600	2300	0.553	0.464	$0.772 \pm 0.015$	2700	2300	0.497	0.433	$0.790 \pm 0.022$
2600	2400	0.582	0.487	$0.735 \pm 0.015$	2700	2400	0.509	0.444	$0.771 \pm 0.014$
2600	2500	0.645	0.541	$0.662 \pm 0.015$	2700	2500	0.533	0.465	$0.736 \pm 0.015$
					2700	2600	0.583	0.508	$0.673 \pm 0.017$

Table A14: The 95% CL observed (Obs.) and expected (Exp.) exclusion limits (in fb) on the  $W_R$  production cross section times branching fraction for  $W_R \rightarrow \mu\mu jj$  as a function of  $W_R$  and  $N_\mu$  mass (in GeV) for  $2800 \leq M_{W_R} \leq 2900$  GeV. This signal acceptance (Acc.) is also included for each  $(M_{W_R}, M_{N_\mu})$  entry.

$M_{W_R}$	$M_{N_\mu}$	Obs.	Exp.	Acc.	$M_{W_R}$	$M_{N_\mu}$	Obs.	Exp.	Acc.
2800	100	71.6	63.4	$0.023 \pm 0.398$	2900	100	73.4	63.2	$0.024 \pm 0.412$
2800	200	8.59	7.62	$0.116 \pm 0.154$	2900	200	9.90	8.53	$0.117 \pm 0.169$
2800	300	2.87	2.55	$0.235 \pm 0.066$	2900	300	3.25	2.80	$0.227 \pm 0.079$
2800	400	1.49	1.32	$0.360 \pm 0.036$	2900	400	1.65	1.42	$0.365 \pm 0.045$
2800	500	0.992	0.879	$0.482 \pm 0.021$	2900	500	1.07	0.919	$0.471 \pm 0.040$
2800	600	0.774	0.686	$0.576 \pm 0.016$	2900	600	0.817	0.703	$0.570 \pm 0.017$
2800	700	0.654	0.580	$0.645 \pm 0.015$	2900	700	0.688	0.593	$0.637 \pm 0.015$
2800	800	0.604	0.535	$0.691 \pm 0.014$	2900	800	0.608	0.524	$0.683 \pm 0.014$
2800	900	0.544	0.482	$0.724 \pm 0.014$	2900	900	0.558	0.481	$0.721 \pm 0.014$
2800	1000	0.516	0.458	$0.752 \pm 0.017$	2900	1000	0.527	0.454	$0.744 \pm 0.014$
2800	1100	0.494	0.438	$0.768 \pm 0.015$	2900	1100	0.503	0.433	$0.767 \pm 0.014$
2800	1200	0.478	0.424	$0.789 \pm 0.015$	2900	1200	0.485	0.417	$0.784 \pm 0.018$
2800	1300	0.464	0.412	$0.800 \pm 0.014$	2900	1300	0.470	0.405	$0.800 \pm 0.014$
2800	1400	0.457	0.406	$0.807 \pm 0.014$	2900	1400	0.461	0.397	$0.807 \pm 0.015$
2800	1500	0.453	0.402	$0.815 \pm 0.015$	2900	1500	0.455	0.392	$0.810 \pm 0.014$
2800	1600	0.450	0.399	$0.820 \pm 0.014$	2900	1600	0.450	0.387	$0.820 \pm 0.015$
2800	1700	0.448	0.397	$0.824 \pm 0.014$	2900	1700	0.450	0.388	$0.820 \pm 0.015$
2800	1800	0.449	0.398	$0.823 \pm 0.014$	2900	1800	0.446	0.384	$0.827 \pm 0.028$
2800	1900	0.450	0.399	$0.821 \pm 0.016$	2900	1900	0.447	0.385	$0.825 \pm 0.017$
2800	2000	0.450	0.399	$0.820 \pm 0.014$	2900	2000	0.445	0.383	$0.828 \pm 0.017$
2800	2100	0.451	0.400	$0.818 \pm 0.014$	2900	2100	0.454	0.391	$0.813 \pm 0.014$
2800	2200	0.457	0.406	$0.807 \pm 0.015$	2900	2200	0.451	0.388	$0.819 \pm 0.016$
2800	2300	0.461	0.409	$0.801 \pm 0.015$	2900	2300	0.454	0.391	$0.812 \pm 0.016$
2800	2400	0.465	0.412	$0.794 \pm 0.015$	2900	2400	0.458	0.395	$0.805 \pm 0.014$
2800	2500	0.477	0.423	$0.774 \pm 0.014$	2900	2500	0.464	0.399	$0.796 \pm 0.014$
2800	2600	0.500	0.443	$0.739 \pm 0.015$	2900	2600	0.477	0.411	$0.773 \pm 0.014$
2800	2700	0.546	0.484	$0.676 \pm 0.016$	2900	2700	0.499	0.429	$0.740 \pm 0.014$
					2900	2800	0.539	0.464	$0.684 \pm 0.020$

Table A15: The 95% CL observed (Obs.) and expected (Exp.) exclusion limits (in fb) on the  $W_R$  production cross section times branching fraction for  $W_R \rightarrow \mu\mu jj$  as a function of  $W_R$  and  $N_\mu$  mass (in GeV) for  $3000 \leq M_{W_R} \leq 3100$  GeV. This signal acceptance (Acc.) is also included for each  $(M_{W_R}, M_{N_\mu})$  entry.

$M_{W_R}$	$M_{N_\mu}$	Obs.	Exp.	Acc.	$M_{W_R}$	$M_{N_\mu}$	Obs.	Exp.	Acc.
3000	100	72.8	63.2	$0.024 \pm 0.428$	3100	100	75.6	65.9	$0.029 \pm 0.439$
3000	200	11.3	9.79	$0.117 \pm 0.185$	3100	200	12.9	11.2	$0.130 \pm 0.197$
3000	300	3.59	3.12	$0.234 \pm 0.094$	3100	300	4.15	3.62	$0.240 \pm 0.104$
3000	400	1.81	1.57	$0.356 \pm 0.052$	3100	400	2.01	1.75	$0.359 \pm 0.060$
3000	500	1.16	1.01	$0.469 \pm 0.031$	3100	500	1.28	1.12	$0.461 \pm 0.037$
3000	600	0.864	0.750	$0.561 \pm 0.019$	3100	600	0.935	0.815	$0.552 \pm 0.024$
3000	700	0.714	0.620	$0.627 \pm 0.016$	3100	700	0.763	0.665	$0.623 \pm 0.021$
3000	800	0.628	0.545	$0.675 \pm 0.015$	3100	800	0.660	0.575	$0.674 \pm 0.016$
3000	900	0.571	0.496	$0.713 \pm 0.016$	3100	900	0.595	0.519	$0.715 \pm 0.015$
3000	1000	0.535	0.465	$0.750 \pm 0.014$	3100	1000	0.554	0.483	$0.738 \pm 0.015$
3000	1100	0.507	0.440	$0.767 \pm 0.015$	3100	1100	0.521	0.454	$0.762 \pm 0.018$
3000	1200	0.488	0.424	$0.780 \pm 0.020$	3100	1200	0.500	0.436	$0.781 \pm 0.017$
3000	1300	0.473	0.410	$0.790 \pm 0.015$	3100	1300	0.483	0.421	$0.793 \pm 0.015$
3000	1400	0.461	0.400	$0.805 \pm 0.018$	3100	1400	0.467	0.407	$0.805 \pm 0.023$
3000	1500	0.451	0.391	$0.816 \pm 0.016$	3100	1500	0.455	0.397	$0.808 \pm 0.018$
3000	1600	0.449	0.390	$0.819 \pm 0.014$	3100	1600	0.451	0.393	$0.818 \pm 0.032$
3000	1700	0.445	0.387	$0.826 \pm 0.017$	3100	1700	0.448	0.390	$0.825 \pm 0.017$
3000	1800	0.446	0.387	$0.824 \pm 0.018$	3100	1800	0.447	0.390	$0.825 \pm 0.032$
3000	1900	0.446	0.387	$0.824 \pm 0.015$	3100	1900	0.448	0.390	$0.825 \pm 0.018$
3000	2000	0.443	0.385	$0.829 \pm 0.031$	3100	2000	0.445	0.387	$0.831 \pm 0.014$
3000	2100	0.444	0.385	$0.828 \pm 0.015$	3100	2100	0.448	0.390	$0.825 \pm 0.041$
3000	2200	0.448	0.389	$0.820 \pm 0.015$	3100	2200	0.446	0.389	$0.828 \pm 0.015$
3000	2300	0.448	0.389	$0.821 \pm 0.026$	3100	2300	0.448	0.390	$0.824 \pm 0.020$
3000	2400	0.451	0.392	$0.815 \pm 0.014$	3100	2400	0.451	0.393	$0.819 \pm 0.015$
3000	2500	0.456	0.396	$0.806 \pm 0.017$	3100	2500	0.455	0.396	$0.812 \pm 0.015$
3000	2600	0.462	0.401	$0.795 \pm 0.015$	3100	2600	0.457	0.399	$0.807 \pm 0.016$
3000	2700	0.471	0.409	$0.780 \pm 0.014$	3100	2700	0.463	0.404	$0.797 \pm 0.017$
3000	2800	0.494	0.429	$0.744 \pm 0.014$	3100	2800	0.475	0.414	$0.777 \pm 0.014$
3000	2900	0.535	0.464	$0.688 \pm 0.024$	3100	2900	0.494	0.431	$0.747 \pm 0.015$
					3100	3000	0.535	0.466	$0.690 \pm 0.019$

Table A16: The 95% CL observed (Obs.) and expected (Exp.) exclusion limits (in fb) on the  $W_R$  production cross section times branching fraction for  $W_R \rightarrow \mu\mu jj$  as a function of  $W_R$  and  $N_\mu$  mass (in GeV) for  $M_{W_R} = 3200$  GeV. This signal acceptance (Acc.) is also included for each  $(M_{W_R}, M_{N_\mu})$  entry.

$M_{W_R}$	$M_{N_\mu}$	Obs.	Exp.	Acc.
3200	100	75.8	66.0	$0.031 \pm 0.449$
3200	200	14.4	12.5	$0.131 \pm 0.206$
3200	300	4.58	3.99	$0.254 \pm 0.111$
3200	400	2.24	1.95	$0.363 \pm 0.070$
3200	500	1.39	1.21	$0.458 \pm 0.050$
3200	600	1.01	0.877	$0.546 \pm 0.029$
3200	700	0.808	0.704	$0.614 \pm 0.020$
3200	800	0.691	0.602	$0.668 \pm 0.016$
3200	900	0.614	0.535	$0.703 \pm 0.018$
3200	1000	0.567	0.494	$0.734 \pm 0.014$
3200	1100	0.531	0.463	$0.762 \pm 0.027$
3200	1200	0.503	0.438	$0.776 \pm 0.015$
3200	1300	0.485	0.422	$0.790 \pm 0.026$
3200	1400	0.468	0.408	$0.799 \pm 0.015$
3200	1500	0.455	0.396	$0.808 \pm 0.016$
3200	1600	0.445	0.388	$0.819 \pm 0.015$
3200	1700	0.444	0.387	$0.820 \pm 0.030$
3200	1800	0.441	0.384	$0.827 \pm 0.018$
3200	1900	0.440	0.383	$0.829 \pm 0.031$
3200	2000	0.438	0.382	$0.832 \pm 0.023$
3200	2100	0.442	0.385	$0.825 \pm 0.018$
3200	2200	0.438	0.382	$0.831 \pm 0.019$
3200	2300	0.441	0.385	$0.826 \pm 0.019$
3200	2400	0.443	0.386	$0.822 \pm 0.015$
3200	2500	0.446	0.389	$0.817 \pm 0.018$
3200	2600	0.449	0.391	$0.811 \pm 0.017$
3200	2700	0.451	0.393	$0.808 \pm 0.021$
3200	2800	0.459	0.399	$0.795 \pm 0.021$
3200	2900	0.471	0.410	$0.774 \pm 0.022$
3200	3000	0.485	0.423	$0.751 \pm 0.015$
3200	3100	0.527	0.459	$0.691 \pm 0.039$

Table A17: The 95% CL observed (Obs.) and expected (Exp.) exclusion limits (in fb) on the  $W_R$  production cross section times branching fraction for  $W_R \rightarrow (ee + \mu\mu)jj$  as a function of  $W_R$  and  $N_\ell$  mass (in GeV) for  $1000 \leq M_{W_R} \leq 1600$  GeV. The signal acceptance (Acc.) is also included for each  $(M_{W_R}, M_{N_\ell})$  entry.

$M_{W_R}$	$M_{N_\ell}$	Obs.	Exp.	Acc.	$M_{W_R}$	$M_{N_\ell}$	Obs.	Exp.	Acc.
1000	100	117	88.5	$0.0695 \pm 0.0650$	1400	100	54.0	71.9	$0.040 \pm 0.109$
1000	200	26.3	19.9	$0.291 \pm 0.018$	1400	200	8.26	11.0	$0.232 \pm 0.034$
1000	300	17.8	13.5	$0.441 \pm 0.010$	1400	300	4.52	6.02	$0.419 \pm 0.016$
1000	400	15.0	11.3	$0.544 \pm 0.009$	1400	400	3.49	4.64	$0.541 \pm 0.011$
1000	500	13.7	10.3	$0.591 \pm 0.009$	1400	500	3.07	4.08	$0.624 \pm 0.009$
1000	600	13.1	9.90	$0.616 \pm 0.008$	1400	600	2.89	3.84	$0.682 \pm 0.009$
1000	700	13.1	9.94	$0.613 \pm 0.008$	1400	700	2.77	3.69	$0.707 \pm 0.009$
1000	800	14.1	10.7	$0.570 \pm 0.008$	1400	800	2.70	3.60	$0.725 \pm 0.008$
1000	900	18.6	14.1	$0.433 \pm 0.009$	1400	900	2.70	3.59	$0.725 \pm 0.008$
1100	100	150	98.2	$0.0582 \pm 0.0760$	1400	1000	2.71	3.61	$0.721 \pm 0.008$
1100	200	27.8	18.1	$0.282 \pm 0.021$	1400	1100	2.76	3.68	$0.708 \pm 0.008$
1100	300	16.4	10.7	$0.435 \pm 0.011$	1400	1200	2.96	3.93	$0.661 \pm 0.009$
1100	400	13.8	9.00	$0.542 \pm 0.009$	1400	1300	3.52	4.68	$0.555 \pm 0.009$
1100	500	12.9	8.43	$0.604 \pm 0.009$	1500	100	46.7	69.1	$0.035 \pm 0.119$
1100	600	12.3	8.04	$0.651 \pm 0.009$	1500	200	6.57	9.72	$0.212 \pm 0.039$
1100	700	12.2	7.95	$0.659 \pm 0.008$	1500	300	3.20	4.74	$0.401 \pm 0.018$
1100	800	12.5	8.19	$0.639 \pm 0.009$	1500	400	2.44	3.61	$0.536 \pm 0.011$
1100	900	13.3	8.68	$0.602 \pm 0.009$	1500	500	2.15	3.19	$0.618 \pm 0.009$
1100	1000	17.0	11.1	$0.470 \pm 0.009$	1500	600	2.04	3.01	$0.680 \pm 0.009$
1200	100	108	89.9	$0.0495 \pm 0.0869$	1500	700	1.98	2.92	$0.711 \pm 0.009$
1200	200	19.5	16.2	$0.267 \pm 0.025$	1500	800	1.94	2.87	$0.735 \pm 0.009$
1200	300	11.9	9.84	$0.434 \pm 0.012$	1500	900	1.92	2.84	$0.742 \pm 0.008$
1200	400	9.54	7.92	$0.549 \pm 0.009$	1500	1000	1.90	2.81	$0.750 \pm 0.008$
1200	500	8.56	7.10	$0.622 \pm 0.009$	1500	1100	1.94	2.87	$0.735 \pm 0.008$
1200	600	8.01	6.65	$0.666 \pm 0.008$	1500	1200	2.01	2.98	$0.708 \pm 0.009$
1200	700	7.86	6.52	$0.679 \pm 0.008$	1500	1300	2.11	3.13	$0.673 \pm 0.008$
1200	800	7.79	6.46	$0.684 \pm 0.008$	1500	1400	2.50	3.69	$0.570 \pm 0.008$
1200	900	7.95	6.60	$0.670 \pm 0.009$	1600	100	46.4	67.3	$0.031 \pm 0.130$
1200	1000	8.53	7.08	$0.624 \pm 0.009$	1600	200	6.48	9.39	$0.204 \pm 0.044$
1200	1100	10.6	8.83	$0.500 \pm 0.008$	1600	300	3.17	4.59	$0.392 \pm 0.020$
1300	100	64.6	72.0	$0.0445 \pm 0.0977$	1600	400	2.36	3.43	$0.527 \pm 0.012$
1300	200	10.1	11.2	$0.246 \pm 0.030$	1600	500	2.04	2.96	$0.620 \pm 0.011$
1300	300	5.36	5.97	$0.437 \pm 0.014$	1600	600	1.87	2.71	$0.674 \pm 0.009$
1300	400	4.26	4.75	$0.551 \pm 0.010$	1600	700	1.82	2.64	$0.718 \pm 0.008$
1300	500	3.90	4.35	$0.628 \pm 0.009$	1600	800	1.77	2.56	$0.742 \pm 0.009$
1300	600	3.76	4.19	$0.679 \pm 0.009$	1600	900	1.74	2.52	$0.755 \pm 0.008$
1300	700	3.71	4.13	$0.694 \pm 0.008$	1600	1000	1.72	2.50	$0.759 \pm 0.008$
1300	800	3.61	4.02	$0.712 \pm 0.009$	1600	1100	1.73	2.50	$0.758 \pm 0.008$
1300	900	3.64	4.05	$0.706 \pm 0.008$	1600	1200	1.75	2.54	$0.746 \pm 0.008$
1300	1000	3.70	4.12	$0.694 \pm 0.009$	1600	1300	1.79	2.60	$0.729 \pm 0.008$
1300	1100	3.96	4.42	$0.647 \pm 0.008$	1600	1400	1.89	2.74	$0.692 \pm 0.009$
1300	1200	4.81	5.36	$0.534 \pm 0.009$	1600	1500	2.22	3.21	$0.590 \pm 0.009$

Table A18: The 95% CL observed (Obs.) and expected (Exp.) exclusion limits (in fb) on the  $W_R$  production cross section times branching fraction for  $W_R \rightarrow (ee + \mu\mu)jj$  as a function of  $W_R$  and  $N_\ell$  mass (in GeV) for  $1700 \leq M_{W_R} \leq 2000$  GeV. The signal acceptance (Acc.) is also included for each  $(M_{W_R}, M_{N_\ell})$  entry.

$M_{W_R}$	$M_{N_\ell}$	Obs.	Exp.	Acc.	$M_{W_R}$	$M_{N_\ell}$	Obs.	Exp.	Acc.
1700	100	60.3	75.0	$0.029 \pm 0.140$	1900	100	117	69.5	$0.022 \pm 0.159$
1700	200	7.31	9.09	$0.187 \pm 0.049$	1900	200	13.0	7.71	$0.154 \pm 0.061$
1700	300	3.13	3.90	$0.373 \pm 0.023$	1900	300	5.37	3.17	$0.338 \pm 0.031$
1700	400	2.21	2.75	$0.516 \pm 0.014$	1900	400	3.63	2.14	$0.492 \pm 0.018$
1700	500	1.88	2.34	$0.609 \pm 0.010$	1900	500	3.01	1.78	$0.596 \pm 0.015$
1700	600	1.76	2.19	$0.670 \pm 0.009$	1900	600	2.71	1.60	$0.667 \pm 0.010$
1700	700	1.72	2.14	$0.714 \pm 0.009$	1900	700	2.58	1.52	$0.709 \pm 0.009$
1700	800	1.67	2.07	$0.747 \pm 0.009$	1900	800	2.51	1.48	$0.743 \pm 0.009$
1700	900	1.64	2.04	$0.763 \pm 0.008$	1900	900	2.45	1.45	$0.764 \pm 0.009$
1700	1000	1.63	2.03	$0.770 \pm 0.008$	1900	1000	2.41	1.42	$0.778 \pm 0.010$
1700	1100	1.62	2.02	$0.772 \pm 0.009$	1900	1100	2.40	1.42	$0.781 \pm 0.009$
1700	1200	1.63	2.03	$0.766 \pm 0.008$	1900	1200	2.39	1.41	$0.783 \pm 0.008$
1700	1300	1.65	2.05	$0.758 \pm 0.009$	1900	1300	2.38	1.41	$0.785 \pm 0.009$
1700	1400	1.70	2.11	$0.736 \pm 0.008$	1900	1400	2.39	1.41	$0.784 \pm 0.008$
1700	1500	1.79	2.22	$0.700 \pm 0.009$	1900	1500	2.44	1.44	$0.767 \pm 0.008$
1700	1600	2.06	2.56	$0.607 \pm 0.009$	1900	1600	2.48	1.47	$0.754 \pm 0.008$
1800	100	81.1	71.6	$0.025 \pm 0.150$	1900	1700	2.62	1.55	$0.713 \pm 0.009$
1800	200	10.2	9.02	$0.170 \pm 0.055$	1900	1800	2.99	1.77	$0.624 \pm 0.009$
1800	300	4.45	3.93	$0.353 \pm 0.025$	2000	100	137	67.6	$0.021 \pm 0.169$
1800	400	3.08	2.72	$0.504 \pm 0.015$	2000	200	15.9	7.84	$0.143 \pm 0.065$
1800	500	2.52	2.23	$0.597 \pm 0.013$	2000	300	6.20	3.06	$0.318 \pm 0.032$
1800	600	2.28	2.01	$0.664 \pm 0.009$	2000	400	3.97	1.96	$0.472 \pm 0.018$
1800	700	2.15	1.90	$0.715 \pm 0.009$	2000	500	3.14	1.55	$0.583 \pm 0.012$
1800	800	2.07	1.83	$0.743 \pm 0.008$	2000	600	2.77	1.36	$0.656 \pm 0.010$
1800	900	2.05	1.81	$0.760 \pm 0.008$	2000	700	2.60	1.28	$0.702 \pm 0.009$
1800	1000	2.02	1.78	$0.772 \pm 0.009$	2000	800	2.48	1.22	$0.738 \pm 0.009$
1800	1100	1.99	1.76	$0.781 \pm 0.010$	2000	900	2.43	1.20	$0.762 \pm 0.008$
1800	1200	1.99	1.76	$0.780 \pm 0.008$	2000	1000	2.40	1.18	$0.780 \pm 0.008$
1800	1300	2.00	1.76	$0.779 \pm 0.008$	2000	1100	2.37	1.17	$0.788 \pm 0.010$
1800	1400	2.03	1.79	$0.766 \pm 0.008$	2000	1200	2.34	1.15	$0.798 \pm 0.008$
1800	1500	2.08	1.84	$0.746 \pm 0.008$	2000	1300	2.33	1.15	$0.799 \pm 0.009$
1800	1600	2.20	1.94	$0.706 \pm 0.010$	2000	1400	2.36	1.16	$0.792 \pm 0.008$
1800	1700	2.54	2.24	$0.612 \pm 0.009$	2000	1500	2.37	1.17	$0.785 \pm 0.009$
					2000	1600	2.40	1.19	$0.776 \pm 0.008$
					2000	1700	2.45	1.21	$0.761 \pm 0.009$
					2000	1800	2.59	1.28	$0.718 \pm 0.009$
					2000	1900	2.96	1.46	$0.629 \pm 0.009$

Table A19: The 95% CL observed (Obs.) and expected (Exp.) exclusion limits (in fb) on the  $W_R$  production cross section times branching fraction for  $W_R \rightarrow (ee + \mu\mu)jj$  as a function of  $W_R$  and  $N_\ell$  mass (in GeV) for  $2100 \leq M_{W_R} \leq 2300$  GeV. The signal acceptance (Acc.) is also included for each  $(M_{W_R}, M_{N_\ell})$  entry.

$M_{W_R}$	$M_{N_\ell}$	Obs.	Exp.	Acc.	$M_{W_R}$	$M_{N_\ell}$	Obs.	Exp.	Acc.
2100	100	172	79.3	$0.022 \pm 0.178$	2300	100	147	77.7	$0.020 \pm 0.197$
2100	200	18.5	8.55	$0.135 \pm 0.070$	2300	200	14.8	7.81	$0.127 \pm 0.082$
2100	300	7.14	3.30	$0.305 \pm 0.034$	2300	300	5.57	2.94	$0.286 \pm 0.041$
2100	400	4.41	2.04	$0.458 \pm 0.019$	2300	400	3.33	1.76	$0.425 \pm 0.023$
2100	500	3.39	1.57	$0.576 \pm 0.016$	2300	500	2.56	1.35	$0.543 \pm 0.015$
2100	600	2.90	1.34	$0.648 \pm 0.010$	2300	600	2.23	1.18	$0.641 \pm 0.011$
2100	700	2.65	1.22	$0.703 \pm 0.009$	2300	700	2.03	1.07	$0.683 \pm 0.010$
2100	800	2.50	1.16	$0.739 \pm 0.009$	2300	800	1.94	1.02	$0.730 \pm 0.009$
2100	900	2.42	1.12	$0.754 \pm 0.009$	2300	900	1.89	0.994	$0.755 \pm 0.009$
2100	1000	2.36	1.09	$0.780 \pm 0.008$	2300	1000	1.83	0.966	$0.774 \pm 0.008$
2100	1100	2.33	1.07	$0.787 \pm 0.008$	2300	1100	1.80	0.950	$0.788 \pm 0.009$
2100	1200	2.31	1.07	$0.793 \pm 0.009$	2300	1200	1.80	0.948	$0.797 \pm 0.009$
2100	1300	2.28	1.05	$0.802 \pm 0.009$	2300	1300	1.78	0.937	$0.806 \pm 0.017$
2100	1400	2.29	1.06	$0.799 \pm 0.009$	2300	1400	1.77	0.933	$0.810 \pm 0.008$
2100	1500	2.29	1.06	$0.797 \pm 0.008$	2300	1500	1.77	0.932	$0.811 \pm 0.009$
2100	1600	2.31	1.07	$0.790 \pm 0.008$	2300	1600	1.77	0.933	$0.809 \pm 0.009$
2100	1700	2.35	1.09	$0.776 \pm 0.009$	2300	1700	1.78	0.939	$0.803 \pm 0.009$
2100	1800	2.41	1.12	$0.756 \pm 0.009$	2300	1800	1.79	0.946	$0.798 \pm 0.017$
2100	1900	2.52	1.16	$0.725 \pm 0.008$	2300	1900	1.82	0.958	$0.787 \pm 0.009$
2100	2000	2.85	1.32	$0.641 \pm 0.009$	2300	2000	1.87	0.988	$0.763 \pm 0.009$
2200	100	159	76.4	$0.021 \pm 0.187$	2300	2100	1.96	1.03	$0.730 \pm 0.010$
2200	200	17.6	8.46	$0.129 \pm 0.076$	2300	2200	2.19	1.15	$0.654 \pm 0.009$
2200	300	6.82	3.28	$0.289 \pm 0.037$					
2200	400	4.30	2.07	$0.446 \pm 0.021$					
2200	500	3.35	1.61	$0.557 \pm 0.014$					
2200	600	2.87	1.38	$0.637 \pm 0.011$					
2200	700	2.60	1.25	$0.696 \pm 0.010$					
2200	800	2.44	1.17	$0.728 \pm 0.009$					
2200	900	2.35	1.13	$0.760 \pm 0.009$					
2200	1000	2.27	1.09	$0.780 \pm 0.008$					
2200	1100	2.23	1.07	$0.788 \pm 0.009$					
2200	1200	2.20	1.06	$0.796 \pm 0.021$					
2200	1300	2.17	1.04	$0.808 \pm 0.009$					
2200	1400	2.19	1.06	$0.798 \pm 0.009$					
2200	1500	2.18	1.05	$0.804 \pm 0.009$					
2200	1600	2.18	1.05	$0.803 \pm 0.009$					
2200	1700	2.20	1.06	$0.795 \pm 0.008$					
2200	1800	2.23	1.07	$0.783 \pm 0.009$					
2200	1900	2.29	1.10	$0.765 \pm 0.009$					
2200	2000	2.40	1.16	$0.728 \pm 0.009$					
2200	2100	2.69	1.29	$0.651 \pm 0.017$					

Table A20: The 95% CL observed (Obs.) and expected (Exp.) exclusion limits (in fb) on the  $W_R$  production cross section times branching fraction for  $W_R \rightarrow (ee + \mu\mu)jj$  as a function of  $W_R$  and  $N_\ell$  mass (in GeV) for  $2400 \leq M_{W_R} \leq 2500$  GeV. The signal acceptance (Acc.) is also included for each  $(M_{W_R}, M_{N_\ell})$  entry.

$M_{W_R}$	$M_{N_\ell}$	Obs.	Exp.	Acc.	$M_{W_R}$	$M_{N_\ell}$	Obs.	Exp.	Acc.
2400	100	151	88.1	$0.022 \pm 0.207$	2500	100	153	98.3	$0.024 \pm 0.217$
2400	200	14.0	8.18	$0.121 \pm 0.088$	2500	200	13.8	8.85	$0.119 \pm 0.095$
2400	300	5.00	2.93	$0.268 \pm 0.044$	2500	300	4.71	3.02	$0.254 \pm 0.049$
2400	400	2.90	1.69	$0.418 \pm 0.032$	2500	400	2.67	1.71	$0.401 \pm 0.032$
2400	500	2.15	1.26	$0.537 \pm 0.016$	2500	500	1.88	1.21	$0.527 \pm 0.018$
2400	600	1.79	1.05	$0.624 \pm 0.012$	2500	600	1.56	0.999	$0.612 \pm 0.013$
2400	700	1.63	0.956	$0.683 \pm 0.010$	2500	700	1.38	0.884	$0.674 \pm 0.011$
2400	800	1.53	0.895	$0.725 \pm 0.009$	2500	800	1.28	0.818	$0.722 \pm 0.009$
2400	900	1.55	0.909	$0.751 \pm 0.010$	2500	900	1.20	0.772	$0.744 \pm 0.009$
2400	1000	1.50	0.880	$0.773 \pm 0.009$	2500	1000	1.17	0.753	$0.771 \pm 0.009$
2400	1100	1.44	0.843	$0.789 \pm 0.008$	2500	1100	1.14	0.733	$0.785 \pm 0.009$
2400	1200	1.40	0.820	$0.803 \pm 0.009$	2500	1200	1.13	0.724	$0.798 \pm 0.009$
2400	1300	1.39	0.815	$0.809 \pm 0.009$	2500	1300	1.12	0.717	$0.805 \pm 0.008$
2400	1400	1.39	0.815	$0.807 \pm 0.008$	2500	1400	1.11	0.712	$0.811 \pm 0.008$
2400	1500	1.39	0.813	$0.810 \pm 0.008$	2500	1500	1.10	0.707	$0.816 \pm 0.009$
2400	1600	1.38	0.809	$0.814 \pm 0.009$	2500	1600	1.09	0.700	$0.824 \pm 0.009$
2400	1700	1.38	0.809	$0.813 \pm 0.012$	2500	1700	1.11	0.710	$0.812 \pm 0.011$
2400	1800	1.40	0.818	$0.804 \pm 0.012$	2500	1800	1.11	0.713	$0.809 \pm 0.010$
2400	1900	1.41	0.825	$0.798 \pm 0.009$	2500	1900	1.11	0.710	$0.812 \pm 0.012$
2400	2000	1.43	0.834	$0.789 \pm 0.008$	2500	2000	1.12	0.718	$0.803 \pm 0.008$
2400	2100	1.46	0.852	$0.772 \pm 0.008$	2500	2100	1.13	0.726	$0.794 \pm 0.008$
2400	2200	1.53	0.894	$0.736 \pm 0.009$	2500	2200	1.17	0.750	$0.769 \pm 0.010$
2400	2300	1.70	0.995	$0.660 \pm 0.011$	2500	2300	1.22	0.781	$0.737 \pm 0.009$
					2500	2400	1.36	0.869	$0.662 \pm 0.009$



Table A21: The 95% CL observed (Obs.) and expected (Exp.) exclusion limits (in fb) on the  $W_R$  production cross section times branching fraction for  $W_R \rightarrow (ee + \mu\mu)jj$  as a function of  $W_R$  and  $N_\ell$  mass (in GeV) for  $2600 \leq M_{W_R} \leq 2700$  GeV. The signal acceptance (Acc.) is also included for each  $(M_{W_R}, M_{N_\ell})$  entry.

$M_{W_R}$	$M_{N_\ell}$	Obs.	Exp.	Acc.	$M_{W_R}$	$M_{N_\ell}$	Obs.	Exp.	Acc.
2600	100	136	98.1	$0.021 \pm 0.225$	2700	100	134	94.6	$0.023 \pm 0.236$
2600	200	13.3	9.58	$0.115 \pm 0.101$	2700	200	14.1	9.94	$0.120 \pm 0.109$
2600	300	4.42	3.19	$0.246 \pm 0.053$	2700	300	4.70	3.31	$0.247 \pm 0.058$
2600	400	2.38	1.72	$0.392 \pm 0.031$	2700	400	2.48	1.75	$0.381 \pm 0.034$
2600	500	1.66	1.20	$0.509 \pm 0.019$	2700	500	1.70	1.20	$0.500 \pm 0.021$
2600	600	1.34	0.966	$0.605 \pm 0.014$	2700	600	1.34	0.940	$0.601 \pm 0.015$
2600	700	1.17	0.842	$0.672 \pm 0.011$	2700	700	1.18	0.831	$0.663 \pm 0.012$
2600	800	1.07	0.774	$0.715 \pm 0.010$	2700	800	1.10	0.772	$0.710 \pm 0.010$
2600	900	1.01	0.731	$0.738 \pm 0.010$	2700	900	1.02	0.715	$0.740 \pm 0.009$
2600	1000	0.965	0.698	$0.765 \pm 0.009$	2700	1000	0.943	0.664	$0.768 \pm 0.009$
2600	1100	0.931	0.672	$0.778 \pm 0.009$	2700	1100	0.914	0.643	$0.780 \pm 0.011$
2600	1200	0.937	0.677	$0.799 \pm 0.009$	2700	1200	0.861	0.606	$0.794 \pm 0.009$
2600	1300	0.909	0.657	$0.803 \pm 0.009$	2700	1300	0.867	0.611	$0.806 \pm 0.009$
2600	1400	0.903	0.652	$0.808 \pm 0.009$	2700	1400	0.882	0.621	$0.810 \pm 0.013$
2600	1500	0.899	0.649	$0.812 \pm 0.009$	2700	1500	0.874	0.615	$0.817 \pm 0.010$
2600	1600	0.888	0.641	$0.821 \pm 0.010$	2700	1600	0.868	0.611	$0.822 \pm 0.010$
2600	1700	0.887	0.641	$0.822 \pm 0.012$	2700	1700	0.870	0.613	$0.819 \pm 0.019$
2600	1800	0.891	0.644	$0.818 \pm 0.018$	2700	1800	0.866	0.610	$0.823 \pm 0.011$
2600	1900	0.894	0.646	$0.816 \pm 0.009$	2700	1900	0.869	0.612	$0.820 \pm 0.009$
2600	2000	0.899	0.650	$0.810 \pm 0.009$	2700	2000	0.870	0.612	$0.820 \pm 0.008$
2600	2100	0.905	0.654	$0.805 \pm 0.009$	2700	2100	0.873	0.614	$0.816 \pm 0.011$
2600	2200	0.917	0.663	$0.794 \pm 0.011$	2700	2200	0.888	0.625	$0.802 \pm 0.009$
2600	2300	0.940	0.679	$0.775 \pm 0.009$	2700	2300	0.899	0.633	$0.792 \pm 0.013$
2600	2400	0.988	0.714	$0.737 \pm 0.009$	2700	2400	0.921	0.648	$0.774 \pm 0.008$
2600	2500	1.10	0.792	$0.664 \pm 0.010$	2700	2500	0.965	0.679	$0.738 \pm 0.009$
					2700	2600	1.05	0.743	$0.674 \pm 0.010$

Table A22: The 95% CL observed (Obs.) and expected (Exp.) exclusion limits (in fb) on the  $W_R$  production cross section times branching fraction for  $W_R \rightarrow (ee + \mu\mu)jj$  as a function of  $W_R$  and  $N_\ell$  mass (in GeV) for  $2800 \leq M_{W_R} \leq 2900$  GeV. The signal acceptance (Acc.) is also included for each  $(M_{W_R}, M_{N_\ell})$  entry.

$M_{W_R}$	$M_{N_\ell}$	Obs.	Exp.	Acc.	$M_{W_R}$	$M_{N_\ell}$	Obs.	Exp.	Acc.
2800	100	143	101	$0.025 \pm 0.248$	2900	100	140	100	$0.027 \pm 0.255$
2800	200	16.5	11.6	$0.123 \pm 0.117$	2900	200	18.1	12.9	$0.123 \pm 0.126$
2800	300	5.46	3.86	$0.245 \pm 0.063$	2900	300	5.90	4.21	$0.236 \pm 0.070$
2800	400	2.81	1.99	$0.372 \pm 0.037$	2900	400	2.97	2.12	$0.377 \pm 0.042$
2800	500	1.86	1.32	$0.494 \pm 0.023$	2900	500	1.91	1.37	$0.485 \pm 0.030$
2800	600	1.45	1.02	$0.589 \pm 0.016$	2900	600	1.46	1.04	$0.582 \pm 0.017$
2800	700	1.22	0.861	$0.655 \pm 0.013$	2900	700	1.22	0.873	$0.647 \pm 0.014$
2800	800	1.12	0.793	$0.699 \pm 0.010$	2900	800	1.08	0.769	$0.692 \pm 0.011$
2800	900	1.01	0.713	$0.731 \pm 0.010$	2900	900	0.986	0.704	$0.729 \pm 0.010$
2800	1000	0.955	0.675	$0.758 \pm 0.011$	2900	1000	0.930	0.664	$0.751 \pm 0.009$
2800	1100	0.913	0.646	$0.773 \pm 0.011$	2900	1100	0.886	0.632	$0.772 \pm 0.015$
2800	1200	0.882	0.624	$0.794 \pm 0.010$	2900	1200	0.853	0.609	$0.790 \pm 0.011$
2800	1300	0.857	0.606	$0.804 \pm 0.009$	2900	1300	0.827	0.590	$0.805 \pm 0.009$
2800	1400	0.844	0.597	$0.811 \pm 0.009$	2900	1400	0.810	0.578	$0.811 \pm 0.009$
2800	1500	0.836	0.591	$0.819 \pm 0.009$	2900	1500	0.800	0.571	$0.814 \pm 0.009$
2800	1600	0.830	0.587	$0.824 \pm 0.009$	2900	1600	0.791	0.565	$0.823 \pm 0.009$
2800	1700	0.826	0.584	$0.827 \pm 0.009$	2900	1700	0.791	0.565	$0.823 \pm 0.010$
2800	1800	0.827	0.585	$0.826 \pm 0.009$	2900	1800	0.783	0.559	$0.831 \pm 0.017$
2800	1900	0.829	0.586	$0.824 \pm 0.009$	2900	1900	0.785	0.561	$0.829 \pm 0.010$
2800	2000	0.830	0.587	$0.823 \pm 0.009$	2900	2000	0.782	0.559	$0.831 \pm 0.021$
2800	2100	0.832	0.588	$0.821 \pm 0.009$	2900	2100	0.797	0.569	$0.816 \pm 0.009$
2800	2200	0.843	0.596	$0.810 \pm 0.009$	2900	2200	0.792	0.565	$0.821 \pm 0.010$
2800	2300	0.850	0.601	$0.803 \pm 0.009$	2900	2300	0.798	0.570	$0.815 \pm 0.010$
2800	2400	0.857	0.606	$0.796 \pm 0.009$	2900	2400	0.805	0.575	$0.808 \pm 0.011$
2800	2500	0.879	0.622	$0.776 \pm 0.008$	2900	2500	0.814	0.581	$0.798 \pm 0.009$
2800	2600	0.921	0.651	$0.741 \pm 0.011$	2900	2600	0.838	0.598	$0.776 \pm 0.010$
2800	2700	1.01	0.711	$0.678 \pm 0.010$	2900	2700	0.876	0.625	$0.742 \pm 0.009$
					2900	2800	0.947	0.676	$0.686 \pm 0.013$

Table A23: The 95% CL observed (Obs.) and expected (Exp.) exclusion limits (in fb) on the  $W_R$  production cross section times branching fraction for  $W_R \rightarrow (ee + \mu\mu)jj$  as a function of  $W_R$  and  $N_\ell$  mass (in GeV) for  $3000 \leq M_{W_R} \leq 3100$  GeV. The signal acceptance (Acc.) is also included for each  $(M_{W_R}, M_{N_\ell})$  entry.

$M_{W_R}$	$M_{N_\ell}$	Obs.	Exp.	Acc.	$M_{W_R}$	$M_{N_\ell}$	Obs.	Exp.	Acc.
3000	100	137	99.7	$0.027 \pm 0.264$	3100	100	141	103	$0.032 \pm 0.269$
3000	200	20.3	14.7	$0.124 \pm 0.135$	3100	200	23.0	16.7	$0.137 \pm 0.142$
3000	300	6.40	4.66	$0.245 \pm 0.078$	3100	300	7.33	5.32	$0.250 \pm 0.086$
3000	400	3.21	2.33	$0.369 \pm 0.048$	3100	400	3.53	2.56	$0.373 \pm 0.054$
3000	500	2.04	1.49	$0.482 \pm 0.030$	3100	500	2.24	1.63	$0.475 \pm 0.034$
3000	600	1.52	1.10	$0.573 \pm 0.019$	3100	600	1.63	1.18	$0.565 \pm 0.022$
3000	700	1.25	0.908	$0.637 \pm 0.014$	3100	700	1.32	0.959	$0.634 \pm 0.018$
3000	800	1.09	0.796	$0.685 \pm 0.012$	3100	800	1.14	0.827	$0.685 \pm 0.012$
3000	900	0.993	0.722	$0.721 \pm 0.011$	3100	900	1.02	0.744	$0.724 \pm 0.012$
3000	1000	0.928	0.675	$0.757 \pm 0.010$	3100	1000	0.952	0.691	$0.745 \pm 0.010$
3000	1100	0.879	0.640	$0.773 \pm 0.011$	3100	1100	0.893	0.648	$0.768 \pm 0.011$
3000	1200	0.845	0.614	$0.785 \pm 0.012$	3100	1200	0.857	0.622	$0.787 \pm 0.016$
3000	1300	0.818	0.595	$0.795 \pm 0.012$	3100	1300	0.827	0.600	$0.798 \pm 0.013$
3000	1400	0.797	0.579	$0.809 \pm 0.011$	3100	1400	0.799	0.580	$0.809 \pm 0.020$
3000	1500	0.779	0.567	$0.820 \pm 0.009$	3100	1500	0.779	0.565	$0.812 \pm 0.010$
3000	1600	0.775	0.564	$0.823 \pm 0.010$	3100	1600	0.772	0.560	$0.823 \pm 0.017$
3000	1700	0.769	0.560	$0.829 \pm 0.010$	3100	1700	0.765	0.556	$0.829 \pm 0.010$
3000	1800	0.771	0.561	$0.827 \pm 0.011$	3100	1800	0.765	0.555	$0.829 \pm 0.017$
3000	1900	0.771	0.561	$0.827 \pm 0.013$	3100	1900	0.765	0.555	$0.828 \pm 0.011$
3000	2000	0.766	0.557	$0.833 \pm 0.016$	3100	2000	0.760	0.552	$0.834 \pm 0.011$
3000	2100	0.767	0.558	$0.831 \pm 0.009$	3100	2100	0.765	0.555	$0.828 \pm 0.024$
3000	2200	0.774	0.563	$0.823 \pm 0.022$	3100	2200	0.762	0.554	$0.831 \pm 0.012$
3000	2300	0.773	0.563	$0.824 \pm 0.014$	3100	2300	0.765	0.556	$0.827 \pm 0.011$
3000	2400	0.779	0.567	$0.818 \pm 0.010$	3100	2400	0.770	0.559	$0.822 \pm 0.009$
3000	2500	0.788	0.573	$0.808 \pm 0.011$	3100	2500	0.777	0.564	$0.814 \pm 0.009$
3000	2600	0.798	0.581	$0.798 \pm 0.009$	3100	2600	0.782	0.567	$0.810 \pm 0.009$
3000	2700	0.814	0.592	$0.782 \pm 0.009$	3100	2700	0.792	0.575	$0.799 \pm 0.010$
3000	2800	0.853	0.621	$0.746 \pm 0.009$	3100	2800	0.812	0.590	$0.779 \pm 0.009$
3000	2900	0.923	0.672	$0.689 \pm 0.013$	3100	2900	0.845	0.613	$0.749 \pm 0.009$
					3100	3000	0.915	0.664	$0.692 \pm 0.013$

Table A24: The 95% CL observed (Obs.) and expected (Exp.) exclusion limits (in fb) on the  $W_R$  production cross section times branching fraction for  $W_R \rightarrow (ee + \mu\mu)jj$  as a function of  $W_R$  and  $N_\ell$  mass (in GeV) for  $M_{W_R} = 3200$  GeV. The signal acceptance (Acc.) is also included for each  $(M_{W_R}, M_{N_\ell})$  entry.

$M_{W_R}$	$M_{N_\ell}$	Obs.	Exp.	Acc.
3200	100	144	104	$0.035 \pm 0.274$
3200	200	25.9	18.7	$0.139 \pm 0.147$
3200	300	8.16	5.90	$0.265 \pm 0.091$
3200	400	3.98	2.88	$0.376 \pm 0.059$
3200	500	2.46	1.78	$0.471 \pm 0.041$
3200	600	1.77	1.28	$0.560 \pm 0.025$
3200	700	1.41	1.02	$0.626 \pm 0.019$
3200	800	1.20	0.871	$0.679 \pm 0.014$
3200	900	1.07	0.772	$0.712 \pm 0.016$
3200	1000	0.983	0.711	$0.741 \pm 0.012$
3200	1100	0.920	0.665	$0.768 \pm 0.016$
3200	1200	0.870	0.629	$0.781 \pm 0.010$
3200	1300	0.838	0.606	$0.795 \pm 0.016$
3200	1400	0.809	0.585	$0.804 \pm 0.013$
3200	1500	0.785	0.568	$0.813 \pm 0.011$
3200	1600	0.769	0.556	$0.823 \pm 0.010$
3200	1700	0.767	0.555	$0.824 \pm 0.016$
3200	1800	0.760	0.550	$0.831 \pm 0.013$
3200	1900	0.758	0.548	$0.832 \pm 0.016$
3200	2000	0.756	0.547	$0.834 \pm 0.020$
3200	2100	0.762	0.551	$0.828 \pm 0.010$
3200	2200	0.756	0.547	$0.835 \pm 0.013$
3200	2300	0.762	0.551	$0.829 \pm 0.011$
3200	2400	0.765	0.553	$0.825 \pm 0.009$
3200	2500	0.770	0.557	$0.819 \pm 0.010$
3200	2600	0.775	0.560	$0.814 \pm 0.010$
3200	2700	0.778	0.563	$0.811 \pm 0.013$
3200	2800	0.791	0.572	$0.797 \pm 0.012$
3200	2900	0.813	0.588	$0.776 \pm 0.013$
3200	3000	0.837	0.605	$0.753 \pm 0.010$
3200	3100	0.909	0.658	$0.693 \pm 0.024$

## B The CMS Collaboration

### Yerevan Physics Institute, Yerevan, Armenia

V. Khachatryan, A.M. Sirunyan, A. Tumasyan

### Institut für Hochenergiephysik der OeAW, Wien, Austria

W. Adam, T. Bergauer, M. Dragicevic, J. Erö, C. Fabjan<sup>1</sup>, M. Friedl, R. Frühwirth<sup>1</sup>, V.M. Ghete, C. Hartl, N. Hörmann, J. Hrubec, M. Jeitler<sup>1</sup>, W. Kiesenhofer, V. Knünz, M. Krammer<sup>1</sup>, I. Krätschmer, D. Liko, I. Mikulec, D. Rabady<sup>2</sup>, B. Rahbaran, H. Rohringer, R. Schöfbeck, J. Strauss, A. Taurok, W. Treberer-Treberspurg, W. Waltenberger, C.-E. Wulz<sup>1</sup>

### National Centre for Particle and High Energy Physics, Minsk, Belarus

V. Mossolov, N. Shumeiko, J. Suarez Gonzalez

### Universiteit Antwerpen, Antwerpen, Belgium

S. Alderweireldt, M. Bansal, S. Bansal, T. Cornelis, E.A. De Wolf, X. Janssen, A. Knutsson, S. Luyckx, S. Ochesanu, B. Roland, R. Rougny, M. Van De Klundert, H. Van Haevermaet, P. Van Mechelen, N. Van Remortel, A. Van Spilbeeck

### Vrije Universiteit Brussel, Brussel, Belgium

F. Blekman, S. Blyweert, J. D'Hondt, N. Daci, N. Heracleous, J. Keaveney, S. Lowette, M. Maes, A. Olbrechts, Q. Python, D. Strom, S. Tavernier, W. Van Doninck, P. Van Mulders, G.P. Van Onsem, I. Vilella

### Université Libre de Bruxelles, Bruxelles, Belgium

C. Caillol, B. Clerbaux, G. De Lentdecker, D. Dobur, L. Favart, A.P.R. Gay, A. Grebenyuk, A. Léonard, A. Mohammadi, L. Perniè<sup>2</sup>, T. Reis, T. Seva, L. Thomas, C. Vander Velde, P. Vanlaer, J. Wang

### Ghent University, Ghent, Belgium

V. Adler, K. Beernaert, L. Benucci, A. Cimmino, S. Costantini, S. Crucy, S. Dildick, A. Fagot, G. Garcia, J. McCartin, A.A. Ocampo Rios, D. Ryckbosch, S. Salva Diblen, M. Sigamani, N. Strobbe, F. Thyssen, M. Tytgat, E. Yazgan, N. Zaganidis

### Université Catholique de Louvain, Louvain-la-Neuve, Belgium

S. Basegmez, C. Beluffi<sup>3</sup>, G. Bruno, R. Castello, A. Caudron, L. Ceard, G.G. Da Silveira, C. Delaere, T. du Pree, D. Favart, L. Forthomme, A. Giammanco<sup>4</sup>, J. Hollar, P. Jez, M. Komm, V. Lemaître, C. Nuttens, D. Pagano, L. Perrini, A. Pin, K. Piotrkowski, A. Popov<sup>5</sup>, L. Quertenmont, M. Selvaggi, M. Vidal Marono, J.M. Vizan Garcia

### Université de Mons, Mons, Belgium

N. Bely, T. Caebergs, E. Daubie, G.H. Hammad

### Centro Brasileiro de Pesquisas Físicas, Rio de Janeiro, Brazil

W.L. Aldá Júnior, G.A. Alves, L. Brito, M. Correa Martins Junior, M.E. Pol

### Universidade do Estado do Rio de Janeiro, Rio de Janeiro, Brazil

W. Carvalho, J. Chinellato<sup>6</sup>, A. Custódio, E.M. Da Costa, D. De Jesus Damiao, C. De Oliveira Martins, S. Fonseca De Souza, H. Malbouisson, D. Matos Figueiredo, L. Mundim, H. Nogima, W.L. Prado Da Silva, J. Santaolalla, A. Santoro, A. Sznajder, E.J. Tonelli Manganote<sup>6</sup>, A. Vilela Pereira

### Universidade Estadual Paulista <sup>a</sup>, Universidade Federal do ABC <sup>b</sup>, São Paulo, Brazil

C.A. Bernardes<sup>b</sup>, T.R. Fernandez Perez Tomei<sup>a</sup>, E.M. Gregores<sup>b</sup>, P.G. Mercadante<sup>b</sup>, S.F. Novaes<sup>a</sup>, Sandra S. Padula<sup>a</sup>

**Institute for Nuclear Research and Nuclear Energy, Sofia, Bulgaria**

A. Aleksandrov, V. Genchev<sup>2</sup>, P. Iaydjiev, A. Marinov, S. Piperov, M. Rodozov, G. Sultanov, M. Vutova

**University of Sofia, Sofia, Bulgaria**

A. Dimitrov, I. Glushkov, R. Hadjiiska, V. Kozhuharov, L. Litov, B. Pavlov, P. Petkov

**Institute of High Energy Physics, Beijing, China**

J.G. Bian, G.M. Chen, H.S. Chen, M. Chen, R. Du, C.H. Jiang, D. Liang, S. Liang, R. Plestina<sup>7</sup>, J. Tao, X. Wang, Z. Wang

**State Key Laboratory of Nuclear Physics and Technology, Peking University, Beijing, China**

C. Asawatangtrakuldee, Y. Ban, Y. Guo, Q. Li, W. Li, S. Liu, Y. Mao, S.J. Qian, D. Wang, L. Zhang, W. Zou

**Universidad de Los Andes, Bogota, Colombia**

C. Avila, L.F. Chaparro Sierra, C. Florez, J.P. Gomez, B. Gomez Moreno, J.C. Sanabria

**Technical University of Split, Split, Croatia**

N. Godinovic, D. Lelas, D. Polic, I. Puljak

**University of Split, Split, Croatia**

Z. Antunovic, M. Kovac

**Institute Rudjer Boskovic, Zagreb, Croatia**

V. Brigljevic, K. Kadija, J. Luetic, D. Mekterovic, L. Sudic

**University of Cyprus, Nicosia, Cyprus**

A. Attikis, G. Mavromanolakis, J. Mousa, C. Nicolaou, F. Ptochos, P.A. Razis

**Charles University, Prague, Czech Republic**

M. Bodlak, M. Finger, M. Finger Jr.<sup>8</sup>

**Academy of Scientific Research and Technology of the Arab Republic of Egypt, Egyptian Network of High Energy Physics, Cairo, Egypt**

Y. Assran<sup>9</sup>, S. Elgammal<sup>10</sup>, M.A. Mahmoud<sup>11</sup>, A. Radi<sup>10,12</sup>

**National Institute of Chemical Physics and Biophysics, Tallinn, Estonia**

M. Kadastik, M. Murumaa, M. Raidal, A. Tiko

**Department of Physics, University of Helsinki, Helsinki, Finland**

P. Eerola, G. Fedi, M. Voutilainen

**Helsinki Institute of Physics, Helsinki, Finland**

J. Härkönen, V. Karimäki, R. Kinnunen, M.J. Kortelainen, T. Lampén, K. Lassila-Perini, S. Lehti, T. Lindén, P. Luukka, T. Mäenpää, T. Peltola, E. Tuominen, J. Tuominiemi, E. Tuovinen, L. Wendland

**Lappeenranta University of Technology, Lappeenranta, Finland**

T. Tuuva

**DSM/IRFU, CEA/Saclay, Gif-sur-Yvette, France**

M. Besancon, F. Couderc, M. Dejardin, D. Denegri, B. Fabbro, J.L. Faure, C. Favaro, F. Ferri, S. Ganjour, A. Givernaud, P. Gras, G. Hamel de Monchenault, P. Jarry, E. Locci, J. Malcles, J. Rander, A. Rosowsky, M. Titov

**Laboratoire Leprince-Ringuet, Ecole Polytechnique, IN2P3-CNRS, Palaiseau, France**

S. Baffioni, F. Beaudette, P. Busson, C. Charlot, T. Dahms, M. Dalchenko, L. Dobrzynski, N. Filipovic, A. Florent, R. Granier de Cassagnac, L. Mastrolorenzo, P. Miné, C. Mironov, I.N. Naranjo, M. Nguyen, C. Ochando, P. Paganini, R. Salerno, J.b. Sauvan, Y. Sirois, C. Veelken, Y. Yilmaz, A. Zabi

**Institut Pluridisciplinaire Hubert Curien, Université de Strasbourg, Université de Haute Alsace Mulhouse, CNRS/IN2P3, Strasbourg, France**

J.-L. Agram<sup>13</sup>, J. Andrea, A. Aubin, D. Bloch, J.-M. Brom, E.C. Chabert, C. Collard, E. Conte<sup>13</sup>, J.-C. Fontaine<sup>13</sup>, D. Gelé, U. Goerlach, C. Goetzmann, A.-C. Le Bihan, P. Van Hove

**Centre de Calcul de l'Institut National de Physique Nucleaire et de Physique des Particules, CNRS/IN2P3, Villeurbanne, France**

S. Gadrat

**Université de Lyon, Université Claude Bernard Lyon 1, CNRS-IN2P3, Institut de Physique Nucléaire de Lyon, Villeurbanne, France**

S. Beauceron, N. Beaupere, G. Boudoul<sup>2</sup>, S. Brochet, C.A. Carrillo Montoya, J. Chasserat, R. Chierici, D. Contardo<sup>2</sup>, P. Depasse, H. El Mamouni, J. Fan, J. Fay, S. Gascon, M. Gouzevitch, B. Ille, T. Kurca, M. Lethuillier, L. Mirabito, S. Perries, J.D. Ruiz Alvarez, D. Sabes, L. Sgandurra, V. Sordini, M. Vander Donckt, P. Verdier, S. Viret, H. Xiao

**Institute of High Energy Physics and Informatization, Tbilisi State University, Tbilisi, Georgia**

I. Bagaturia

**RWTH Aachen University, I. Physikalisches Institut, Aachen, Germany**

C. Autermann, S. Beranek, M. Bontenackels, M. Edelhoff, L. Feld, O. Hindrichs, K. Klein, A. Ostapchuk, A. Perieanu, F. Raupach, J. Sammet, S. Schael, H. Weber, B. Wittmer, V. Zhukov<sup>5</sup>

**RWTH Aachen University, III. Physikalisches Institut A, Aachen, Germany**

M. Ata, E. Dietz-Laursonn, D. Duchardt, M. Erdmann, R. Fischer, A. Güth, T. Hebbeker, C. Heidemann, K. Hoepfner, D. Klingebiel, S. Knutzen, P. Kreuzer, M. Merschmeyer, A. Meyer, P. Millet, M. Olschewski, K. Padeken, P. Papacz, H. Reithler, S.A. Schmitz, L. Sonnenschein, D. Teyssier, S. Thüer, M. Weber

**RWTH Aachen University, III. Physikalisches Institut B, Aachen, Germany**

V. Cherepanov, Y. Erdogan, G. Flügge, H. Geenen, M. Geisler, W. Haj Ahmad, F. Hoehle, B. Kargoll, T. Kress, Y. Kuessel, J. Lingemann<sup>2</sup>, A. Nowack, I.M. Nugent, L. Perchalla, O. Pooth, A. Stahl

**Deutsches Elektronen-Synchrotron, Hamburg, Germany**

I. Asin, N. Bartosik, J. Behr, W. Behrenhoff, U. Behrens, A.J. Bell, M. Bergholz<sup>14</sup>, A. Bethani, K. Borras, A. Burgmeier, A. Cakir, L. Calligaris, A. Campbell, S. Choudhury, F. Costanza, C. Diez Pardos, S. Dooling, T. Dorland, G. Eckerlin, D. Eckstein, T. Eichhorn, G. Flucke, J. Garay Garcia, A. Geiser, P. Gunnellini, J. Hauk, G. Hellwig, M. Hempel, D. Horton, H. Jung, A. Kalogeropoulos, M. Kasemann, P. Katsas, J. Kieseler, C. Kleinwort, D. Krücker, W. Lange, J. Leonard, K. Lipka, A. Lobanov, W. Lohmann<sup>14</sup>, B. Lutz, R. Mankel, I. Marfin, I.-A. Melzer-Pellmann, A.B. Meyer, J. Mnich, A. Mussgiller, S. Naumann-Emme, A. Nayak, O. Novgorodova, F. Nowak, E. Ntomari, H. Perrey, D. Pitzl, R. Placakyte, A. Raspereza, P.M. Ribeiro Cipriano, E. Ron, M.Ö. Sahin, J. Salfeld-Nebgen, P. Saxena, R. Schmidt<sup>14</sup>, T. Schoerner-Sadenius, M. Schröder, C. Seitz, S. Spannagel, A.D.R. Vargas Trevino, R. Walsh, C. Wissing

**University of Hamburg, Hamburg, Germany**

M. Aldaya Martin, V. Blobel, M. Centis Vignali, A.r. Draeger, J. Erfle, E. Garutti, K. Goebel, M. Görner, J. Haller, M. Hoffmann, R.S. Höing, H. Kirschenmann, R. Klanner, R. Kogler, J. Lange, T. Lapsien, T. Lenz, I. Marchesini, J. Ott, T. Peiffer, N. Pietsch, T. Pöhlsen, D. Rathjens, C. Sander, H. Schettler, P. Schleper, E. Schlieckau, A. Schmidt, M. Seidel, J. Sibille<sup>15</sup>, V. Sola, H. Stadie, G. Steinbrück, D. Troendle, E. Usai, L. Vanelderen

**Institut für Experimentelle Kernphysik, Karlsruhe, Germany**

C. Barth, C. Baus, J. Berger, C. Böser, E. Butz, T. Chwalek, W. De Boer, A. Descroix, A. Dierlamm, M. Feindt, F. Frensch, M. Giffels, F. Hartmann<sup>2</sup>, T. Hauth<sup>2</sup>, U. Husemann, I. Katkov<sup>5</sup>, A. Kornmayer<sup>2</sup>, E. Kuznetsova, P. Lobelle Pardo, M.U. Mozer, Th. Müller, A. Nürnberg, G. Quast, K. Rabbertz, F. Ratnikov, S. Röcker, H.J. Simonis, F.M. Stober, R. Ulrich, J. Wagner-Kuhr, S. Wayand, T. Weiler, R. Wolf

**Institute of Nuclear and Particle Physics (INPP), NCSR Demokritos, Aghia Paraskevi, Greece**

G. Anagnostou, G. Daskalakis, T. Gerasis, V.A. Giakoumopoulou, A. Kyriakis, D. Loukas, A. Markou, C. Markou, A. Psallidas, I. Topsis-Giotis

**University of Athens, Athens, Greece**

A. Panagiotou, N. Saoulidou, E. Stiliaris

**University of Ioánnina, Ioánnina, Greece**

X. Aslanoglou, I. Evangelou, G. Flouris, C. Foudas, P. Kokkas, N. Manthos, I. Papadopoulos, E. Paradas

**Wigner Research Centre for Physics, Budapest, Hungary**

G. Bencze, C. Hajdu, P. Hidas, D. Horvath<sup>16</sup>, F. Sikler, V. Veszpremi, G. Vesztergombi<sup>17</sup>, A.J. Zsigmond

**Institute of Nuclear Research ATOMKI, Debrecen, Hungary**

N. Beni, S. Czellar, J. Karancsi<sup>18</sup>, J. Molnar, J. Palinkas, Z. Szillasi

**University of Debrecen, Debrecen, Hungary**

P. Raics, Z.L. Trocsanyi, B. Ujvari

**National Institute of Science Education and Research, Bhubaneswar, India**

S.K. Swain

**Panjab University, Chandigarh, India**

S.B. Beri, V. Bhatnagar, N. Dhingra, R. Gupta, U. Bhawandeep, A.K. Kalsi, M. Kaur, M. Mittal, N. Nishu, J.B. Singh

**University of Delhi, Delhi, India**

Ashok Kumar, Arun Kumar, S. Ahuja, A. Bhardwaj, B.C. Choudhary, A. Kumar, S. Malhotra, M. Naimuddin, K. Ranjan, V. Sharma

**Saha Institute of Nuclear Physics, Kolkata, India**

S. Banerjee, S. Bhattacharya, K. Chatterjee, S. Dutta, B. Gomber, Sa. Jain, Sh. Jain, R. Khurana, A. Modak, S. Mukherjee, D. Roy, S. Sarkar, M. Sharan

**Bhabha Atomic Research Centre, Mumbai, India**

A. Abdulsalam, D. Dutta, S. Kailas, V. Kumar, A.K. Mohanty<sup>2</sup>, L.M. Pant, P. Shukla, A. Topkar

**Tata Institute of Fundamental Research, Mumbai, India**

T. Aziz, S. Banerjee, S. Bhowmik<sup>19</sup>, R.M. Chatterjee, R.K. Dewanjee, S. Dugad, S. Ganguly,



S. Ghosh, M. Guchait, A. Gurtu<sup>20</sup>, G. Kole, S. Kumar, M. Maity<sup>19</sup>, G. Majumder, K. Mazumdar, G.B. Mohanty, B. Parida, K. Sudhakar, N. Wickramage<sup>21</sup>

**Institute for Research in Fundamental Sciences (IPM), Tehran, Iran**

H. Bakhshiansohi, H. Behnamian, S.M. Etesami<sup>22</sup>, A. Fahim<sup>23</sup>, R. Goldouzian, A. Jafari, M. Khakzad, M. Mohammadi Najafabadi, M. Naseri, S. Paktinat Mehdiabadi, B. Safarzadeh<sup>24</sup>, M. Zeinali

**University College Dublin, Dublin, Ireland**

M. Felcini, M. Grunewald

**INFN Sezione di Bari <sup>a</sup>, Università di Bari <sup>b</sup>, Politecnico di Bari <sup>c</sup>, Bari, Italy**

M. Abbrescia<sup>a,b</sup>, L. Barbone<sup>a,b</sup>, C. Calabria<sup>a,b</sup>, S.S. Chhibra<sup>a,b</sup>, A. Colaleo<sup>a</sup>, D. Creanza<sup>a,c</sup>, N. De Filippis<sup>a,c</sup>, M. De Palma<sup>a,b</sup>, L. Fiore<sup>a</sup>, G. Iaselli<sup>a,c</sup>, G. Maggi<sup>a,c</sup>, M. Maggi<sup>a</sup>, S. My<sup>a,c</sup>, S. Nuzzo<sup>a,b</sup>, A. Pompili<sup>a,b</sup>, G. Pugliese<sup>a,c</sup>, R. Radogna<sup>a,b,2</sup>, G. Selvaggi<sup>a,b</sup>, L. Silvestris<sup>a,2</sup>, G. Singh<sup>a,b</sup>, R. Venditti<sup>a,b</sup>, P. Verwilligen<sup>a</sup>, G. Zito<sup>a</sup>

**INFN Sezione di Bologna <sup>a</sup>, Università di Bologna <sup>b</sup>, Bologna, Italy**

G. Abbiendi<sup>a</sup>, A.C. Benvenuti<sup>a</sup>, D. Bonacorsi<sup>a,b</sup>, S. Braibant-Giacomelli<sup>a,b</sup>, L. Brigliadori<sup>a,b</sup>, R. Campanini<sup>a,b</sup>, P. Capiluppi<sup>a,b</sup>, A. Castro<sup>a,b</sup>, F.R. Cavallo<sup>a</sup>, G. Codispoti<sup>a,b</sup>, M. Cuffiani<sup>a,b</sup>, G.M. Dallavalle<sup>a</sup>, F. Fabbri<sup>a</sup>, A. Fanfani<sup>a,b</sup>, D. Fasanella<sup>a,b</sup>, P. Giacomelli<sup>a</sup>, C. Grandi<sup>a</sup>, L. Guiducci<sup>a,b</sup>, S. Marcellini<sup>a</sup>, G. Masetti<sup>a,2</sup>, A. Montanari<sup>a</sup>, F.L. Navarria<sup>a,b</sup>, A. Perrotta<sup>a</sup>, F. Primavera<sup>a,b</sup>, A.M. Rossi<sup>a,b</sup>, T. Rovelli<sup>a,b</sup>, G.P. Siroli<sup>a,b</sup>, N. Tosi<sup>a,b</sup>, R. Travaglini<sup>a,b</sup>

**INFN Sezione di Catania <sup>a</sup>, Università di Catania <sup>b</sup>, CSFNSM <sup>c</sup>, Catania, Italy**

S. Albergo<sup>a,b</sup>, G. Cappello<sup>a</sup>, M. Chiorboli<sup>a,b</sup>, S. Costa<sup>a,b</sup>, F. Giordano<sup>a,c,2</sup>, R. Potenza<sup>a,b</sup>, A. Tricoli<sup>a,b</sup>, C. Tuve<sup>a,b</sup>

**INFN Sezione di Firenze <sup>a</sup>, Università di Firenze <sup>b</sup>, Firenze, Italy**

G. Barbagli<sup>a</sup>, V. Ciulli<sup>a,b</sup>, C. Civinini<sup>a</sup>, R. D'Alessandro<sup>a,b</sup>, E. Focardi<sup>a,b</sup>, E. Gallo<sup>a</sup>, S. Gonzi<sup>a,b</sup>, V. Gori<sup>a,b,2</sup>, P. Lenzi<sup>a,b</sup>, M. Meschini<sup>a</sup>, S. Paoletti<sup>a</sup>, G. Sguazzoni<sup>a</sup>, A. Tropiano<sup>a,b</sup>

**INFN Laboratori Nazionali di Frascati, Frascati, Italy**

L. Benussi, S. Bianco, F. Fabbri, D. Piccolo

**INFN Sezione di Genova <sup>a</sup>, Università di Genova <sup>b</sup>, Genova, Italy**

F. Ferro<sup>a</sup>, M. Lo Vetere<sup>a,b</sup>, E. Robutti<sup>a</sup>, S. Tosi<sup>a,b</sup>

**INFN Sezione di Milano-Bicocca <sup>a</sup>, Università di Milano-Bicocca <sup>b</sup>, Milano, Italy**

M.E. Dinardo<sup>a,b</sup>, P. Dini<sup>a</sup>, S. Fiorendi<sup>a,b,2</sup>, S. Gennai<sup>a,2</sup>, R. Gerosa<sup>2</sup>, A. Ghezzi<sup>a,b</sup>, P. Govoni<sup>a,b</sup>, M.T. Lucchini<sup>a,b,2</sup>, S. Malvezzi<sup>a</sup>, R.A. Manzoni<sup>a,b</sup>, A. Martelli<sup>a,b</sup>, B. Marzocchi, D. Menasce<sup>a</sup>, L. Moroni<sup>a</sup>, M. Paganoni<sup>a,b</sup>, S. Ragazzi<sup>a,b</sup>, N. Redaelli<sup>a</sup>, T. Tabarelli de Fatis<sup>a,b</sup>

**INFN Sezione di Napoli <sup>a</sup>, Università di Napoli 'Federico II' <sup>b</sup>, Università della Basilicata (Potenza) <sup>c</sup>, Università G. Marconi (Roma) <sup>d</sup>, Napoli, Italy**

S. Buontempo<sup>a</sup>, N. Cavallo<sup>a,c</sup>, S. Di Guida<sup>a,d,2</sup>, F. Fabozzi<sup>a,c</sup>, A.O.M. Iorio<sup>a,b</sup>, L. Lista<sup>a</sup>, S. Meola<sup>a,d,2</sup>, M. Merola<sup>a</sup>, P. Paolucci<sup>a,2</sup>

**INFN Sezione di Padova <sup>a</sup>, Università di Padova <sup>b</sup>, Università di Trento (Trento) <sup>c</sup>, Padova, Italy**

P. Azzi<sup>a</sup>, N. Bacchetta<sup>a</sup>, D. Bisello<sup>a,b</sup>, A. Branca<sup>a,b</sup>, R. Carlin<sup>a,b</sup>, P. Checchia<sup>a</sup>, M. Dall'Osso<sup>a,b</sup>, T. Dorigo<sup>a</sup>, M. Galanti<sup>a,b</sup>, F. Gasparini<sup>a,b</sup>, U. Gasparini<sup>a,b</sup>, P. Giubilato<sup>a,b</sup>, F. Gonella<sup>a</sup>, A. Gozzelino<sup>a</sup>, K. Kanishchev<sup>a,c</sup>, S. Lacaprara<sup>a</sup>, M. Margoni<sup>a,b</sup>, A.T. Meneguzzo<sup>a,b</sup>, F. Montecassiano<sup>a</sup>, J. Pazzini<sup>a,b</sup>, N. Pozzobon<sup>a,b</sup>, P. Ronchese<sup>a,b</sup>, F. Simonetto<sup>a,b</sup>, E. Torassa<sup>a</sup>, M. Tosi<sup>a,b</sup>, P. Zotto<sup>a,b</sup>, A. Zucchetta<sup>a,b</sup>

**INFN Sezione di Pavia <sup>a</sup>, Università di Pavia <sup>b</sup>, Pavia, Italy**M. Gabusi<sup>a,b</sup>, S.P. Ratti<sup>a,b</sup>, C. Riccardi<sup>a,b</sup>, P. Salvini<sup>a</sup>, P. Vitulo<sup>a,b</sup>**INFN Sezione di Perugia <sup>a</sup>, Università di Perugia <sup>b</sup>, Perugia, Italy**M. Biasini<sup>a,b</sup>, G.M. Bilei<sup>a</sup>, D. Ciangottini<sup>a,b</sup>, L. Fanò<sup>a,b</sup>, P. Lariccia<sup>a,b</sup>, G. Mantovani<sup>a,b</sup>, M. Menichelli<sup>a</sup>, F. Romeo<sup>a,b</sup>, A. Saha<sup>a</sup>, A. Santocchia<sup>a,b</sup>, A. Spiezia<sup>a,b,2</sup>**INFN Sezione di Pisa <sup>a</sup>, Università di Pisa <sup>b</sup>, Scuola Normale Superiore di Pisa <sup>c</sup>, Pisa, Italy**K. Androsov<sup>a,25</sup>, P. Azzurri<sup>a</sup>, G. Bagliesi<sup>a</sup>, J. Bernardini<sup>a</sup>, T. Boccali<sup>a</sup>, G. Broccolo<sup>a,c</sup>, R. Castaldi<sup>a</sup>, M.A. Ciocci<sup>a,25</sup>, R. Dell'Orso<sup>a</sup>, S. Donato<sup>a,c</sup>, F. Fiori<sup>a,c</sup>, L. Foà<sup>a,c</sup>, A. Giassi<sup>a</sup>, M.T. Grippo<sup>a,25</sup>, F. Ligabue<sup>a,c</sup>, T. Lomtadze<sup>a</sup>, L. Martini<sup>a,b</sup>, A. Messineo<sup>a,b</sup>, C.S. Moon<sup>a,26</sup>, F. Palla<sup>a,2</sup>, A. Rizzi<sup>a,b</sup>, A. Savoy-Navarro<sup>a,27</sup>, A.T. Serban<sup>a</sup>, P. Spagnolo<sup>a</sup>, P. Squillacioti<sup>a,25</sup>, R. Tenchini<sup>a</sup>, G. Tonelli<sup>a,b</sup>, A. Venturi<sup>a</sup>, P.G. Verdini<sup>a</sup>, C. Vernieri<sup>a,c,2</sup>**INFN Sezione di Roma <sup>a</sup>, Università di Roma <sup>b</sup>, Roma, Italy**L. Barone<sup>a,b</sup>, F. Cavallari<sup>a</sup>, D. Del Re<sup>a,b</sup>, M. Diemoz<sup>a</sup>, M. Grassi<sup>a,b</sup>, C. Jorda<sup>a</sup>, E. Longo<sup>a,b</sup>, F. Margaroli<sup>a,b</sup>, P. Meridiani<sup>a</sup>, F. Micheli<sup>a,b,2</sup>, S. Nourbakhsh<sup>a,b</sup>, G. Organtini<sup>a,b</sup>, R. Paramatti<sup>a</sup>, S. Rahatlou<sup>a,b</sup>, C. Rovelli<sup>a</sup>, F. Santanastasio<sup>a,b</sup>, L. Soffi<sup>a,b,2</sup>, P. Traczyk<sup>a,b</sup>**INFN Sezione di Torino <sup>a</sup>, Università di Torino <sup>b</sup>, Università del Piemonte Orientale (Novara) <sup>c</sup>, Torino, Italy**N. Amapane<sup>a,b</sup>, R. Arcidiacono<sup>a,c</sup>, S. Argiro<sup>a,b,2</sup>, M. Arneodo<sup>a,c</sup>, R. Bellan<sup>a,b</sup>, C. Biino<sup>a</sup>, N. Cartiglia<sup>a</sup>, S. Casasso<sup>a,b,2</sup>, M. Costa<sup>a,b</sup>, A. Degano<sup>a,b</sup>, N. Demaria<sup>a</sup>, L. Finco<sup>a,b</sup>, C. Mariotti<sup>a</sup>, S. Maselli<sup>a</sup>, E. Migliore<sup>a,b</sup>, V. Monaco<sup>a,b</sup>, M. Musich<sup>a</sup>, M.M. Obertino<sup>a,c,2</sup>, G. Ortona<sup>a,b</sup>, L. Pacher<sup>a,b</sup>, N. Pastrone<sup>a</sup>, M. Pelliccioni<sup>a</sup>, G.L. Pinna Angioni<sup>a,b</sup>, A. Potenza<sup>a,b</sup>, A. Romero<sup>a,b</sup>, M. Ruspa<sup>a,c</sup>, R. Sacchi<sup>a,b</sup>, A. Solano<sup>a,b</sup>, A. Staiano<sup>a</sup>, U. Tamponi<sup>a</sup>**INFN Sezione di Trieste <sup>a</sup>, Università di Trieste <sup>b</sup>, Trieste, Italy**S. Belforte<sup>a</sup>, V. Candelise<sup>a,b</sup>, M. Casarsa<sup>a</sup>, F. Cossutti<sup>a</sup>, G. Della Ricca<sup>a,b</sup>, B. Gobbo<sup>a</sup>, C. La Licata<sup>a,b</sup>, M. Marone<sup>a,b</sup>, D. Montanino<sup>a,b</sup>, A. Schizzi<sup>a,b,2</sup>, T. Umer<sup>a,b</sup>, A. Zanetti<sup>a</sup>**Chonbuk National University, Chonju, Korea**

T.J. Kim

**Kangwon National University, Chunchon, Korea**

S. Chang, A. Kropivnitskaya, S.K. Nam

**Kyungpook National University, Daegu, Korea**

D.H. Kim, G.N. Kim, M.S. Kim, D.J. Kong, S. Lee, Y.D. Oh, H. Park, A. Sakharov, D.C. Son

**Chonnam National University, Institute for Universe and Elementary Particles, Kwangju, Korea**

J.Y. Kim, S. Song

**Korea University, Seoul, Korea**

S. Choi, D. Gyun, B. Hong, M. Jo, H. Kim, Y. Kim, B. Lee, K.S. Lee, S.K. Park, Y. Roh

**University of Seoul, Seoul, Korea**

M. Choi, J.H. Kim, I.C. Park, S. Park, G. Ryu, M.S. Ryu

**Sungkyunkwan University, Suwon, Korea**

Y. Choi, Y.K. Choi, J. Goh, D. Kim, E. Kwon, J. Lee, H. Seo, I. Yu

**Vilnius University, Vilnius, Lithuania**

A. Juodagalvis

**National Centre for Particle Physics, Universiti Malaya, Kuala Lumpur, Malaysia**

J.R. Komaragiri, M.A.B. Md Ali

**Centro de Investigacion y de Estudios Avanzados del IPN, Mexico City, Mexico**

H. Castilla-Valdez, E. De La Cruz-Burelo, I. Heredia-de La Cruz<sup>28</sup>, R. Lopez-Fernandez, A. Sanchez-Hernandez

**Universidad Iberoamericana, Mexico City, Mexico**

S. Carrillo Moreno, F. Vazquez Valencia

**Benemerita Universidad Autonoma de Puebla, Puebla, Mexico**

I. Pedraza, H.A. Salazar Ibarguen

**Universidad Autónoma de San Luis Potosí, San Luis Potosí, Mexico**

E. Casimiro Linares, A. Morelos Pineda

**University of Auckland, Auckland, New Zealand**

D. Krofcheck

**University of Canterbury, Christchurch, New Zealand**

P.H. Butler, S. Reucroft

**National Centre for Physics, Quaid-I-Azam University, Islamabad, Pakistan**

A. Ahmad, M. Ahmad, Q. Hassan, H.R. Hoorani, S. Khalid, W.A. Khan, T. Khurshid, M.A. Shah, M. Shoaib

**National Centre for Nuclear Research, Swierk, Poland**

H. Bialkowska, M. Bluj, B. Boimska, T. Frueboes, M. Górski, M. Kazana, K. Nawrocki, K. Romanowska-Rybinska, M. Szleper, P. Zalewski

**Institute of Experimental Physics, Faculty of Physics, University of Warsaw, Warsaw, Poland**

G. Brona, K. Bunkowski, M. Cwiok, W. Dominik, K. Doroba, A. Kalinowski, M. Konecki, J. Krolikowski, M. Misiura, M. Olszewski, W. Wolszczak

**Laboratório de Instrumentação e Física Experimental de Partículas, Lisboa, Portugal**

P. Bargassa, C. Beirão Da Cruz E Silva, P. Faccioli, P.G. Ferreira Parracho, M. Gallinaro, F. Nguyen, J. Rodrigues Antunes, J. Seixas, J. Varela, P. Vischia

**Joint Institute for Nuclear Research, Dubna, Russia**

P. Bunin, M. Gavrilenko, I. Golutvin, A. Kamenev, V. Karjavin, V. Konoplyanikov, A. Lanev, A. Malakhov, V. Matveev<sup>29</sup>, P. Moisezenz, V. Palichik, V. Perelygin, M. Savina, S. Shmatov, S. Shulha, N. Skatchkov, V. Smirnov, A. Zarubin

**Petersburg Nuclear Physics Institute, Gatchina (St. Petersburg), Russia**

V. Golovtsov, Y. Ivanov, V. Kim<sup>30</sup>, P. Levchenko, V. Murzin, V. Oreshkin, I. Smirnov, V. Sulimov, L. Uvarov, S. Vavilov, A. Vorobyev, An. Vorobyev

**Institute for Nuclear Research, Moscow, Russia**

Yu. Andreev, A. Dermenev, S. Gninenko, N. Golubev, M. Kirsanov, N. Krasnikov, A. Pashenkov, D. Tlisov, A. Toropin

**Institute for Theoretical and Experimental Physics, Moscow, Russia**

V. Epshteyn, V. Gavrilov, N. Lychkovskaya, V. Popov, G. Safronov, S. Semenov, A. Spiridonov, V. Stolin, E. Vlasov, A. Zhokin

**P.N. Lebedev Physical Institute, Moscow, Russia**

V. Andreev, M. Azarkin, I. Dremin, M. Kirakosyan, A. Leonidov, G. Mesyats, S.V. Rusakov, A. Vinogradov

**Skobeltsyn Institute of Nuclear Physics, Lomonosov Moscow State University, Moscow, Russia**

A. Belyaev, E. Boos, V. Bunichev, M. Dubinin<sup>31</sup>, L. Dudko, A. Ershov, A. Gribushin, V. Klyukhin, O. Kodolova, I. Lokhtin, S. Obraztsov, S. Petrushanko, V. Savrin

**State Research Center of Russian Federation, Institute for High Energy Physics, Protvino, Russia**

I. Azhgirey, I. Bayshev, S. Bitioukov, V. Kachanov, A. Kalinin, D. Konstantinov, V. Krychkin, V. Petrov, R. Ryutin, A. Sobol, L. Tourtchanovitch, S. Troshin, N. Tyurin, A. Uzunian, A. Volkov

**University of Belgrade, Faculty of Physics and Vinca Institute of Nuclear Sciences, Belgrade, Serbia**

P. Adzic<sup>32</sup>, M. Ekmedzic, J. Milosevic, V. Rekovic

**Centro de Investigaciones Energéticas Medioambientales y Tecnológicas (CIEMAT), Madrid, Spain**

J. Alcaraz Maestre, C. Battilana, E. Calvo, M. Cerrada, M. Chamizo Llatas, N. Colino, B. De La Cruz, A. Delgado Peris, D. Domínguez Vázquez, A. Escalante Del Valle, C. Fernandez Bedoya, J.P. Fernández Ramos, J. Flix, M.C. Fouz, P. Garcia-Abia, O. Gonzalez Lopez, S. Goy Lopez, J.M. Hernandez, M.I. Josa, G. Merino, E. Navarro De Martino, A. Pérez-Calero Yzquierdo, J. Puerta Pelayo, A. Quintario Olmeda, I. Redondo, L. Romero, M.S. Soares

**Universidad Autónoma de Madrid, Madrid, Spain**

C. Albajar, J.F. de Trocóniz, M. Missiroli, D. Moran

**Universidad de Oviedo, Oviedo, Spain**

H. Brun, J. Cuevas, J. Fernandez Menendez, S. Folgueras, I. Gonzalez Caballero, L. Lloret Iglesias

**Instituto de Física de Cantabria (IFCA), CSIC-Universidad de Cantabria, Santander, Spain**

J.A. Brochero Cifuentes, I.J. Cabrillo, A. Calderon, J. Duarte Campderros, M. Fernandez, G. Gomez, A. Graziano, A. Lopez Virto, J. Marco, R. Marco, C. Martinez Rivero, F. Matorras, F.J. Munoz Sanchez, J. Piedra Gomez, T. Rodrigo, A.Y. Rodríguez-Marrero, A. Ruiz-Jimeno, L. Scodellaro, I. Vila, R. Vilar Cortabitarte

**CERN, European Organization for Nuclear Research, Geneva, Switzerland**

D. Abbaneo, E. Auffray, G. Auzinger, M. Bachtis, P. Baillon, A.H. Ball, D. Barney, A. Benaglia, J. Bendavid, L. Benhabib, J.F. Benitez, C. Bernet<sup>7</sup>, G. Bianchi, P. Bloch, A. Bocci, A. Bonato, O. Bondu, C. Botta, H. Breuker, T. Camporesi, G. Cerminara, S. Colafranceschi<sup>33</sup>, M. D'Alfonso, D. d'Enterria, A. Dabrowski, A. David, F. De Guio, A. De Roeck, S. De Visscher, M. Dobson, M. Dordevic, N. Dupont-Sagorin, A. Elliott-Peisert, J. Eugster, G. Franzoni, W. Funk, D. Gigi, K. Gill, D. Giordano, M. Girone, F. Glege, R. Guida, S. Gundacker, M. Guthoff, J. Hammer, M. Hansen, P. Harris, J. Hegeman, V. Innocente, P. Janot, K. Kousouris, K. Krajczar, P. Lecoq, C. Lourenço, N. Magini, L. Malgeri, M. Mannelli, J. Marrouche, L. Masetti, F. Meijers, S. Mersi, E. Meschi, F. Moortgat, S. Morovic, M. Mulders, P. Musella, L. Orsini, L. Pape, E. Perez, L. Perrozzi, A. Petrilli, G. Petrucciani, A. Pfeiffer, M. Pierini, M. Pimiä, D. Piparo, M. Plagge, A. Racz, G. Rolandi<sup>34</sup>, M. Rovere, H. Sakulin, C. Schäfer, C. Schwick, A. Sharma, P. Siegrist, P. Silva, M. Simon, P. Sphicas<sup>35</sup>, D. Spiga, J. Steggemann, B. Stieger, M. Stoye, D. Treille, A. Tsiros, G.I. Veres<sup>17</sup>, J.R. Vlimant, N. Wardle, H.K. Wöhri, H. Wollny, W.D. Zeuner

**Paul Scherrer Institut, Villigen, Switzerland**

W. Bertl, K. Deiters, W. Erdmann, R. Horisberger, Q. Ingram, H.C. Kaestli, S. König, D. Kotlinski, U. Langenegger, D. Renker, T. Rohe

**Institute for Particle Physics, ETH Zurich, Zurich, Switzerland**

F. Bachmair, L. Bäni, L. Bianchini, P. Bortignon, M.A. Buchmann, B. Casal, N. Chanon, A. Deisher, G. Dissertori, M. Dittmar, M. Donegà, M. Dünser, P. Eller, C. Grab, D. Hits, W. Lustermann, B. Mangano, A.C. Marini, P. Martinez Ruiz del Arbol, D. Meister, N. Mohr, C. Nägeli<sup>36</sup>, F. Nessi-Tedaldi, F. Pandolfi, F. Pauss, M. Peruzzi, M. Quittnat, L. Rebane, M. Rossini, A. Starodumov<sup>37</sup>, M. Takahashi, K. Theofilatos, R. Wallny, H.A. Weber

**Universität Zürich, Zurich, Switzerland**

C. Amsler<sup>38</sup>, M.F. Canelli, V. Chiochia, A. De Cosa, A. Hinzmann, T. Hreus, B. Kilminster, B. Millan Mejias, J. Ngadiuba, P. Robmann, F.J. Ronga, S. Taroni, M. Verzetti, Y. Yang

**National Central University, Chung-Li, Taiwan**

M. Cardaci, K.H. Chen, C. Ferro, C.M. Kuo, W. Lin, Y.J. Lu, R. Volpe, S.S. Yu

**National Taiwan University (NTU), Taipei, Taiwan**

P. Chang, Y.H. Chang, Y.W. Chang, Y. Chao, K.F. Chen, P.H. Chen, C. Dietz, U. Grundler, W.-S. Hou, K.Y. Kao, Y.J. Lei, Y.F. Liu, R.-S. Lu, D. Majumder, E. Petrakou, Y.M. Tzeng, R. Wilken

**Chulalongkorn University, Faculty of Science, Department of Physics, Bangkok, Thailand**

B. Asavapibhop, N. Srimanobhas, N. Suwonjandee

**Cukurova University, Adana, Turkey**

A. Adiguzel, M.N. Bakirci<sup>39</sup>, S. Cerci<sup>40</sup>, C. Dozen, I. Dumanoglu, E. Eskut, S. Girgis, G. Gokbulut, E. Gurpinar, I. Hos, E.E. Kangal, A. Kayis Topaksu, G. Onengut<sup>41</sup>, K. Ozdemir, S. Ozturk<sup>39</sup>, A. Polatoz, K. Sogut<sup>42</sup>, D. Sunar Cerci<sup>40</sup>, B. Tali<sup>40</sup>, H. Topakli<sup>39</sup>, M. Vergili

**Middle East Technical University, Physics Department, Ankara, Turkey**

I.V. Akin, B. Bilin, S. Bilmis, H. Gamsizkan, G. Karapinar<sup>43</sup>, K. Ocalan, S. Sekmen, U.E. Surat, M. Yalvac, M. Zeyrek

**Bogazici University, Istanbul, Turkey**

E. Gülmez, B. Isildak<sup>44</sup>, M. Kaya<sup>45</sup>, O. Kaya<sup>45</sup>

**Istanbul Technical University, Istanbul, Turkey**

H. Bahtiyar<sup>46</sup>, E. Barlas, K. Cankocak, F.I. Vardarli, M. Yücel

**National Scientific Center, Kharkov Institute of Physics and Technology, Kharkov, Ukraine**

L. Levchuk, P. Sorokin

**University of Bristol, Bristol, United Kingdom**

J.J. Brooke, E. Clement, D. Cussans, H. Flacher, R. Frazier, J. Goldstein, M. Grimes, G.P. Heath, H.F. Heath, J. Jacob, L. Kreczko, C. Lucas, Z. Meng, D.M. Newbold<sup>47</sup>, S. Paramesvaran, A. Poll, S. Senkin, V.J. Smith, T. Williams

**Rutherford Appleton Laboratory, Didcot, United Kingdom**

K.W. Bell, A. Belyaev<sup>48</sup>, C. Brew, R.M. Brown, D.J.A. Cockerill, J.A. Coughlan, K. Harder, S. Harper, E. Olaiya, D. Petyt, C.H. Shepherd-Themistocleous, A. Thea, I.R. Tomalin, W.J. Womersley, S.D. Worm

**Imperial College, London, United Kingdom**

M. Baber, R. Bainbridge, O. Buchmuller, D. Burton, D. Colling, N. Cripps, M. Cutajar, P. Dauncey, G. Davies, M. Della Negra, P. Dunne, W. Ferguson, J. Fulcher, D. Futyan, A. Gilbert,

G. Hall, G. Iles, M. Jarvis, G. Karapostoli, M. Kenzie, R. Lane, R. Lucas<sup>47</sup>, L. Lyons, A.-M. Magnan, S. Malik, B. Mathias, J. Nash, A. Nikitenko<sup>37</sup>, J. Pela, M. Pesaresi, K. Petridis, D.M. Raymond, S. Rogerson, A. Rose, C. Seez, P. Sharp<sup>†</sup>, A. Tapper, M. Vazquez Acosta, T. Virdee

**Brunel University, Uxbridge, United Kingdom**

J.E. Cole, P.R. Hobson, A. Khan, P. Kyberd, D. Leggat, D. Leslie, W. Martin, I.D. Reid, P. Symonds, L. Teodorescu, M. Turner

**Baylor University, Waco, USA**

J. Dittmann, K. Hatakeyama, A. Kasmi, H. Liu, T. Scarborough

**The University of Alabama, Tuscaloosa, USA**

O. Charaf, S.I. Cooper, C. Henderson, P. Rumerio

**Boston University, Boston, USA**

A. Avetisyan, T. Bose, C. Fantasia, A. Heister, P. Lawson, C. Richardson, J. Rohlf, D. Sperka, J. St. John, L. Sulak

**Brown University, Providence, USA**

J. Alimena, E. Berry, S. Bhattacharya, G. Christopher, D. Cutts, Z. Demiragli, A. Ferapontov, A. Garabedian, U. Heintz, G. Kukartsev, E. Laird, G. Landsberg, M. Luk, M. Narain, M. Segala, T. Sinthuprasith, T. Speer, J. Swanson

**University of California, Davis, Davis, USA**

R. Breedon, G. Breto, M. Calderon De La Barca Sanchez, S. Chauhan, M. Chertok, J. Conway, R. Conway, P.T. Cox, R. Erbacher, M. Gardner, W. Ko, R. Lander, T. Miceli, M. Mulhearn, D. Pellett, J. Pilot, F. Ricci-Tam, M. Searle, S. Shalhout, J. Smith, M. Squires, D. Stolp, M. Tripathi, S. Wilbur, R. Yohay

**University of California, Los Angeles, USA**

R. Cousins, P. Everaerts, C. Farrell, J. Hauser, M. Ignatenko, G. Rakness, E. Takasugi, V. Valuev, M. Weber

**University of California, Riverside, Riverside, USA**

J. Babb, K. Burt, R. Clare, J. Ellison, J.W. Gary, G. Hanson, J. Heilman, M. Ivova Rikova, P. Jandir, E. Kennedy, F. Lacroix, H. Liu, O.R. Long, A. Luthra, M. Malberti, H. Nguyen, M. Olmedo Negrete, A. Shrinivas, S. Sumowidagdo, S. Wimpenny

**University of California, San Diego, La Jolla, USA**

W. Andrews, J.G. Branson, G.B. Cerati, S. Cittolin, R.T. D'Agnolo, D. Evans, A. Holzner, R. Kelley, D. Klein, M. Lebourgeois, J. Letts, I. Macneill, D. Olivito, S. Padhi, C. Palmer, M. Pieri, M. Sani, V. Sharma, S. Simon, E. Sudano, M. Tadel, Y. Tu, A. Vartak, C. Welke, F. Würthwein, A. Yagil, J. Yoo

**University of California, Santa Barbara, Santa Barbara, USA**

D. Barge, J. Bradmiller-Feld, C. Campagnari, T. Danielson, A. Dishaw, K. Flowers, M. Franco Sevilla, P. Geffert, C. George, F. Golf, L. Gouskos, J. Incandela, C. Justus, N. Mccoll, J. Richman, D. Stuart, W. To, C. West

**California Institute of Technology, Pasadena, USA**

A. Apresyan, A. Bornheim, J. Bunn, Y. Chen, E. Di Marco, J. Duarte, A. Mott, H.B. Newman, C. Pena, C. Rogan, M. Spiropulu, V. Timciuc, R. Wilkinson, S. Xie, R.Y. Zhu

**Carnegie Mellon University, Pittsburgh, USA**

V. Azzolini, A. Calamba, T. Ferguson, Y. Iiyama, M. Paulini, J. Russ, H. Vogel, I. Vorobiev

**University of Colorado at Boulder, Boulder, USA**

J.P. Cumalat, W.T. Ford, A. Gaz, E. Luiggi Lopez, U. Nauenberg, J.G. Smith, K. Stenson, K.A. Ulmer, S.R. Wagner

**Cornell University, Ithaca, USA**

J. Alexander, A. Chatterjee, J. Chu, S. Dittmer, N. Eggert, N. Mirman, G. Nicolas Kaufman, J.R. Patterson, A. Ryd, E. Salvati, L. Skinnari, W. Sun, W.D. Teo, J. Thom, J. Thompson, J. Tucker, Y. Weng, L. Winstrom, P. Wittich

**Fairfield University, Fairfield, USA**

D. Winn

**Fermi National Accelerator Laboratory, Batavia, USA**

S. Abdullin, M. Albrow, J. Anderson, G. Apollinari, L.A.T. Bauerdick, A. Beretvas, J. Berryhill, P.C. Bhat, K. Burkett, J.N. Butler, H.W.K. Cheung, F. Chlebana, S. Cihangir, V.D. Elvira, I. Fisk, J. Freeman, Y. Gao, E. Gottschalk, L. Gray, D. Green, S. Grünendahl, O. Gutsche, J. Hanlon, D. Hare, R.M. Harris, J. Hirschauer, B. Hooberman, S. Jindariani, M. Johnson, U. Joshi, K. Kaadze, B. Klima, B. Kreis, S. Kwan, J. Linacre, D. Lincoln, R. Lipton, T. Liu, J. Lykken, K. Maeshima, J.M. Marraffino, V.I. Martinez Outschoorn, S. Maruyama, D. Mason, P. McBride, K. Mishra, S. Mrenna, Y. Musienko<sup>29</sup>, S. Nahn, C. Newman-Holmes, V. O'Dell, O. Prokofyev, E. Sexton-Kennedy, S. Sharma, A. Soha, W.J. Spalding, L. Spiegel, L. Taylor, S. Tkaczyk, N.V. Tran, L. Uplegger, E.W. Vaandering, R. Vidal, A. Whitbeck, J. Whitmore, F. Yang

**University of Florida, Gainesville, USA**

D. Acosta, P. Avery, D. Bourilkov, M. Carver, T. Cheng, D. Curry, S. Das, M. De Gruttola, G.P. Di Giovanni, R.D. Field, M. Fisher, I.K. Furic, J. Hugon, J. Konigsberg, A. Korytov, T. Kypreos, J.F. Low, K. Matchev, P. Milenovic<sup>49</sup>, G. Mitselmakher, L. Muniz, A. Rinkevicius, L. Shchutska, N. Skhirtladze, M. Snowball, J. Yelton, M. Zakaria

**Florida International University, Miami, USA**

S. Hewamanage, S. Linn, P. Markowitz, G. Martinez, J.L. Rodriguez

**Florida State University, Tallahassee, USA**

T. Adams, A. Askew, J. Bochenek, B. Diamond, J. Haas, S. Hagopian, V. Hagopian, K.F. Johnson, H. Prosper, V. Veeraraghavan, M. Weinberg

**Florida Institute of Technology, Melbourne, USA**

M.M. Baarmand, M. Hohlmann, H. Kalakhety, F. Yumiceva

**University of Illinois at Chicago (UIC), Chicago, USA**

M.R. Adams, L. Apanasevich, V.E. Bazterra, D. Berry, R.R. Betts, I. Bucinskaite, R. Cavanaugh, O. Evdokimov, L. Gauthier, C.E. Gerber, D.J. Hofman, S. Khalatyan, P. Kurt, D.H. Moon, C. O'Brien, C. Silkworth, P. Turner, N. Varelas

**The University of Iowa, Iowa City, USA**

E.A. Albayrak<sup>46</sup>, B. Bilki<sup>50</sup>, W. Clarida, K. Dilsiz, F. Duru, M. Haytmyradov, J.-P. Merlo, H. Mermerkaya<sup>51</sup>, A. Mestvirishvili, A. Moeller, J. Nachtman, H. Ogul, Y. Onel, F. Ozok<sup>46</sup>, A. Penzo, R. Rahmat, S. Sen, P. Tan, E. Tiras, J. Wetzel, T. Yetkin<sup>52</sup>, K. Yi

**Johns Hopkins University, Baltimore, USA**

B.A. Barnett, B. Blumenfeld, S. Bolognesi, D. Fehling, A.V. Gritsan, P. Maksimovic, C. Martin, M. Swartz

**The University of Kansas, Lawrence, USA**

P. Baringer, A. Bean, G. Benelli, C. Bruner, J. Gray, R.P. Kenny III, M. Malek, M. Murray, D. Noonan, S. Sanders, J. Sekaric, R. Stringer, Q. Wang, J.S. Wood

**Kansas State University, Manhattan, USA**

A.F. Barfuss, I. Chakaberia, A. Ivanov, S. Khalil, M. Makouski, Y. Maravin, L.K. Saini, S. Shrestha, I. Svintradze

**Lawrence Livermore National Laboratory, Livermore, USA**

J. Gronberg, D. Lange, F. Rebassoo, D. Wright

**University of Maryland, College Park, USA**

A. Baden, A. Belloni, B. Calvert, S.C. Eno, J.A. Gomez, N.J. Hadley, R.G. Kellogg, T. Kolberg, Y. Lu, M. Marionneau, A.C. Mignerey, K. Pedro, A. Skuja, M.B. Tonjes, S.C. Tonwar

**Massachusetts Institute of Technology, Cambridge, USA**

A. Apyan, R. Barbieri, G. Bauer, W. Busza, I.A. Cali, M. Chan, L. Di Matteo, V. Dutta, G. Gomez Ceballos, M. Goncharov, D. Gulhan, M. Klute, Y.S. Lai, Y.-J. Lee, A. Levin, P.D. Luckey, T. Ma, C. Paus, D. Ralph, C. Roland, G. Roland, G.S.F. Stephans, F. Stöckli, K. Sumorok, D. Velicanu, J. Veverka, B. Wyslouch, M. Yang, M. Zanetti, V. Zhukova

**University of Minnesota, Minneapolis, USA**

B. Dahmes, A. Gude, S.C. Kao, K. Klapoetke, Y. Kubota, J. Mans, N. Pastika, R. Rusack, A. Singovsky, N. Tambe, J. Turkewitz

**University of Mississippi, Oxford, USA**

J.G. Acosta, S. Oliveros

**University of Nebraska-Lincoln, Lincoln, USA**

E. Avdeeva, K. Bloom, S. Bose, D.R. Claes, A. Dominguez, R. Gonzalez Suarez, J. Keller, D. Knowlton, I. Kravchenko, J. Lazo-Flores, S. Malik, F. Meier, G.R. Snow

**State University of New York at Buffalo, Buffalo, USA**

J. Dolen, A. Godshalk, I. Iashvili, A. Kharchilava, A. Kumar, S. Rappoccio

**Northeastern University, Boston, USA**

G. Alverson, E. Barberis, D. Baumgartel, M. Chasco, J. Haley, A. Massironi, D.M. Morse, D. Nash, T. Orimoto, D. Trocino, R.j. Wang, D. Wood, J. Zhang

**Northwestern University, Evanston, USA**

K.A. Hahn, A. Kubik, N. Mucia, N. Odell, B. Pollack, A. Pozdnyakov, M. Schmitt, S. Stoynev, K. Sung, M. Velasco, S. Won

**University of Notre Dame, Notre Dame, USA**

A. Brinkerhoff, K.M. Chan, A. Drozdetskiy, M. Hildreth, C. Jessop, D.J. Karmgard, N. Kellams, K. Lannon, W. Luo, S. Lynch, N. Marinelli, T. Pearson, M. Planer, R. Ruchti, N. Valls, M. Wayne, M. Wolf, A. Woodard

**The Ohio State University, Columbus, USA**

L. Antonelli, J. Brinson, B. Bylsma, L.S. Durkin, S. Flowers, C. Hill, R. Hughes, K. Kotov, T.Y. Ling, D. Puigh, M. Rodenburg, G. Smith, C. Vuosalo, B.L. Winer, H. Wolfe, H.W. Wulsin

**Princeton University, Princeton, USA**

O. Driga, P. Elmer, P. Hebda, A. Hunt, S.A. Koay, P. Lujan, D. Marlow, T. Medvedeva, M. Mooney, J. Olsen, P. Piroué, X. Quan, H. Saka, D. Stickland<sup>2</sup>, C. Tully, J.S. Werner, S.C. Zenz, A. Zuranski



**University of Puerto Rico, Mayaguez, USA**

E. Brownson, H. Mendez, J.E. Ramirez Vargas

**Purdue University, West Lafayette, USA**

E. Alagoz, V.E. Barnes, D. Benedetti, G. Bolla, D. Bortoletto, M. De Mattia, Z. Hu, M.K. Jha, M. Jones, K. Jung, M. Kress, N. Leonardo, D. Lopes Pegna, V. Maroussov, P. Merkel, D.H. Miller, N. Neumeister, B.C. Radburn-Smith, X. Shi, I. Shipsey, D. Silvers, A. Svyatkovskiy, F. Wang, W. Xie, L. Xu, H.D. Yoo, J. Zablocki, Y. Zheng

**Purdue University Calumet, Hammond, USA**

N. Parashar, J. Stupak

**Rice University, Houston, USA**

A. Adair, B. Akgun, K.M. Ecklund, F.J.M. Geurts, W. Li, B. Michlin, B.P. Padley, R. Redjimi, J. Roberts, J. Zabel

**University of Rochester, Rochester, USA**

B. Betchart, A. Bodek, R. Covarelli, P. de Barbaro, R. Demina, Y. Eshaq, T. Ferbel, A. Garcia-Bellido, P. Goldenzweig, J. Han, A. Harel, A. Khukhunaishvili, G. Petrillo, D. Vishnevskiy

**The Rockefeller University, New York, USA**

R. Ciesielski, L. Demortier, K. Goulianos, G. Lungu, C. Mesropian

**Rutgers, The State University of New Jersey, Piscataway, USA**

S. Arora, A. Barker, J.P. Chou, C. Contreras-Campana, E. Contreras-Campana, D. Duggan, D. Ferencek, Y. Gershtein, R. Gray, E. Halkiadakis, D. Hidas, A. Lath, S. Panwalkar, M. Park, R. Patel, S. Salur, S. Schnetzer, S. Somalwar, R. Stone, S. Thomas, P. Thomassen, M. Walker

**University of Tennessee, Knoxville, USA**

K. Rose, S. Spanier, A. York

**Texas A&M University, College Station, USA**

O. Bouhali<sup>53</sup>, R. Eusebi, W. Flanagan, J. Gilmore, T. Kamon<sup>54</sup>, V. Khotilovich, V. Krutelyov, R. Montalvo, I. Osipenkov, Y. Pakhotin, A. Perloff, J. Roe, A. Rose, A. Safonov, T. Sakuma, I. Suarez, A. Tatarinov

**Texas Tech University, Lubbock, USA**

N. Akchurin, C. Cowden, J. Damgov, C. Dragoiu, P.R. Duderu, J. Faulkner, K. Kovitangoon, S. Kunori, S.W. Lee, T. Libeiro, I. Volobouev

**Vanderbilt University, Nashville, USA**

E. Appelt, A.G. Delannoy, S. Greene, A. Gurrola, W. Johns, C. Maguire, Y. Mao, A. Melo, M. Sharma, P. Sheldon, B. Snook, S. Tuo, J. Velkovska

**University of Virginia, Charlottesville, USA**

M.W. Arenton, S. Boutle, B. Cox, B. Francis, J. Goodell, R. Hirosky, A. Ledovskoy, H. Li, C. Lin, C. Neu, J. Wood

**Wayne State University, Detroit, USA**

R. Harr, P.E. Karchin, C. Kottachchi Kankanamge Don, P. Lamichhane, J. Sturdy

**University of Wisconsin, Madison, USA**

D.A. Belknap, D. Carlsmith, M. Cepeda, S. Dasu, S. Duric, E. Friis, R. Hall-Wilton, M. Herndon, A. Hervé, P. Klabbers, A. Lanaro, C. Lazaridis, A. Levine, R. Loveless, A. Mohapatra, I. Ojalvo, T. Perry, G.A. Pierro, G. Polese, I. Ross, T. Sarangi, A. Savin, W.H. Smith, N. Woods

†: Deceased

- 1: Also at Vienna University of Technology, Vienna, Austria
- 2: Also at CERN, European Organization for Nuclear Research, Geneva, Switzerland
- 3: Also at Institut Pluridisciplinaire Hubert Curien, Université de Strasbourg, Université de Haute Alsace Mulhouse, CNRS/IN2P3, Strasbourg, France
- 4: Also at National Institute of Chemical Physics and Biophysics, Tallinn, Estonia
- 5: Also at Skobeltsyn Institute of Nuclear Physics, Lomonosov Moscow State University, Moscow, Russia
- 6: Also at Universidade Estadual de Campinas, Campinas, Brazil
- 7: Also at Laboratoire Leprince-Ringuet, Ecole Polytechnique, IN2P3-CNRS, Palaiseau, France
- 8: Also at Joint Institute for Nuclear Research, Dubna, Russia
- 9: Also at Suez University, Suez, Egypt
- 10: Also at British University in Egypt, Cairo, Egypt
- 11: Also at Fayoum University, El-Fayoum, Egypt
- 12: Now at Ain Shams University, Cairo, Egypt
- 13: Also at Université de Haute Alsace, Mulhouse, France
- 14: Also at Brandenburg University of Technology, Cottbus, Germany
- 15: Also at The University of Kansas, Lawrence, USA
- 16: Also at Institute of Nuclear Research ATOMKI, Debrecen, Hungary
- 17: Also at Eötvös Loránd University, Budapest, Hungary
- 18: Also at University of Debrecen, Debrecen, Hungary
- 19: Also at University of Visva-Bharati, Santiniketan, India
- 20: Now at King Abdulaziz University, Jeddah, Saudi Arabia
- 21: Also at University of Ruhuna, Matara, Sri Lanka
- 22: Also at Isfahan University of Technology, Isfahan, Iran
- 23: Also at Sharif University of Technology, Tehran, Iran
- 24: Also at Plasma Physics Research Center, Science and Research Branch, Islamic Azad University, Tehran, Iran
- 25: Also at Università degli Studi di Siena, Siena, Italy
- 26: Also at Centre National de la Recherche Scientifique (CNRS) - IN2P3, Paris, France
- 27: Also at Purdue University, West Lafayette, USA
- 28: Also at Universidad Michoacana de San Nicolas de Hidalgo, Morelia, Mexico
- 29: Also at Institute for Nuclear Research, Moscow, Russia
- 30: Also at St. Petersburg State Polytechnical University, St. Petersburg, Russia
- 31: Also at California Institute of Technology, Pasadena, USA
- 32: Also at Faculty of Physics, University of Belgrade, Belgrade, Serbia
- 33: Also at Facoltà Ingegneria, Università di Roma, Roma, Italy
- 34: Also at Scuola Normale e Sezione dell'INFN, Pisa, Italy
- 35: Also at University of Athens, Athens, Greece
- 36: Also at Paul Scherrer Institut, Villigen, Switzerland
- 37: Also at Institute for Theoretical and Experimental Physics, Moscow, Russia
- 38: Also at Albert Einstein Center for Fundamental Physics, Bern, Switzerland
- 39: Also at Gaziosmanpasa University, Tokat, Turkey
- 40: Also at Adiyaman University, Adiyaman, Turkey
- 41: Also at Cag University, Mersin, Turkey
- 42: Also at Mersin University, Mersin, Turkey
- 43: Also at Izmir Institute of Technology, Izmir, Turkey
- 44: Also at Ozyegin University, Istanbul, Turkey
- 45: Also at Kafkas University, Kars, Turkey

46: Also at Mimar Sinan University, Istanbul, Istanbul, Turkey

47: Also at Rutherford Appleton Laboratory, Didcot, United Kingdom

48: Also at School of Physics and Astronomy, University of Southampton, Southampton, United Kingdom

49: Also at University of Belgrade, Faculty of Physics and Vinca Institute of Nuclear Sciences, Belgrade, Serbia

50: Also at Argonne National Laboratory, Argonne, USA

51: Also at Erzincan University, Erzincan, Turkey

52: Also at Yildiz Technical University, Istanbul, Turkey

53: Also at Texas A&M University at Qatar, Doha, Qatar

54: Also at Kyungpook National University, Daegu, Korea